A METHODOLOGY FOR THE DETERMINATION OF OPTIMAL OPERATIONAL SCHEDULES OF HYBRID ELECTRIC ARCHITECTURES

A Thesis

Presented to

The Academic Faculty

by

David Russell Trawick

In Partial Fulfillment

of the Requirements for the Degree

Doctor of Philosophy in the

School of Aerospace Engineering

Georgia Institute of Technology

May 2018

A METHODOLOGY FOR THE DETERMINATION OF OPTIMAL OPERATIONAL SCHEDULES OF HYBRID ELECTRIC ARCHITECTURES

Approved by:

Dr. Dimitri Mavris, Advisor
Daniel Guggenheim School of
Aerospace Engineering
Georgia Institute of Technology

Dr. Daniel P. Schrage
Daniel Guggenheim School of
Aerospace Engineering
Georgia Institute of Technology

Dr. Jimmy Tai
Daniel Guggenheim School of
Aerospace Engineering
Georgia Institute of Technology

Dr. Graeme Kennedy
Daniel Guggenheim School of
Aerospace Engineering
Georgia Institute of Technology

Dr. Michael Armstrong
Aerospace Engineer
*Rolls-Royce North American
Technologies, Inc.*

Date Approved: December 7, 2017

ACKNOWLEDGEMENTS

His support was instrumental in allowing me to meet the final deadlines and start my employment as planned.

I must also thank my parents, Charles and Susan Trawick for their immense support, financial, emotional, and editorial, throughout my Georgia Tech career. Their encouragement and practical assistance were key to my success at Georgia Tech. In addition they are among the few to take the time to read this thesis during its development, and their feedback was invaluable for improving the accessibility and quality of this document.

Finally, I would like to thank my fellow students at ASDL for their encouragement, support and example. These include but are not limited to Imon Chakraborty, Mario Lee, Metin Ozcan, David Moroniti and Tom Neumann. Special thanks is due to Andrew Burrell who has not only been a sounding board for my work throughout my time at ASDL, but who also generously donated weeks of computing time toward my thesis on his powerful personal computer.

TABLE OF CONTENTS

LIST OF TABLES

Page

LIST OF FIGURES

Page

LIST OF SYMBOLS AND ABBREVIATIONS

Δt	Simulation Time Step
AC	Alternating Current
Adv	Advanced
BLI	Boundary Layer Ingestion
CDCS	Charge Depleting Charge Sustaining
CMC	Ceramic Matrix Composites
CO_2	Carbon Dioxide
DC	Direct Current
EADS	European Aeronautic Defence and Space
EMCS	Equivalent Minimum Consumption Strategy
g	Acceleration Due to Earth's Gravity
GM	General Motors
hFan	Hybrid Turbofan
HPT	High Pressure Turbine
HTS	High Temperature Superconductor
I	Electric Current
λ	Optimal Control Costate
LPT	Low Pressure Turbine
MATLAB	Matrix Laboratory
MTOW	Maximum Takeoff Weight
NPSS	Numerical Propulsion System Simulation
P_e	Electric Power

PR	Pressure Ratio
R	Electrical Resistance
TOGW	Takeoff Gross Weight
TSFC	Thrust Specific Fuel Consumption
SOC	State of Charge
SUGAR	Subsonic Ultra Green Aircraft Research
UAV	Unmanned Aerial Vehicle
UTRC	United Technologies Research Center
V	Voltage
VTOL	Vertical Takeoff and Landing
W_f	Mass of Fuel
$\dot{w}_f$	Fuel Burn rate

SUMMARY

Hybrid electric aircraft have been proposed as a means to achieve the ambitious fuel burn reduction goals which have been set for future air transports. Hybrid aircraft supplement the fuel they carry with batteries. This results in propulsion systems which can meet a thrust requirement in multiple ways until the battery runs out of charge. The choice of when to supplement the gas turbine with electrical power can change the fuel burn even if the same total amount of battery is used. This is due both to the weight change from fuel burn being different than that for battery usage and also to the changing fuel efficiency resulting from adding electrical power. In return, fuel efficiency depends on the thrust being produced, the electricity added and the flight condition. Choosing the proper power schedule for the electric motors is essential to an efficient flight and to an accurate estimate of fuel burn during design.

This thesis set out to determine a methodology for choosing the best power scheduling method for hybrid aircraft. In order to define this methodology, several research questions were posed: what impact do the power schedules have on the mission level fuel burn, what factors in the hybrid system design and operation have the greatest impact on the ideal power schedule, what baseline methods and optimization techniques provide the best performance and how does the choice of the best power schedules affect the larger problems in hybrid electric aircraft design and sizing.

An examination of the literature found that a small number of hybrid power schedules have been used in hybrid aircraft studies, but more advanced methods have been used to address the problem for hybrid cars. Based on the literature, hypotheses were formed for the research questions, and a methodology based on the hypotheses was

proposed for choosing a power scheduling method, called the Systematic Hybrid Aircraft Power Schedule Optimizer (SHAPSO). A set of experiments to settle the research questions was planned, with the intention of revising SHAPSO as needed if the hypotheses were disproven.

Before any experiments could be conducted on the performance of different hybrid power schedulers and scheduling methods, a hybrid system model had to be constructed. A set of hybrid electric component models was constructed within the gas turbine modeling tool NPSS in order to add hybrid capability to the tool. This enabled the modeling of a hybrid turbofan engine at a fidelity sufficient to capture the efficiency changes of each component due to the interactions between the electric power system and the gas turbine. With this model in hand, the drag polar and aircraft size and weight were all that were required to model the hybrid system. To enable the use of computationally expensive optimization techniques, a surrogate model was made of the hybrid turbofan. This reduced the computational burden of a call to the engine at the cost of baking in the component efficiencies assumed in the modeling phase. The battery was modeled separately from the surrogate to enable its size and efficiency to vary from case to case as required.

The first experiment involved testing several candidate power schedules and scheduling methods on a simple mission consisting of a single cruise segment at a constant Mach number and altitude. Three baseline power schedules were run, Constant Power, Power at Start and Power at End. These were compared in their resulting fuel burns against each other, as well as against the Optimal Control method and the global optimization method Dynamic Programming. Dynamic Programming found that the ideal

power schedule was linear, slowly increasing in power over the mission with a slope and height dependent on the battery size and mission length. Optimal Control found a similar power schedule with a lesser slope. Its fuel burn was only marginally worse than Dynamic Programming. Constant Power consumed only slightly more fuel than Optimal Control, but End Power burned 2-3% more fuel than Constant Power and Start Power another .5% more fuel than End Power. A Linear Power schedule was also found that showed marginally better performance than Dynamic Programming due to the resolution limitations of its implementation. These results showed that the power schedule does make a difference in fuel burn, but disproved the hypotheses that End Power was the best of the baseline schedules. The results also indicated that the most significant factor in the ideal power schedule was not the reduction of system weight from burning fuel earlier rather than later, as had been hypothesized. Instead the results suggested that the resistance of the battery may be the dominant factor determining the optimal power usage schedule. However the research questions could not be conclusively answered until a more complete mission was tested. In addition the margin of difference in fuel burn between Constant Power, Optimal Control and Dynamic Programming was found to be extremely small, requiring care to be taken to zero other errors.

Experiment #2 was similar to Experiment #1 but also included a climb segment and a descent segment to capture a more complete mission. The descent segment could not use hybrid power due to the operating assumptions of the hybrid turbofan, but the climb segment could use hybrid power and did so throughout drastically changing flight conditions. The methods tested were End Power, Climb Power, Constant Power, Optimal Control and Dynamic Programming. These were the same methods as in Experiment #1,

with the exceptions that the Start Power method was replaced with a Climb Power method and that the Linear schedule, found to be optimum in Experiment #1, was omitted. These changes were made because Start Power was the worst method in Experiment #1 but Climb Power has been proposed by other studies in the literature. Also the power schedules found by Dynamic Programming in Experiment #2 were not linear, eliminating the utility of the Linear power schedule. During the setup of Experiment #2 it was found that the fit of the hybrid engine surrogate model had to be very tight, as the optimizers would otherwise find any beneficial errors in the surrogate model and base their power schedules around these inaccurate efficiency gains. The length of the mission and the size of the battery were varied, as was the battery resistance in order to evaluate their impact on the power schedules.

The Experiment #2 results showed that the best of the baseline schedules was Constant Power, which did nearly as well as Dynamic Programming. Varying the battery resistance greatly reduced the difference between Constant Power and the other baselines but did not eliminate it, showing that the battery resistance was the primary factor driving the power schedules. Optimal Control did not always do better than Constant Power. This inspired two different improvements to the Optimal Control method to allow it to favor fuel more at one end of the mission than the other. These improved versions were able to match or slightly improve Dynamic Programming's fuel burn due to the resolution limits on Dynamic Programming. The improved versions of Optimal Control required an increase in computational burden compared to the original Optimal Control but were still an order of magnitude faster than Dynamic Programming.

Experiment #3 demonstrated part of the analysis that would be required to choose a battery size for a particular aircraft. End Power, Climb Power, Constant Power, Optimal Control, Weighted Optimal Control, and 2 Level Optimal Control were used to find the required fuel to fly distances from 500 to 2,000 nautical miles with each of four different batteries weighing 5,000, 10,000, 15,000, or 20,000 lbs. These fuel burns were then compared to the required fuel for the same system with no battery attached, flying on fuel alone. The total energy savings was then plotted against range for each battery and method. This chart could then be used to determine the most appropriate battery pack for a given mission set.

The Experiment #3 results showed a significantly higher energy savings across the energy limited region of the chart for Constant Power compared to the other baseline methods. This showed the impact that power schedules can have on energy consumption. Even when the battery resistance was lowered, the differences became smaller but persisted across the ranges examined. The other methods made marginal improvements to the Constant Power energy savings, on the order of .1% of the total energy at each range.

Based on these results the procedure within SHAPSO for choosing the appropriate power scheduling method for any hybrid electric architecture was updated. In the final version of SHAPSO, after defining the architecture itself, the optimization problem has to be defined, specifying the metric of interest and the available degrees of freedom. Once this is known the hybrid architecture has to be modeled at fidelity sufficient to capture the tradeoffs inherent to the problem. If this model takes too long to be used with the global optimization method of choice, a surrogate model is then made with a tight fit to capture the details of the model but speed execution. When the most

appropriate baseline schedule is unknown, candidate schedules are tested against one another to find the best. This baseline schedule is then compared to a global optimizer at a number of points to determine the difference between the baseline and ideal performance. If that difference is less than the accepted error of the model, the methodology chooses the baseline schedule for future operation of the architecture, until the model changes or the error is reduced. If the difference is more than the accepted error of the model the methodology tests other methods such as Optimal Control in increasing order of computational cost, until one is found that is closer to the ideal result than the error margin. If no method yields results closer than the error margin, the best of the methods and the global optimizer itself are compared and the methodology chooses between them depending on the relative cost of computational time and model performance.

This thesis improves the state of the art by establishing a consistent process for power schedule selection, SHAPSO, which is different than that used in previous studies. It also establishes the ideal power schedules for a common hybrid electric architecture, although the specific results are a function of the modeling, sizing and operational assumptions baked into the NPSS model. Future work would include readdressing some of these assumptions, adding degrees of freedom to the optimization problem, and including other factors in the objective function along with fuel cost, such as engine maintenance and battery costs. Future work would also include testing the methodology on a different hybrid electric architecture, preferably one with an ideal power schedule significantly better than any baseline schedule. This methodology would then enable

greater fuel savings with a fixed hardware aircraft and thus increase the utility of hybrid electric architectures.

INTRODUCTION

Since the beginning of the 21st century there has been a renewed focus on reducing the CO_2 emissions and improving the fuel efficiency of new transport aircraft. This focus has been shared by airframers, engine manufacturers and regulatory agencies. In 2007 NASA set goals for upcoming generations of aircraft, setting the ambitious goal of a 70% reduction in fuel burn by aircraft entering service in 2030-2035 when compared to a 2005 baseline vehicle [1]. These goals have been updated since, with the 2016 revision shown in Table 1 below. In addition to evolutionary improvements to current conventional aircraft, these high goals have inspired revolutionary aircraft concepts such as drastic changes in planform and attempts to utilize boundary layer ingestion[2]. Other concepts have taken aim at the fuel burning propulsion system itself and have proposed augmenting the traditional gas turbine with electrical propulsion components to increase the efficiency of the system and supplement the fossil fuel burning gas turbines with electric power[4].

Table 1: NASA's Technology Goals for Future Subsonic Vehicles v2016.1[3]

Technology Benefits	Technology Generations (Technology Readiness Level = 5-6)		
	Near Term 2015-2025	Mid Term 2025-2035	Far Term Beyond 2035
Noise (cum below Stage 4)	22-32 dB	32-42 dB	42-52 dB
LTO NOx Emissions (below CAEP 6)	70-75%	80%	> 80%
Cruise NOx Emissions (rel. to 2005 best in class)	65-70%	80%	> 80%
Aircraft Fuel/Energy Consumption (rel. to 2005 best in class)	40-50%	50-60%	60-80%

Several different architectures have been proposed which use electrical components to augment the traditional gas turbine. These can be broadly characterized as Hybrid Electric systems, in which batteries are used as energy sources or energy storage elements, and Turboelectric systems, in which electrical components are used for power transmission but not significant storage[5, 6]. The two primary families of hybrid electric propulsion systems are the Series Hybrid, in which all thrust is produced using electric motors powered by batteries and gas turbine driven generators, and the Parallel Hybrid, in which gas burning engines producing thrust are augmented with electric power coming from batteries[7]. Both of these architectures have been proposed for use in air transports. Well studied examples are the parallel hybrid Boeing SUGAR Volt, the series hybrid NASA N3-X[8], and the EADS/Rolls-Royce eConcept which shows a compromise position--a series-parallel hybrid in which the generator produces thrust and is augmented by batteries[9, 10]. Similar architectures have been used for non-aerospace applications for years. Examples are series hybrid diesel-electric locomotives, parallel hybrid diesel-electric submarines and series/parallel hybrid cars such as the GM Chevrolet Volt[11]. However, only recent and anticipated advances in power and energy density have made electric power systems light enough to contemplate their use in civil air transports[12].

These and other aircraft concepts are being developed to see how they compare as future air transports in the Far Term timeframe. Conceptual design processes such as Schutte et al.'s Environmental Design Space[13] size aircraft based on each architecture to perform missions of various ranges and payloads. These processes evaluate the aircraft performance over these missions in comparison to performance of other architectures and concepts. In the process the mission fuel burn over on-design missions and off-design

2

missions is evaluated through simulation of said missions. This is straightforward until aircraft with multiple energy sources are evaluated. These aircraft with multiple energy sources include hybrid electric vehicles.

For conventional aircraft, there is only one engine command which can produce the required thrust; however hybrid aircraft have a continuous range of power settings in which the sum of the electric and gas turbine systems produce the same thrust setting[14]. The decision on when to use battery and when to use fuel can alter the fuel burn of the mission. This is due to changes in vehicle weight over the mission, which change the thrust requirement, and changes in engine efficiency from hybrid power, which are a function of the thrust. The problem is further complicated by the limited amount of battery energy available before the battery is depleted. Without an optimal power schedule, the hybrid electric concepts are at a disadvantage against other Far Term concepts whose fuel burn is better understood.

Hybrid electric cars have addressed this problem with myriad control schemes, from hard coded rules to Stochastic Dynamic Programming[15]. Strategies which are optimized for the mission type at hand perform well; for example, the default behavior on the Chevrolet Volt, using battery only until it is depleted[16], works well for short trips in city driving. This strategy is not as effective over longer trips, where other strategies can result in fuel savings of 10% over certain distances[17]. Different optimization techniques have been used to find these strategies, and can be adapted to find the optimal power split for hybrid aircraft.

In order to choose the proper power scheduling method for a particular hybrid electric aircraft, a systematic procedure is required to evaluate different methods and

select the most appropriate one. In some cases the ideal schedule may be simple, while in others a computationally intensive method may be required to find the minimum fuel burn. In some cases the savings from the ideal schedule may be small enough that using a lower performing schedule may be justified by the increase in computation speed. The threshold where this switchover occurs will also vary based on the confidence in the precision of the model, the current stage of design and the number of ideal scenarios required for the related analysis.

This thesis sets out to define a methodology for determining the optimal operational schedules of hybrid electric architectures. This methodology should be capable of determining the optimal electric power schedule to be used for a given hybrid electric architecture, depending on the available computational resources and the fidelity of the available models. This should enable evaluation of hybrid electric architectures while taking their optimized performance into account and to better reflect how these architectures will be used in the Far Term timeframe.

Introduction : The Far Term Efficiency Goals

Motivation: Hybrid Power Scheduling Problem

Purpose: Develop a Methodology for the Determination of Optimal
Operational Schedules for Hybrid Architectures

Chapter 2: Background Information

Definitions: Different Kinds of Hybrids

Example Hybrid Concepts:
SUGAR Volt, STARC-ABL, N3-X , eConcept , etc.

Energy Management In Hybrid Concepts

Chapter 3: Methodology Formulation

Statement of Purpose: To Develop a Methodology for the Determination
of Optimal Operational Schedules of Hybrid Electric Architectures

Research Questions and Hypotheses #1-#5

Proposed Methodology:
Systematic Hybrid Aircraft Power Schedule Optimizer: SHAPSO

Experimental Plan

Chapter 4: Framework for Hybrid Electric Aircraft Power Schedule Testing

Example Hybrid Electric Concept

Optimization Problem Definition

Modeling the Hybrid Electric Architecture

> Modeling Assumptions
>
> Modeling of Electric Components
>
> Modeling of Hybrid Engines
>
> Modeling of Airframe
>
> Mission Modeling

Chapter 5: Implementation and Results of Experiments

Experimental Setup

Experiment #1: Constant Speed Cruise Segment

Experiment #2: Application to Entire Mission

Experiment #3: Application to Battery Sizing Trade Study

Revisiting the Research Questions

Chapter 6: Conclusions and Future Work

Summary of Experimental Results and Changes to SHAPSO

Potential Improvements to the Methodology

Contributions

Future Work

Figure 1: Thesis Outline

5

The outline of this thesis is shown in Figure 1. As shown in the figure, Chapter 2 will discuss future hybrid electric aircraft concepts and the problem of finding the optimal power schedules for each. It will include a discussion of power schedule control in previous simulations. Chapter 3 will address the purpose of this thesis, identify and attempt to answer research questions pertaining to the purpose, and propose a methodology and an experimental plan to settle the research questions. Chapter 4 will discuss in detail the modeling of the hybrid electric architectures and the different optimization algorithms which are required to complete the experiments. Chapter 5 will describe the implementation and results of the experiments planned in Chapter 3. Chapter 6 will discuss the results, the factors which determined them and propose any changes to the methodology based on the results. In addition Chapter 6 will discuss the contributions of this thesis and the remaining future work.

CHAPTER 2

BACKGROUND INFORMATION

In order to better understand the problem of hybrid electric power scheduling in aircraft, it is necessary to examine the literature on hybrid aircraft and related problems. It is particularly helpful to have an understanding of the hybrid electric concepts which have been proposed and the degrees of freedom they add to the power control problem. This chapter will discuss several hybrid and turboelectric concepts in detail, demonstrating the diversity of proposed propulsion concepts and revealing the difficulty in modeling them without taking their differences into account.

Definitions of Hybrid Architectures

When discussing the integration of electric power components into the propulsion system of an aircraft, it is important to define the different categories of hybrid and turboelectric power system architectures. This thesis adopts the convention described in Figure 2 below for distinguishing between the different architectures.

Parallel Hybrid:

Battery	Electricity	Motor	Common Shaft/Gearbox	Fan

(Gas Turbine)

Turboelectric:

Gas Turbine	Shaft	Generator	Electricity	Motor	Shaft	Fan

Series/Parallel Hybrid:

Gas Turbine	Shaft	Generator	Electricity	Motor	Shaft	Fan
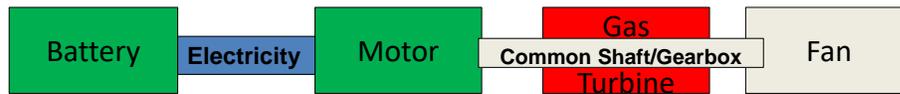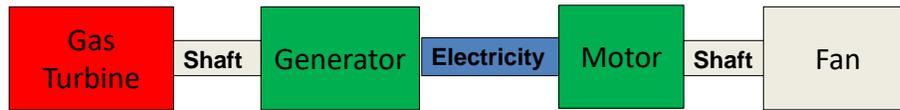
Battery — Electricity
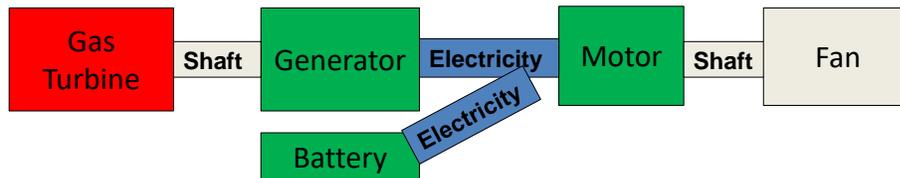
Figure 2: Hybrid Definition Diagram

A parallel hybrid is defined as a vehicle which draws its energy from both a battery and a conventionally fueled engine, with power from the gas turbine and the electric motors both mechanically driving fans. This can be accomplished by driving the same fans through use of common shafts or gearboxes, or by driving independent fans, but there is no intermediate conversion of the mechanical energy from the gas turbine into electrical energy before it is used to drive the fans.

In contrast a turboelectric, also known as a series hybrid propulsion system, does not contain significant energy storage elements, but uses a gas turbine as a source of electric power. This electric power is then used to drive one or more electric fans to produce thrust. An intermediate position exists between the turboelectric and conventional gas turbine architectures in which a gas turbine simultaneously drives a generator as in the turboelectric case and directly drives a propulsive fan. This partially

turboelectric architecture is still not a hybrid because it lacks a battery for electrical energy storage.

The series/parallel hybrid concept is the intermediate position between the parallel hybrid and the turboelectric system. A gas turbine is used to generate electrical energy but a battery is also present to store electric energy, recharged either between missions or in flight by the gas turbine when the power required for thrust is low.

Other configurations can be conceived to interlink these components to produce a propulsion system; however these are representative of the design space. The key distinction to be made is between the hybrid systems and the non-hybrid systems. Under this convention, a configuration is a hybrid only if it possesses a battery for electric energy storage. The problem then becomes determining when this energy storage should be used during a mission.

Hybrid Electric and Turboelectric Aircraft Concepts

Since NASA set the Far Term goals for fuel burn, many different hybrid electric aircraft architectures have been proposed and studied in various levels of detail. Many combine the fuel savings of hybrid technology with other advanced technologies such as truss braced wings or boundary layer ingestion to achieve the Far Term goals. Four different concepts are discussed in detail below as examples of the four primary hybrid architectures: parallel hybrid, partially turboelectric, turboelectric, and series/parallel hybrid.

Boeing SUGAR Volt

Figure 3: Boeing SUGAR Volt [18]

In the Phase I report of the Subsonic Ultra Green Aircraft Research (SUGAR) project, Boeing established current gen and Far Term baselines before evaluating several approaches to the Far Term goals[19]. Among the concepts explored in detail was the SUGAR Volt, a high wing regional aircraft with several propulsion system options. These options included a totally battery powered system, a fuel cell/Brayton cycle hybrid system and a battery/Brayton cycle hybrid system developed in partnership with GE and called the hFan[20]. The fuel cell and pure battery options were shown to be unfeasible with the projected power densities and efficiencies of the Far Term timeframe; however, the hFan proved promising enough for further study.

This hFan became the archetypical hybrid electric turbofan engine, consisting of a gas turbine engine augmented by adding an electric motor to the fan shaft, as shown in Figure 4 below. This depicts a traditional turbofan engine, with a number of technology improvements from the Far Term era added and called out, including the hybrid motor shown mounted inside the tail cone, taking advantage of the empty space aft of the turbine. There is variation in where on the fan shaft the motor is mounted, from its termination at the tail cone as in the original drawing in Figure 4, to between the compressor and the fan[21], to a ring motor mounted on the tips of the fan and the nacelle[22].
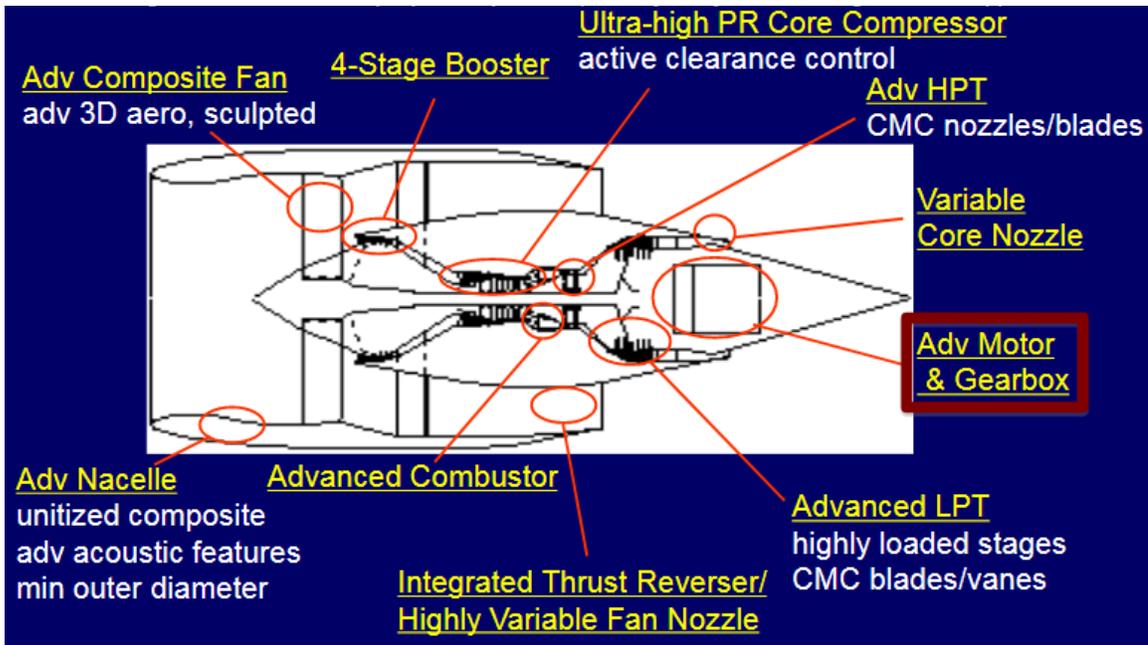
Figure 4: GE "hfan" from Boeing Far Term Study[23]

After borrowing a drag polar from the SUGAR High concept, Boeing explored the tradeoffs inherent to hybrids, in particular the benefits of flying at Maximum Takeoff

Gross Weight (TOGW) at all but the shortest missions. As shown in Figure 5 they investigated using any excess lifting capacity to carry more batteries. For this reason, they analyzed increasing the Maximum TOGW (MTOW) of the aircraft, increasing the wing area and structural weight, in order to allow more batteries to be carried and increase the potential fuel savings. This strategy is opposite the ordinary trend of reducing weight whenever possible, but was found to provide 10% fuel savings due to the additional battery energy[19].
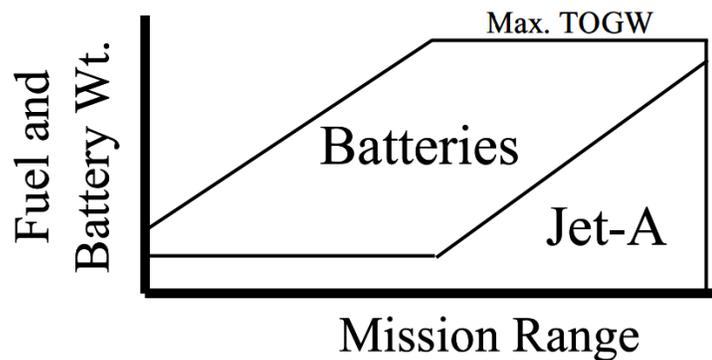
Figure 5: Battery and Fuel Weight Vs. Range[19]

The variable proportions of battery weight to fuel (Jet-A) seen in Figure 5 show that the proportion of electric power to gas power is not constant with range. In fact the Boeing SUGAR Phase I report discusses differing uses of battery vs. jet fuel over the flight envelope, with longer range missions only using electric power for takeoff assist. An additional requirement for use at smaller airports is also discussed as a factor when choosing the amount of battery to load. This is because using battery for takeoff assist only minimizes takeoff weight while increasing takeoff thrust. As such the system would

have capability to independently select power levels to be used during takeoff, climb, and cruise depending on the length of the mission and the weight/takeoff budget available[19].

The SUGAR Phase II part 2 report[18] contains further refinements of the SUGAR volt design, exploring motor powers up to 8,000 HP. At this level the airplane could fly in cruise without using the gas turbine at all. This enables a "core shutdown" mission profile where the gas turbine is fully shut off partway through cruise and left off for the rest of the mission. In order to carry enough batteries to power an 8,000 HP motor, the core shutdown capable concept had its MTOW increased to 190,000 lbs. This was compared to the 150,000 lb. weight for the 1380 HP power assist baseline. The 8,000 HP motor achieved 10% fuel savings due to the increase in battery energy carried. The SUGAR Phase II part 2 report also considered regenerating electric power during descent to recharge the battery and increase the descent angle. This strategy was dismissed by the realization that any energy recovered could be reduced more simply by gliding at a shallower angle toward the airport.

Since the SUGAR Volt was proposed, it has been used as a prototypical design in works considering hybrid aircraft. Jagannath et al. [24] computed the performance of a similar parallel hybrid aircraft using a modified Breguet range equation set, assuming fixed levels of hybrid power during different segments of the aircraft's mission. Similarly, Singh et al. used a similar propulsion system to the SUGAR Volt as his example when developing a hybrid system to minimize cost at current energy prices [25]. The SUGAR Volt is easy to use as a standard due to the abundant data provided about its airframe and propulsion systems in the SUGAR reports[18, 19].

Other engine manufacturers have also proposed engines and corresponding vehicles along the same lines as the hFan and the SUGAR volt. UTRC's Parallel Hybrid Geared Turbofan has the same general architecture as the SUGAR Volt. It exploits the hybrid power by shrinking the gas turbine core to make it ideal for cruising thrust while requiring electric power to provide the climb thrust[26]. Rolls-Royce's Electrically Variable Engine is more similar to the hFan. It is sized to handle the entire mission without use of batteries but utilizes battery power to reduce fuel burn and overall emissions[27]. An X-plane concept has also been proposed, constructed out of a heavily modified DC-9 with a truss braced wing and hybrid engines added[28].

STARC-ABL

Figure 6: STARC-ABL Concept Aircraft[29]

A different application of electrical propulsion to a conventional airframe is the STARC-ABL concept proposed by Welstead et al. in 2016[30]. This concept, seen in

Figure 6, consists of a conventional fuselage with engines similar to the hFan used by the SUGAR Volt. However, instead of battery power being added to the fan as in the SUGAR Volt, electrical power is extracted from both engines and used to power a tail cone thruster for Boundary Layer Ingestion (BLI). This thruster is sized and mounted to ingest the boundary layer at the aft end of the fuselage, providing a drag reduction and effectively increasing the bypass ratio[29]. As presented it is a partially turboelectric concept, but with the addition of a battery it could become a series/parallel hybrid[5].

NASA N3-X
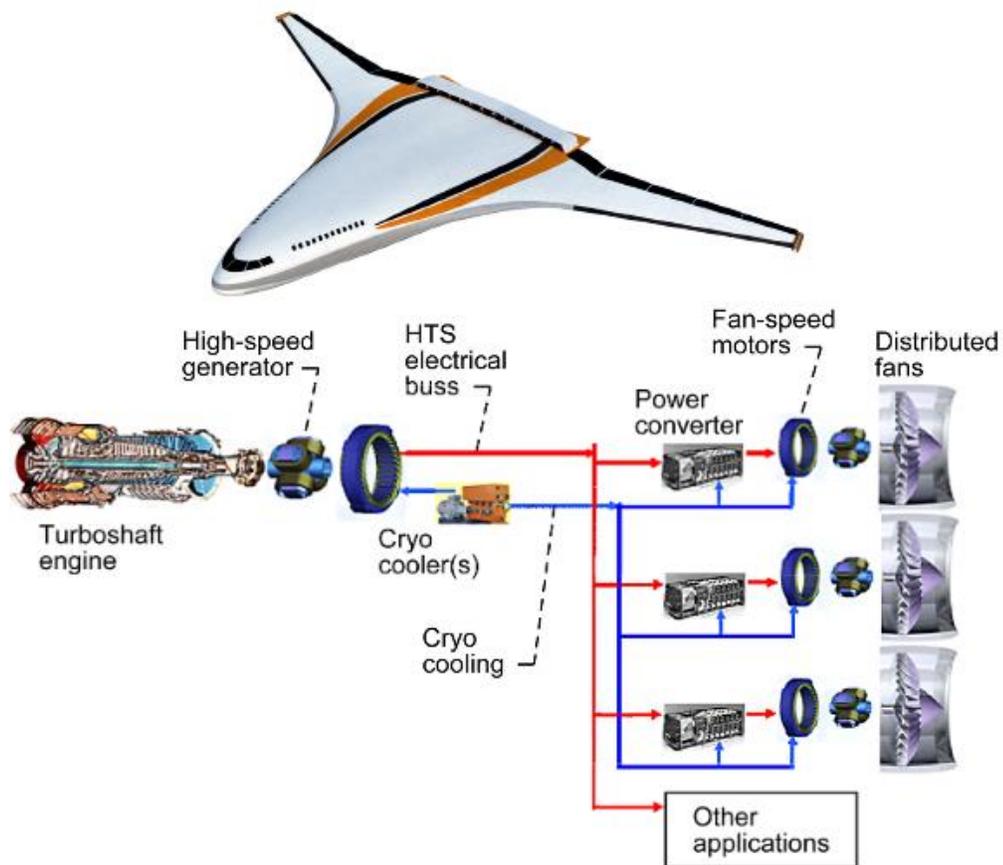
Figure 7: NASA N3-X Concept and Subset of Propulsion System[8, 31]

STARC-ABL was originally proposed as a more conventional turboelectric alternative to the NASA N3-X, which was proposed by Felder et al. in 2009. This vehicle, shown in Figure 7, is a radical shift in aircraft design capable of meeting the CO_2 goals for long range high payload missions. A turboelectric drive consisting of 14 electric fans driven by two wingtip mounted gas turbine generators increases propulsive efficiency by increasing the effective bypass ratio and combines favorably with a hybrid wing body planform with BLI to enable a considerable reduction in TSFC. To overcome the turboelectric efficiency penalty from transforming power from mechanical to electrical and back, High Temperature Superconductors (HTS) are used in the power transmission system and for all motors and generators. HTS operations require a cooling system to maintain superconductivity, so cryogenic fuels (hydrogen and methane) and cryocooling are considered by Felder et al.[8]

Further work has refined the N3-X concept. Brown includes updated weight and efficiency estimates for the hybrid components using state of the art superconductors. He anticipates a complete hybrid powertrain efficiency of 98% and weight under 27,000 lbs. not including the gas turbine and the fans themselves[12]. Armstrong et al. approached the problem of flight reliability by laying out the power system architecture with the redundancy and protection systems necessary to keep a Turbo Electric Distributed Propulsion air transport flying in the event of engine, fan, or power system component failure. Armstrong et al. also explored the DC transmission voltage taking arcing considerations into account and added a small amount of electrical energy storage to handle transient loads[32]. Others have refined the aerodynamics of the concept[33], the

16

mail-slot nacelle[34], the noise and emissions[35], and the overall economic viability of the concept[36].

EADS/Rolls-Royce eConcept

Figure 8: EADS/Rolls-Royce eConcept Vehicle[10]

The eConcept vehicle, seen in Figure 8, is a series/parallel hybrid concept which uses six distributed BLI fans powered by a single turbogenerator and a large energy storage system. The decoupling of the propulsion from the power generation allows the two systems to be sized and operated differently. The turbine is sized for cruise operation and dependent on batteries for supplemental power during takeoff and climb. During cruise and descent the turbine's excess power allows the batteries to be recharged.

Aiming at an entry into service date of 2050, the eConcept assumes superconducting machines and power transmission in addition to lithium air batteries with a specific energy density in excess of 1 kWh/kg [9, 10, 37].

Two different operating assumptions have been proposed for the eConcept's battery usage: either the battery will be recharged on the ground between flights as in the SUGAR Volt[37], or it will be recharged by the gas turbine during cruise and by regenerative braking by the fans during descent[9]. The second method would reduce the infrastructure requirements on the ground by not requiring battery chargers at airports. The choice between these two alternatives could change the sizing of the system and would certainly change the ideal battery usage schedule.

Other Hybrid Concepts

Other hybrid aircraft concepts have been proposed. These range from a smaller turboprop similar to the SUGAR Volt[38], to a nearer term turboelectric distributed concept with a more conventional airframe and either superconducting or non-superconducting electrical systems [39, 40]. In addition, hybrid electric aircraft have been proposed at smaller scales, including general aviation[41] and multiple Unmanned Arial Vehicles (UAVs). In the case of UAV's the hybrid technology often buys its way onto the proposed aircraft for reasons other than efficiency. This would include adding Vertical Takeoff and Landing (VTOL)[42] or adding quiet loiter capability using electric motors and some electric energy storage to aircraft which retain the range provided by their internal combustion engines[43].

The hybrid electric concepts detailed above show the principal features of the design space as well as hybrid electric technology's potential to supplement the energy provided from fuel, increase the effective bypass ratio, and enable drag reductions through BLI. They also demonstrate the different levels of coupling between the hybrid components and the gas turbine components, aerodynamically and electrically, from the tightly coupled SUGAR Volt, where the gas turbine sits behind the electrically augmented fan to the nearly independent eConcept, whose battery enables the electric fans and gas turbine to be controlled separately.

Energy Management in Hybrid Concepts

Analysis of any aircraft with multiple propulsion systems is dependent on assumptions of how the thrust requirement will be distributed between them. For aircraft with a single power source, such as conventional air transports and the N3-X, the most fuel efficient mission is accomplished with the most fuel efficient operation which meets the thrust demand at each instant. For conventional aircraft this is symmetric thrust between all engines. However, the N3-X can maintain straight flight while generating most of its electricity from one engine and idling the other. As long as the inactive engine has to be idling (and cannot be shutdown), the fuel required to keep the idling engine burning keeps this from being more efficient than operating the engines symmetrically except at low altitudes and power settings[44]. In contrast to conventional single power source aircraft, aircraft which have multiple power sources, for example batteries and fuel, which have differing costs and effects on aircraft weight, are no longer necessarily optimized over a mission by an instantaneous optimization.

19

The SUGAR Phase II study evaluated the SUGAR Volt under different power assumptions to arrive at the 7500 HP motor equipped "engine shut down" power schedule alongside 1380 HP and 1750 HP motor equipped alternatives which were operated at maximum power throughout the mission[18]. The studies of the eConcept vehicle took the opposite approach: the gas turbine engine was simulated at full power over the entire mission with the batteries charging or discharging at whatever level was required to meet the thrust requirements. Both of these approaches allow the aircraft to be simulated, however a better use of the batteries was not attempted. In fact the SUGAR Phase II report states that its approach was taken due to time constraints and further optimization was planned [18]. Later studies of a SUGAR Volt type hybrid have used alternative power scheduling methods such as a piecewise linear schedule [45]or a different power for cruise and climb[46], but no single optimal schedule or method for optimizing schedules has been generally accepted for these hybrid aircraft.

This chapter has demonstrated the diversity of hybrid electric and turboelectric aircraft and propulsion system concepts. Each of these systems introduces additional control variables into the propulsion system operation, which must be set in order to simulate the system and determine its performance. For turboelectric systems such as the N3-X or STARC-ABL these variables can be set by instantaneously optimizing for fuel burn, but on hybrid systems the battery constraint limits the total amount of electric energy available during a mission. It is therefore necessary to use power differently depending on the available battery power and mission being flown. Different strategies for using the power during each mission have been proposed, but the industry has not

settled on a proper methodology for selecting a power schedule or schedule optimization

method.

CHAPTER 3

METHODOLOGY FORMULATION

In the previous chapter a representative set of hybrid and turboelectric aircraft were shown to have additional degrees of freedom in their propulsion system control compared to conventional aircraft. The control of these new degrees of freedom for turboelectric aircraft is performed by optimizing the instantaneous fuel burn across the mission. For hybrid aircraft, however, there is a complicating constraint on control caused by the limited electrical energy available from the battery. Due to this constraint the power schedules must be different on every mission depending on the mission requirements and available battery. There is a gap in the literature on what the power schedules should be and what methods should be used to select them. For this reason the purpose of this thesis is as follows:

Statement of Purpose
To Develop a Methodology for the Determination of Optimal Operational Schedules of Hybrid Electric Architectures

This chapter will address a number of research questions and develop hypotheses pertaining to this purpose before proposing a methodology to meet the purpose.

Research Question #1: How Important Is It to Use the Optimal Power Schedule?

Although it is clear that a power schedule must be used which utilizes all the available energy in the battery in order to minimize fuel burn, the impact of using one such schedule rather than another is not as clear. To determine the magnitude of

difference a power schedule can make, plug in hybrid electric cars should be examined as the closest analog system to hybrid aircraft that is currently in widespread service.

Hybrid Car Power Control Schemes

The designers of hybrid electric cars have addressed the problem of power splits and battery energy management in their quest for increased miles per gallon. In recent years over 90% of the hybrid car fleet has adopted a transmission allowing electrical and gas power to be used in any ratio (within power limits) regardless of wheel speed [47]. The primary difference in the power scheduling of hybrid electric cars and hybrid electric aircraft is the stochastic nature of the power demands for automobiles. This is due to unknown terrain, traffic, and even required range from the car's perspective when the journey begins. To deal with this, the Voltec system used by the Chevrolet Volt and shown in Figure 9 below, includes three clutches enabling the system to operate in four different modes during forward propulsion: one-motor all electric, two-motor all electric, series hybrid, and a parallel hybrid mode which uses the hybrid system as a continuously variable transmission.
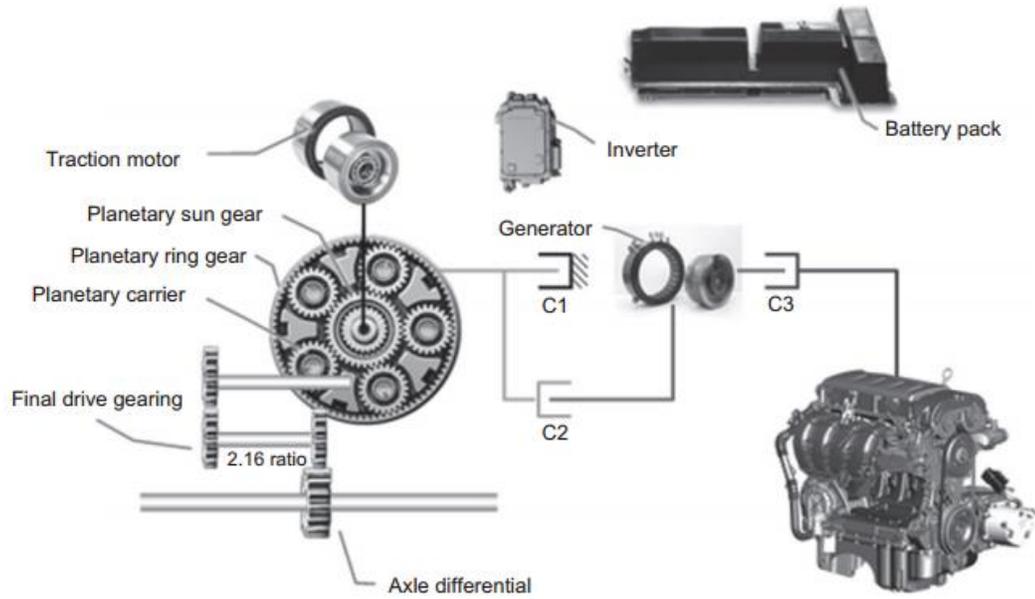
Figure 9: Voltec Electric Drive System from Chevrolet Volt [11]

The Voltec system switches between the four modes based on the current location of the system on one of two torque/speed maps shown in Figure 10 below[11]. The map on the left is all electric while the one on the right is hybrid.
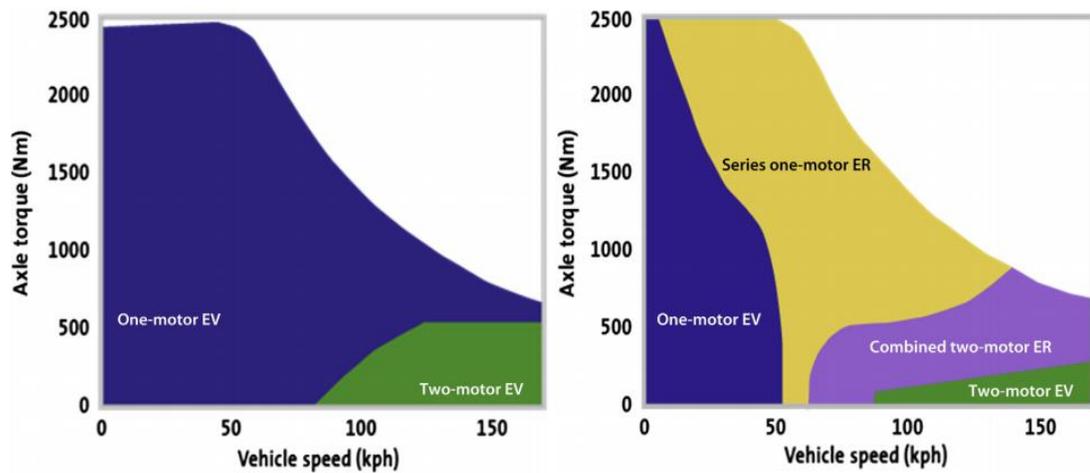
Figure 10: Propulsion Mode Maps for Chevy Volt[11]

The Chevrolet Volt switches between these two maps depending on the state of charge of the battery-if the battery is above the sustain level the system will stay on the all-electric map on the left, otherwise it will switch to the second map on the right. The driver can only set the current torque requirement with the throttle pedal and has the ability to raise the sustain level to ensure sufficient torque for mountain driving and to force a switch to the second map to preserve electricity for later[11].

This system of rules is called the Charge Depleting Charge Sustaining (CDCS) strategy, and it results in the car using its batteries for the first 40 miles or so and using fuel for the rest of the journey. This is fine for typical use, as a range of 40 miles a day means that the gas engine will rarely be turned on by a typical commuter. This has led to plug in hybrids such as the Volt also being known as Extended Range Electric Vehicles[48]. However for long journeys the CDCS strategy is not the best use of the battery pack. Tribioli et al. demonstrated an alternative battery usage strategy which spreads the battery over the first 110 miles before dropping to an all fuel mode. This strategy consumes 20% less fuel over that distance than the CDCS method used by Chevrolet[17].

The fuel burn minimization problem for hybrid cars can be formally stated as in Equation 1[49]:

$$Minimize \ M_f = \int_{T_{start}}^{T_{end}} \dot{m}_f(t)dt \tag{1}$$

Where M_f is the total mission fuel burn and $\dot{m}_f$ is the instantaneous fuel burn. The instantaneous fuel burn is the nonlinear function of the power demand and the applied electric power seen in Equation 2 below.

$$\dot{m}_f(t) = f_{engine}\big(P_r(t), P_e(t)\big) \tag{2}$$

The electric power, P_e, is the free input controlled to minimize M_f. P_e may be positive or negative, but is subject to constraints on its magnitude and on the electric energy storage E_s seen in Equations 3 thru 6 below. $f_{storage}$ includes efficiency losses in the storage and power transmission systems, which will change when the system is recharging

$$P_{e,min} \leq P_e(t) \leq P_{e,max} \tag{3}$$

$$E_s(t) = E_{s,start} - \int_{T_{start}}^{t} f_{storage}\big(P_e(\tau)\big)d\tau \tag{4}$$

$$E_s(T_{start}) = E_{s,start} \, , \; E_s(T_{end}) = E_{s,end} \tag{5}$$

$$E_{s,min} \leq E_s(t) \leq E_{s,max} \tag{6}$$

This framework can capture plug in hybrids as well as hybrids in which the electric energy is all ultimately derived in fuel through the $E_{s,start}$ and $E_{s,end}$ parameters. These are assumed to be equal in the non-plugin case but are often equal to $E_{s,max}$ and $E_{s,min}$ in the plugin case.

Unlike most other parameters in the equation, the required power is not known ahead of time, requiring solutions which can be computed as the car moves along. Numerous test cycles have been used for testing proposed power split algorithms, such as the Japanese Drive Cycle[49], the FUDS cycle for urban driving [47], and the New European Driving Cycle[50] shown in Figure 11 as a velocity profile. This figure shows the unpredictable patterns of braking and acceleration experienced by an automobile. Strategies employed to solve this required power problem include Model Predictive

26

Control, Dynamic Programming, and Optimal Control. These are then often used to find

a rule based strategy to quickly implement power changes in cars on the road [49, 51].
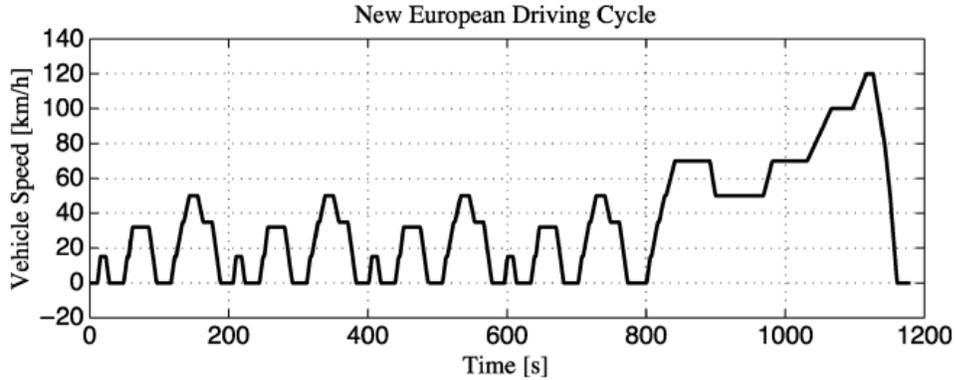
Figure 11: New European Driving Cycle[50]

Model Predictive Control

Model predictive control has been used to reduce the scale of the fuel burn

minimization problem stated previously in Equation 1 by only considering a short amount

of time in the future. This results in a formulation of the problem seen in Equation 7

below, adapted from Borhan et al.[52]

$$Minimize\ J = \int_{t}^{t+\Delta t} \left(k_f \dot{w}_f(\tau) + k_e P_e(\tau) \right) d\tau \tag{7}$$

In this equation k_f and k_e are weighting factors for fuel and stored electric energy,

respectively. The other equations are as before, except that the final state of the battery is

not known. The penalty factors weighting battery use along with fuel use are included to

compensate for this lack of knowledge. It can be observed that this problem collapses to

instantaneous optimization if Δt is taken small enough. If Δt is large enough it will have

to solve the entire mission in advance. These equations are implemented in practice as summations over discrete time steps.[52]

To handle the unknown future demands of the driver, Ripaccioli et al.[53] used Markov chains to predict the most likely power requirements for the system. The Markov chains were derived from previous driving data such as standard driving cycles, and provide a probability that the next power demand will have one of a set of possible predetermined values. This enabled a 13% improvement in fuel burn when compared to a system expecting the current power demand to continue indefinitely. However a prescient system which knew the certain power demands in advance achieved a 29% fuel burn improvement in the same study [53].

Hybrid Aircraft Considerations

The hybrid electric aircraft control problem has some key differences from the hybrid electric car control problem. As previously mentioned, commercial air transports such as the SUGAR Volt are not subjected to unpredictable patterns of braking and accelerations such as those modeled by the New European Driving Cycle. Instead flights are planned before takeoff, with optimized trajectories within the constraints given by air traffic control and the current weather conditions. Although some of these constraints have random or unknown components, the problem can be considered as less stochastic than the car control problem, and during early design phases considered as nonrandom.

The aircraft mission typically consists of a single takeoff, climb, cruise, descent, and landing and does not have the many starts and stops of a car mission. Although some energy could be recovered during landing[54], regenerative braking on aircraft is not the

great energy source it is for automobiles and other land based hybrids[55]. However, there is one source of load variation that is unique to aircraft: a significant change in the mass of the vehicle as fuel is burned.

According to the Phase I report[19] the Boeing SUGAR Volt has a fuel capacity of 5,250 gallons of jet fuel. This amount of fuel weighs over 34500 lbs. which is over 20% of the 154,900 lb. max weight of the aircraft. For comparison, the 2018 Chevrolet Volt has a fuel capacity of 8.9 gallons of gasoline, less than 2% of its 3543 lb. curb weight[56]. During a flight mission, whenever fuel is burned the aircraft weight decreases, but when electricity is used the battery maintains its weight. This weight change affects not only the amount of energy required to climb but also the amount of induced drag encountered by the aircraft during cruise. For a hybrid aircraft, this means that the total fuel burn should be less when using a power schedule which favors jet fuel at the beginning of the mission and electricity towards the end. This can be illustrated using the following notional charts:
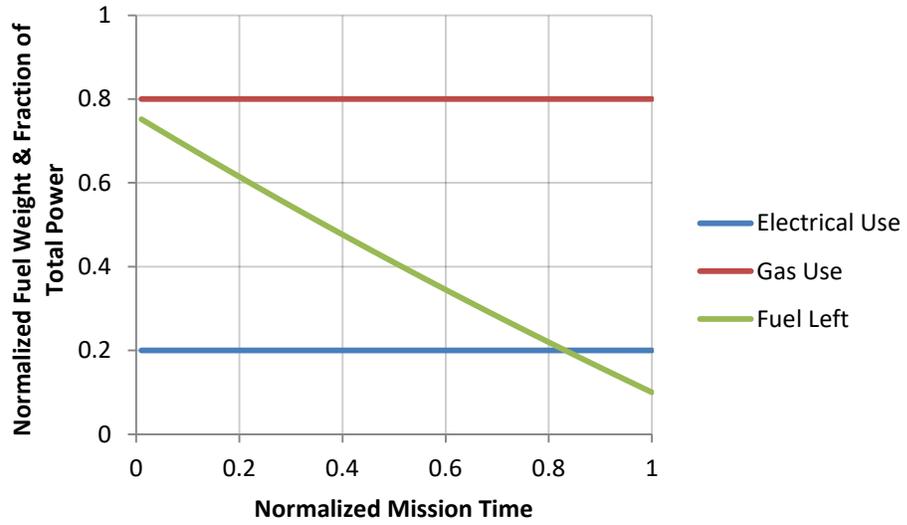
Figure 12: Notional Mission Using Constant Power
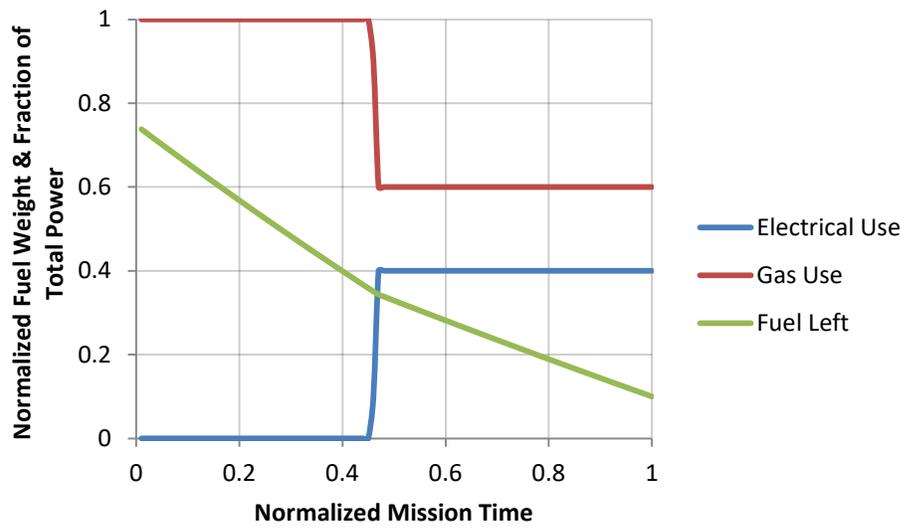
Figure 13: Notional Mission Using Battery at End
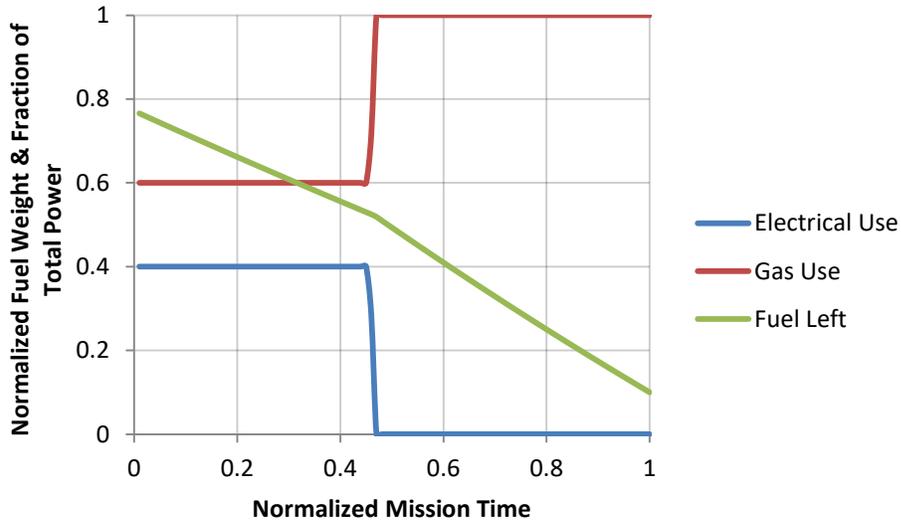
Figure 14: Notional Mission Using Battery at Start

In Figure 12 thru Figure 14 three different power schedules are shown for a notional system flying a constant cruise with a constant specific fuel consumption (SFC) and electrical efficiency. In Figure 12 the electrical power provides a constant fraction of the thrust throughout the mission, but in Figure 13 the battery is used at twice the power level for the second half of the mission, and not at all for the first half. In Figure 14 the battery is instead used at the beginning. In the latter two cases the transition from battery to none was adjusted to cause the same amount of battery energy to be used in all three cases. The bend in the fuel weight histories when the power system changes modes can be clearly seen in the figures, and although they all have the same amount of fuel at the end of the mission, the system that uses the battery at the beginning (Figure 14) uses 2% more fuel in total than the constant power system (Figure 12), and the system that uses the battery at the end (Figure 13) uses 2% less than the constant system (Figure 12). This effect is reflected in their different initial fuel levels.

31

This notional example employs a heavily abstracted hybrid; however it illustrates a potential effect which can drive the selection of an optimal power schedule. That effect is the change in weight from burning fuel earlier rather than later. Based on this example and anticipating some fraction of the 20% savings seen in hybrid cars from improving the power schedule, Hypothesis #1 was proposed:

Hypothesis #1

The use of optimal power schedules over a typical aircraft mission will yield significant savings in fuel burn.

Research Question #2: What Factors Determine the Optimal Power Schedule?

In the previous section the reduction in vehicle weight from burning fuel earlier rather than later was identified as a factor that determines the relative performance of different power schedules. However, this notional example is very simple and does not include all the factors which may affect the optimal power schedule. These factors can be identified by considering the nature of the hybrid propulsion system and the missions in which it is used.

Factors Inherent to the Vehicle and Propulsion System

The hybrid electric powertrain endeavors to displace fuel by applying a finite amount of electrical energy. The efficiency of the hybrid system in delivering this energy to the propulsion components limits the amount of fuel that the system can offset. In addition, any variations of that efficiency with power level are factors affecting the optimal power usage schedule.

<u>Electrical System Efficiencies</u>

One variation of efficiency with power level is the discharge efficiency of the battery itself. Under steady load, a lithium ion battery can be modeled as an ideal battery with a series resistance. This resistance causes a loss proportionate to the square of the current drawn from the battery[57]. This loss penalizes use of higher power levels and therefore drives the optimal power schedule towards a constant power draw at the lowest level which uses all of the energy in the battery.

Other resistive losses in the system are found in the power cables between the battery and the motor and in the windings of the propulsion motors. However, unlike the losses in the battery, the resistance losses in the power cables can be decreased by using power electronics to increase the transmission voltage. This reduces the amount of current required to transmit the power. Increasing the transmission voltage can also enable a decrease in conductor weight but causes an increase in the required insulation and makes any protection equipment heavier[58]. In proposals which include superconducting technology, the cables and motors can have their DC resistive losses eliminated entirely at the cost of the added weight of thermal insulation and the cooling weight and energy consumption of the cooling system for the superconductors[12].

The power electronics used to increase and regulate the DC voltage for power transmission from the batteries as well as the inverters used to drive the electric motors are other sources of power loss. These power electronic devices have efficiency maps which show a significant drop in efficiency at partial power levels[59]. These losses can be avoided by using a modular design, in which the power conversion is performed by a number of smaller modules acting in parallel. One possible design is shown below in

Figure 15. This design allows some modules to be deactivated at lower power levels while the remaining modules operate at peak efficiency[60].
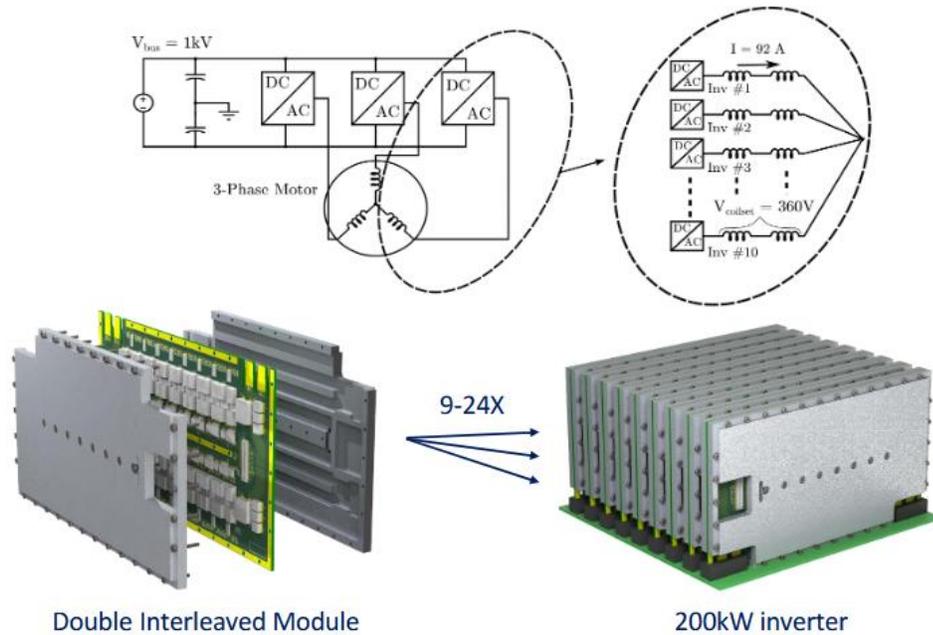
Figure 15: Scalable Inverter Module from UIUC[60]

The motor itself has losses including the resistance loss mentioned previously as well as windage loss, backiron loss, and bearing losses[61]. Unlike the resistance loss, these other losses are not a function of the motor power for most motor types. Instead these losses are a function of the motor speed and the amount of aerodynamic, electrodynamic and mechanical friction that must be overcome to turn at that speed. The losses are therefore more of a function of the mechanical coupling of the electric motor to the propulsion system rather than the power of the motor.

Impact of Hybrid Components on Propulsion System

The hybrid aircraft concepts discussed in Chapter 2 display some variety in coupling electric power into the propulsion system. The more turboelectric concepts such as the eConcept use electric fans to provide most of the thrust whether the gas turbines or the batteries are supplying the power. These systems' battery power schedules are therefore only affected by the battery resistance and the drop in efficiency of the gas turbine at lower power levels. The gas turbine's drop in efficiency at lower power levels is significant at altitude if the assumption is made that the gas turbine is not shut down[44].

Hybrids which have an electric motor mounted on the shaft of an otherwise conventional turbofan have a much tighter coupling between the gas turbine and the hybrid components. That is because they are directly connected mechanically and share a common aerodynamic flow. When the gas turbine is idled back as the electrical power provides a fraction of the thrust, an operability bleed may be required between the low pressure compressor and the high pressure compressor. The low pressure compressor is coupled to the motor and is spinning at a high power level, but the high pressure compressor is not mechanically coupled to the motor and is spinning at a low power level due to the reduced fuel flow. The operability bleed leaks a fraction of the core flow of air into the bypass stream in order to reduce flow through the core and protect the low pressure compressor from stalling [62]. The impact that this has on the efficiency of the gas turbine as a whole when changes are made in hybrid power could drive the optimal power usage schedule.

Factors Inherent to the Mission

The mission of an aircraft could be considered as a schedule of flight conditions and thrust requirements that the propulsion system has to handle and provide. It would not be surprising if these schedules had an effect on the optimal hybrid power usage schedule. The change in flight conditions also has a great impact on the performance of a gas turbine and was the deciding factor in the optimal setting of the turboelectric N3-X concept[44]. The effect of the changing flight conditions can be confounded with the changing thrust requirements since a typical mission consists of a single climb and descent, conducted at full and idle power respectively, with an intermediate power setting only seeing significant use in the cruise segment, at a high altitude and Mach number.

As mentioned in chapter 2, some hybrids have their power schedules fixed by this change between climb and cruise, as the gas turbine is sized too small to be able to provide the required climb thrust without the hybrid[26]. Aircraft without this constraint may still have their optimal power schedule driven by the changes in gas turbine efficiency and the acceptance of hybrid power as the thrust and flight conditions change. The weight change from burning fuel discussed earlier can compound with this effect as well, since reducing the vehicle weight lessens the amount of time spent in climb and reduces the required thrust during cruise.

Examining this research question has identified several potential factors that could determine the optimal hybrid power schedule for aircraft, including battery resistance and the mission requirements. The dependence of these factors on the specific architecture and sizing philosophy was also examined. Due to the large fuel fraction of aircraft weight compared to cars, the effect of burning fuel early to save weight seems to be the most

significant of these effects for parallel hybrids unconstrained by a sized down core. For this reason Hypothesis #2 was made as follows.

Hypothesis #2

The reduction in aircraft weight resulting from burning fuel early in a mission is the dominant factor determining the optimal power usage schedule.

Research Question #3: What is the Appropriate Baseline Schedule?

For any particular mission the power schedule can have any conceivable shape. The power schedule is constrained only by the maximum hybrid power the system can provide, the minimum power required by the system to meet the thrust requirements if any, the maximum amount of charging the system can accept and the total size of the battery, which effectively limits the integral of the power schedule to the available energy. In the absence of a known optimum scheduler or an optimization method, the shape of the power schedule can still be selected based on some understanding of the problem in an attempt to minimize the fuel burn of the system.

Each study of a hybrid electric aircraft has had to make some assumption about the power schedule in order to perform its analysis. The Boeing SUGAR studies have assumed a constant power use throughout climb and cruise for their primary designs but have also examined saving the power until the end of the mission, shutting down the gas turbine entirely and flying the last part of the mission using an 8,000 HP motor in their "core shutdown" case[18]. Other studies have adopted a piecewise linear schedule, defined by power levels at the beginning and end of climb and cruise. After finding the global optimum of this four variable scheme, these studies devised a pattern to follow,

37

allowing the schedule to be set with a single variable to keep their variable count down[45]. Another scheme that has been used is to set the climb power to maximum and the cruise power to the constant value which zeros out the battery[46].

The choice of a baseline schedule comes down to the answer to Research Question #2. If the dominant effect on the power schedule is the battery resistance, the baseline should be a constant power schedule. If the difference between climb and cruise is dominant, the baseline should be to use electric power at one level during climb and one level during cruise, likely at full power during climb. Hypothesis #2 states that the dominant factor will be the change in weight from burning fuel earlier rather than later, therefore Hypothesis #3 must be as follows.

Hypothesis #3

The best baseline hybrid power schedule is to use the battery power as late in the mission as possible.

Research Question #4: What Methods Can Be Used to Find Better Hybrid Power Schedules?

The multiple potential driving factors in determining the ideal hybrid schedule are unlikely to cause the optimum to be one of the baseline schedules. In addition, just looking at the baseline schedules will never reveal how far the performance of the best of them is from the performance of the global optimum. Considering the entire power schedule space using a full factorial examination of all possible schedules is not very feasible. The number of potential schedules is

$$N_{timesteps}{}^{N_{PowerLevels}}$$

(8)

before the battery energy constraint is applied. Even with the constraint applied, for any reasonably high resolution this is infeasible.

Dynamic Programming

Various authors have addressed the determination of the ideal power schedule when modeling hybrid aircraft. Bradley et al. [63] used a Dynamic Programming algorithm for their hybrid UAV modeling to decide when to use the battery to maximize endurance. Originally proposed in 1952 by Richard Bellman to tackle the time to climb problem[64], Dynamic Programming is based on Bellman's Principle of Optimality, which states "An optimal policy has the property that, whatever the initial state and initial decision are, the remaining decisions must constitute an optimal policy with regard to the state resulting from the first decision."[65]. Stated more plainly, this means that the path from any point on the optimal path to the end state must also be optimal.

Bradley e. al.'s implemented of Dynamic Programming by to discretizing the mission space into time steps and possible states of charge, then considering the possible ways to go from one charge state to another during one time step. This leads to an intractably large set of paths, especially when the mission is broken up into 10,000 time steps with 20,000 possible states of charge. However if an algorithm starts from the end of the mission where the final state is known (no fuel, empty battery), and works backwards, then at each time step the ideal method from getting from each state of charge to the end can be found and all other paths from that state of charge can be discarded.

This reduces the number of steps to be evaluated from 20,000^10,000 to 10,000*20,000^2[63]. Dynamic Programming has also been applied to the car power management problem by authors including Lin et al.[51], Musardo et al.[66], and Kolmonovski et al.[67].

Operation of Dynamic Programming for Hybrid Power Schedule Optimization

The application of Dynamic Programming to the hybrid power scheduling problem can best be explained by demonstrating the first few steps of its implementation. First the mission is divided into time steps such as the segments discussed above, and at the beginning of each segment the aircraft battery can only have specific values of State of Charge (SOC). This is as seen in the notional Figure 16.
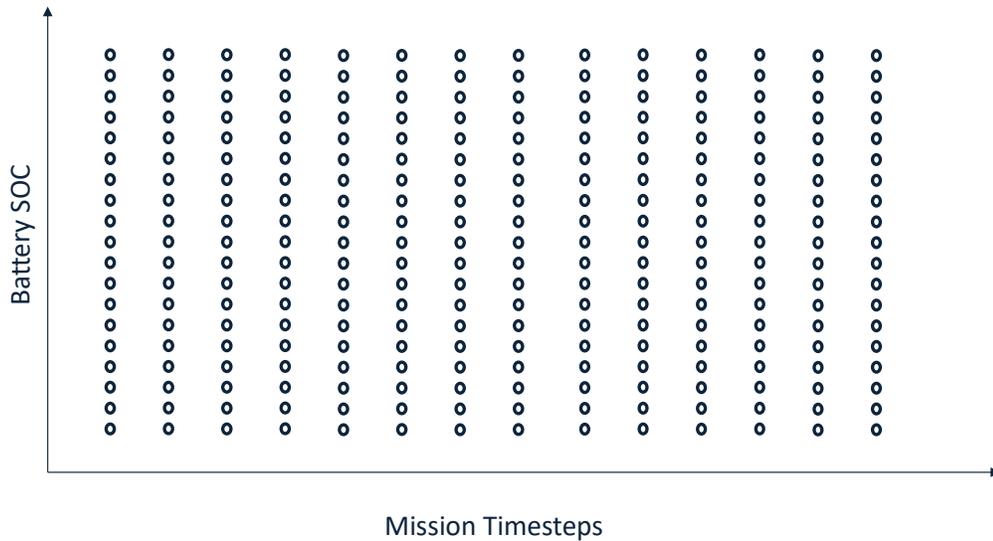
Figure 16: Discretization of Mission and State of Charge for Dynamic Programming

The algorithm begins at the last time step, n, in which the required P_e to go to the known final state from each possible battery state in time step n-1 is computed along with the corresponding fuel burn as shown in Figure 17. This gives the minimum fuel, M_{fi}, which must still be in the aircraft at each of these states, which allows the corresponding aircraft weight to be computed as well.
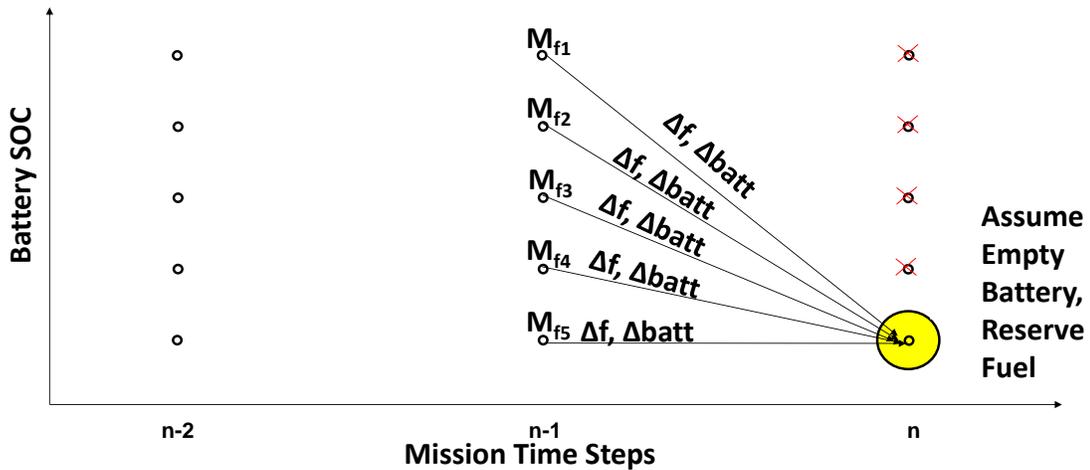
Figure 17: Last Three Time Steps in Dynamic Programming

As the process continues to the time n-2 there are many different paths to the final state at step n for each n-2 state, each of which is computed as shown in Figure 18. One of these paths will have a minimum fuel burn, and the others can be discarded, as the global optimum path will be locally optimal according to Bellman's principle of optimality.

$$M_f = min(M_{f1}+\Delta f1, M_{f2}+\Delta f2, M_{f3}+\Delta f3, M_{f4}+\Delta f4, M_{f5}+\Delta f5) = M_{f3}+\Delta f3$$
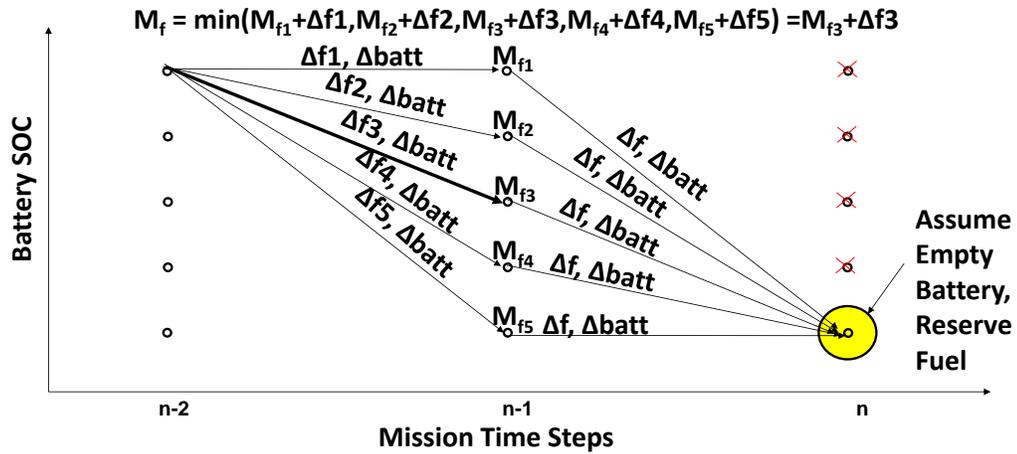
Figure 18: Optimal Path from Charge State 1, Time Step n-2, to End

This process is repeated for each state of charge at time step n-2, and the majority of paths from time step n-2 to the end are eliminated leaving only those shown in Figure 19. Each state must only remember the minimum fuel to get to the end and the path that corresponds to it. This process can then be repeated until the starting state of charge at the starting time step is reached, at which point the minimum fuel burn and corresponding strategy will be known.
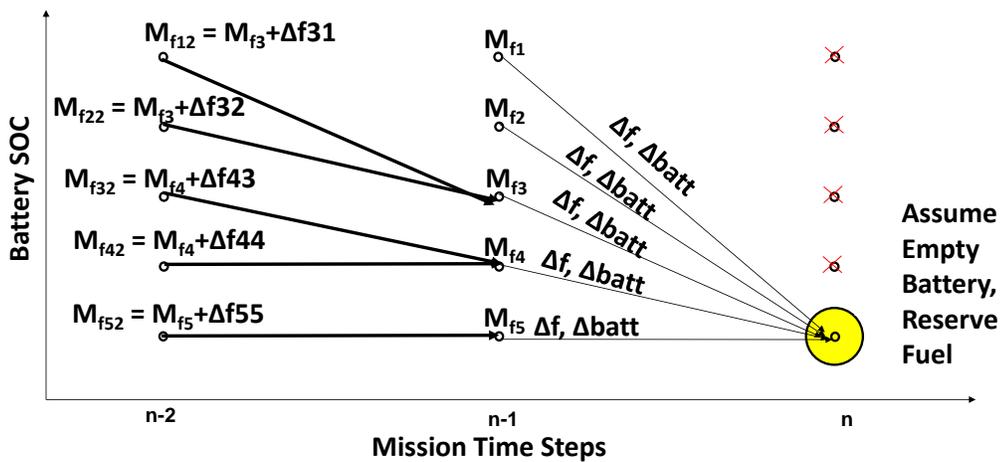
Figure 19: Best Paths for Last Two Time Steps

42

<u>Drawbacks of Dynamic Programming</u>

In a survey paper, Perullo et al.[68] examined different potential approaches to the hybrid power scheduling problem, including Dynamic Programming, which he dismissed as being too slow for use with higher fidelity tools. Lin et al.[51], Musardo et al.[66], and Kolmonovski et al.[67], applied Dynamic Programming to hybrid cars and also noted that Dynamic Programming is not capable of real time operation because of its requirement for complete knowledge of the power demand. They used it either to find the power schedule with the minimum possible fuel burn for a vehicle or to tune a set of rules for use in real time. Kolmonovski went further and noted that the actual power demands of real road vehicles cannot be known in advance, and require Markov chain based Stochastic Dynamic Programming. Another alternative method was demonstrated by Miyazawa et al.[69], who, while optimizing the trajectory in space of aircraft at constant airspeed, used Dynamic Programming iteratively on a subset of the space centered on a candidate solution until the solution could not be improved. These modifications improved the computation time of Dynamic Programming but lost the guarantee of finding the global optimum promised by the optimality principle.

Optimal Control

Because other authors have found Dynamic Programming to be too time consuming they have only used it to check their answers developed using Optimal Control[17]. Optimal Control theory focuses on finding a continuous solution to an optimization problem, as opposed to Dynamic Programming's discretization. This continuous solution is found by application of Pontryagin's Minimum Principle which

establishes necessary conditions for control inputs to be optimal[70]. In particular the Hamiltonian must be minimized by the control inputs at all times. For each instant of the hybrid car problem, the Hamiltonian is given in Equation 9 below, where P_e is the control variable, SOC is the State of Charge of the battery, and λ is the costate. [71]

$$H = \dot{w}_f(P_e) + \lambda S\dot{O}C(P_e, SOC) \tag{9}$$

This costate determines the relative cost of electric power compared to fuel, and must be chosen before the P_e which minimizes H can be found. Kim et al. [71] found that if $S\dot{O}C$ is not a function of SOC, which was the case for the Toyota Prius battery when SOC only varies over a small range, λ becomes a constant, chosen to cause the system to meet the desired SOC(T_{end}) value. Having picked the proper value of λ for several standard driving cycles, Kim et al. demonstrated performance that nearly equaled Dynamic Programming which he used to find the true optimum. [71]

Building on the success of this method, other authors have attacked the problem by looking at the energy stored in the batteries of non-plugin hybrids as though it was equivalent to an additional fuel tank[72, 73]. Sciaretta et al. in particular minimizes a metric J given by Equation 10 below, where ΔE_f is the fuel energy in one time step, ΔE_e is the electrical energy over the one time step, and s(t) is an equivalence function which determines the relative cost of electricity and fuel.

$$J = \Delta E_f + s(t)\Delta E_e \tag{10}$$

Sciaratta et al. calls s(t) the heart of the EMCS (Equivalent Minimum Consumption Strategy), and develops it as a function of the system efficiency in charging and discharging, the expected free recharge energy (a function of terrain/traffic conditions selected by the user), the state of charge of the battery, and the probability that

44

the system will have a net loss or gain in stored charge over the mission. This probabilistic approach allows the system to operate in real time without knowing the mission cycle in advance [73].

Optimal control has also been used in flightpath optimization, in which air transports select altitude and airspeed schedules to minimize fuel consumption within constraints set by air traffic control rules and a required arrival time. Varying airspeed alone using Optimal Control while on a fixed flight path and arrival time was found by Franco et al.[74] to save half a percent of fuel burn when the arrival time is nonstandard.

Tibioli et al. [17] and the other hybrid car researchers who used Optimal Control checked by Dynamic Programming have indicated that Dynamic Programming is an effective, if time consuming method whose guarantee of global optimum gives it a slightly better solution than Optimal Control. Expecting these trends to continue for hybrid aircraft, Hypothesis #4 is stated as follows:

Hypothesis #4

Dynamic Programming will prove effective in finding the global optimum hybrid power schedule but take too long to be practical in design. Optimal Control will find almost as good a solution quickly enough to be practical.

Research Question #5: How Does the Choice of Optimal Schedules Affect Other Problems in Hybrid System Design?
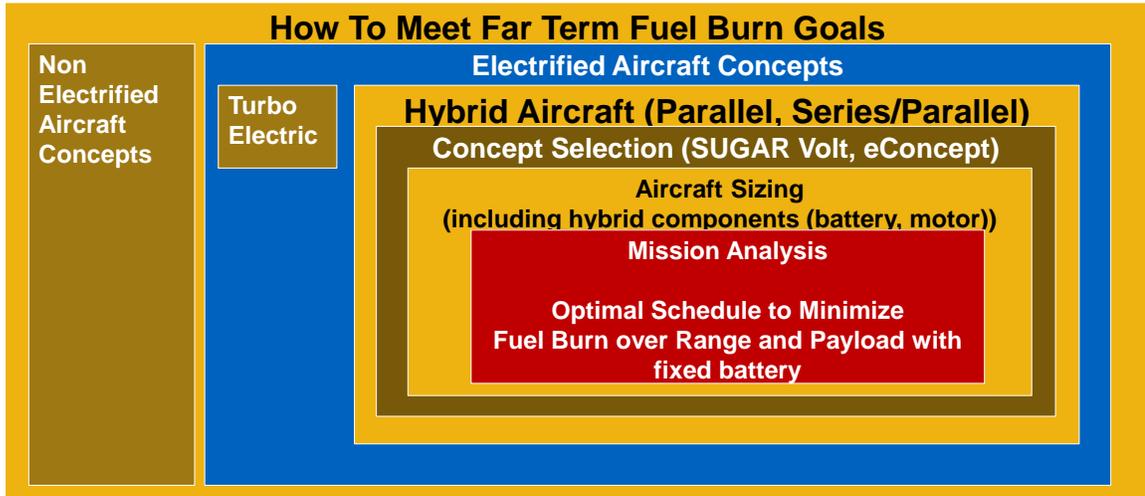
Figure 20: Diagram of Nested Problems

The hybrid power scheduling problem for aircraft is a nested problem within those that have to be solved to reach the Far Term fuel burn goals mentioned in the introduction. This is conceptualized in Figure 20 above. In order to determine the performance of a hybrid aircraft concept, and in order to find the optimal size of its hybrid components, a power schedule must be found or assumed. Optimizing that power schedule may allow a smaller battery pack to be chosen or may demonstrate that one concept has higher fuel savings potential in comparison to other concepts.

An example of the battery sizing trade is shown in Figure 21, a plot of fuel burn savings and energy savings vs. range for aircraft at MTOW with different sized batteries. Each of the battery curves show a peak fuel savings point, corresponding to the shortest range at which the entire battery can be emptied during the hybrid mission. At ranges less

than this, the power schedule uses full hybrid power whenever the propulsion system can accept it. At longer ranges the power schedule is constrained by the energy in the battery. It is in these longer capacity limited segments that an optimized power schedule could be found to increase the performance[46].
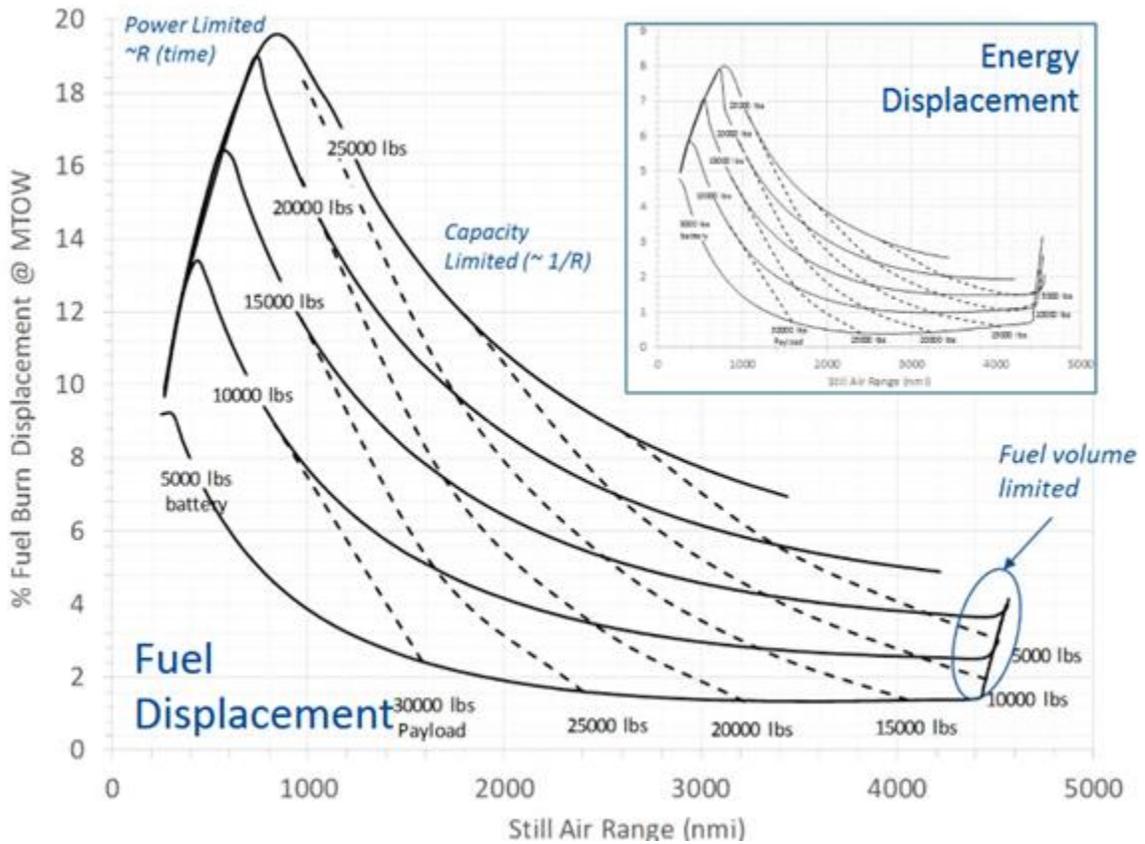
Figure 21: Battery Sizing Trade for Rolls-Royce's Electrically Variable Engine (EVE)[46]

The choice of which power system to use for a proposed aircraft is a function of the expected use of the aircraft in the airlines' fleets. Examining the use profile of single aisle aircraft in 2013 seen in Figure 22, many missions are short enough that even the smaller batteries considered in Figure 21 could power the hybrid systems at full power

during the entire mission. However for all but the largest battery sizes, a majority of the missions are longer than the power limited range [14].
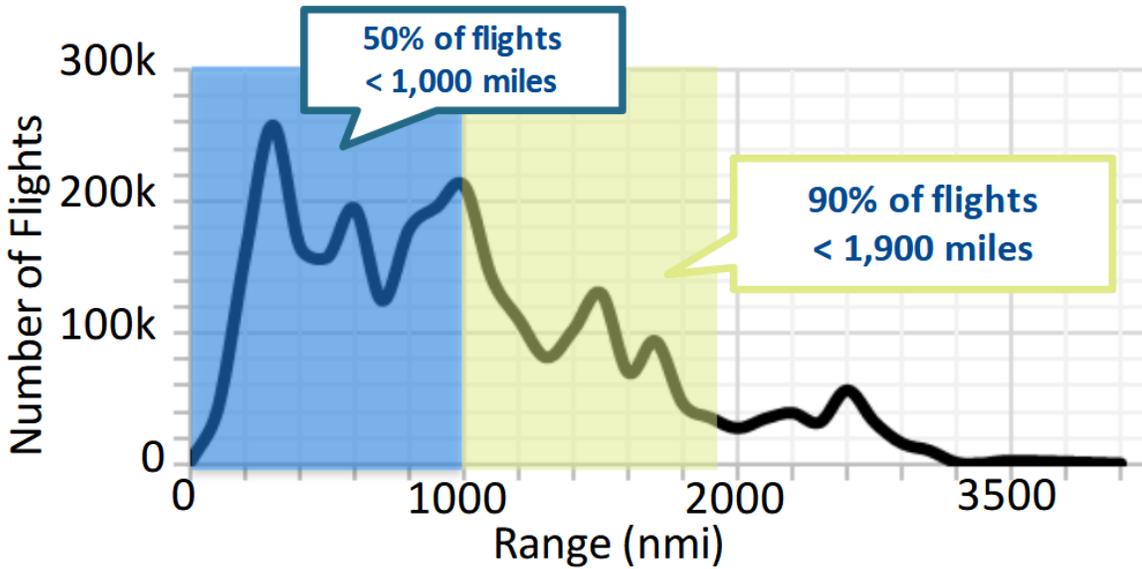
Figure 22: Typical Single Aisle Fleet Operations (2013)[14]

Considering that it is not possible to further optimize the power usage schedule in the power limited case, Hypothesis #5 is as follows.

Hypothesis #5

Using the proper power schedule will improve performance when the system is battery capacity limited.

Optimizing the power schedule should cause benefit in the battery sizing, aircraft/engine sizing, and concept selection problems depending on the proposed mission set. Proposing a mission set and solving these problems is beyond the scope of this thesis.

Revisiting the Research Questions

In pursuit of the purpose stated above, To Develop a Methodology for the Determination of Optimal Operational Schedules of Hybrid Electric Architectures, the research questions and hypotheses were as follows:

Research Question #1: How important is it to use the optimal power schedule?

Hypothesis #1: The use of optimal power schedules over a typical aircraft mission will yield significant savings in fuel burn.

Research Question #2: What factors determine the optimal power schedule?

Hypothesis #2: The reduction in aircraft weight resulting from burning fuel early in a mission is the dominant factor determining the optimal power usage schedule.

Research Question #3: What is the appropriate baseline schedule?

Hypothesis #3: The best baseline hybrid power schedule is to use the battery power as late in the mission as possible.

Research Question #4: What methods can be used to find better hybrid power schedules?

Hypothesis #4: Dynamic Programming will prove effective in finding the global optimum hybrid power schedule but take too long to be practical in design. Optimal Control will find almost as good a solution quickly enough to be practical.

Research Question #5: How does the choice of optimal schedules affect other problems in hybrid system design?

Hypothesis #5: Using the proper power schedule will improve performance when the system is battery capacity limited.

Assuming these hypotheses are correct, a methodology can be to determine the optimum operational schedules of any aircraft's hybrid electric architecture.

Proposed Methodology

Define System	Define Optimization Problem	Create Detailed Model	Determine Appropriate Power Scheduling Method	Find & Apply Power Schedules

- Architecture
- Technology Level
- Size
- Hybridization Level
- Battery Size

- Objective Function and Free Variables
- *Find* $P_e(t)$
- $min\ J = \int w_f dt$

- Architecture
- Technology Level
- Hybridization Level

- Follow Procedure

- Battery Sizing Study, Other Trades on System Design

Figure 23: Systematic Hybrid Aircraft Power Schedule Optimizer (SHAPSO)

This thesis proposes a methodology called the Systematic Hybrid Aircraft Power Schedule Optimizer (SHAPSO). This methodology, shown in graphical form in Figure 23, starts with the system definition in which a particular hybrid aircraft is defined in terms of the propulsion architecture and sizing. At this stage the technology level for all calculations and assumptions is defined. The battery size and the hybridization level, that is the ratio of electric power system size to conventional engine size, are also specified.

With the system defined it is possible to define the optimization problem which needs to be solved by an optimal operational schedule. The optimization problem is defined in terms of the number of free variables the system has, the objective function which defines the best optimization, and the constraints on the systems operation. In the typical problem such as that considered by hybrid cars, the overall power output of the hybrid system and the vehicle position are controlled by the driver or pilot and are a function of the terrain or environment. Thus they are not free variables to be controlled by any optimizer. So at this defining stage these systems would only have the power division between the battery and the fuel as a free variable. The objective function can be defined here as minimization of total mission fuel burn, as shown in Figure 23 and in Equation 11:

$$Minimize\ J = \int_{t_{start}}^{t_{finish}} \dot{w}_f dt \tag{11}$$

where J is the objective function, $\dot{w}_f$ is the fuel burn, and t_{start} and t_{end} are the start and end times of the mission respectively. In addition, system constraints such as starting and ending states of charge and other limits on power level are identified at this stage and included in the rest of the analysis.

After the optimization problem is defined for a set system and technology level, it is possible to select or construct models of that system of a sufficient fidelity to capture the trades being optimized. These can be simple models of the parts of the system not directly affected by the hybrid power system state, such as the aircraft structure or aerodynamics, coupled with detailed models of the propulsion system itself. An example would be using component level models of the gas turbine to find exactly how its

performance is affected by the electric power being used at any time while using far simpler models for the aerodynamics or fuselage mass. In this fashion a point mass and basic wing area/drag polar combination can be used in the same model as a detailed Numerical Propulsion System Simulation (NPSS) model of a gas turbine.

With detailed models in hand the optimization of the power schedules can be approached using the sub-procedure shown in Figure 24. Because a later step includes applying a global optimizer to the problem, it is necessary to first check and see if the model can be executed quickly enough to use such the global optimizer with the available computational resources. Engine models made in tools such as NPSS can take several seconds to converge for a single time step of the simulation, but global optimizers can require many millions of time steps to be simulated. An engine deck can be created to speed this up by running the complex engine model at a sufficient number of points throughout the likely operational space (in flight condition and power settings), and recording the performance of the engine. These recorded points can then be used to approximate the behavior of the full model with an execution time that can be as short as a table lookup. Using the engine deck for all algorithms avoids inaccuracies that could happen if one algorithm used the engine model directly while another used the engine deck. It provides commonality between the tests which helps reveal the difference between the power schedules.
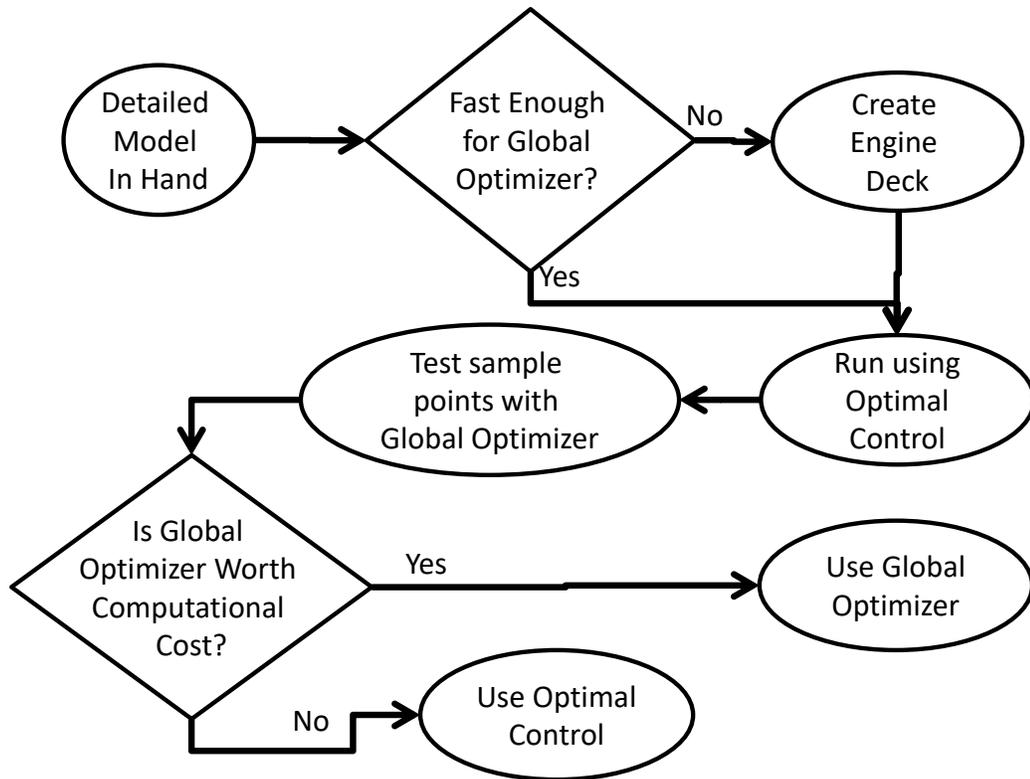
Figure 24: Procedure for Selecting Power Schedule Optimizer

With the engine deck in hand, the system can be simulated using Optimal Control on any possible mission. Sweeping the range with different battery sizes and comparing the fuel burn to the fuel burn of the system with no battery should yield curves similar to Figure 21 on page 46. The fuel burn could be computed for all payload/range combinations and multiplied by each flight's frequency to come up with a fleet fuel savings.

The next step in the procedure is to check the performance of Optimal Control at a small number of payload/range combinations using the global optimizer, Dynamic Programming. The number of points chosen depends on the available computational resources and the variation of missions of interest. Not only is the total fuel burn

determined for each method of interest but the power schedules as well. A comparison of the power schedules would reveal if Dynamic Programming is finding an entirely different solution or just one slightly different from the Optimal Control solution.

The final decision point in this sub-procedure is to evaluate the difference between the Optimal Control results and those from the global optimizer. It may be that the global solution is better than the Optimal Control solution by a large enough margin to justify using the global optimizer despite the high computational cost. If this is not the case, then Optimal Control should be used on the hybrid architecture to find the optimal schedules for each case required.

After this power scheduling method is chosen it is possible to perform the final step of SHAPSO and determine the power schedules for the system and apply them to the model to find the mission performance. The optimized power schedules will require less fuel and can be fed back into the sizing step to enable more accurate trades in the aircraft, propulsion system, and hybrid power system sizing.

Testing the Methodology

The SHAPSO methodology could be applied to any hybrid architecture and shown to determine a method for finding the optimal power schedule. However this would not directly prove that SHAPSO should be adopted in future hybrid studies. Because SHAPSO is based on the hypotheses posed to the research questions, its value can better be assessed after performing a series of experiments to test the hypotheses themselves. These experiments will consist of tests of different power schedules and

methods of optimization on a hybrid aircraft concept. The resulting schedules and fuel burns will be sufficient to address the research questions. Therefore a modeling framework must be constructed sufficient to conduct tests of different power schedules and scheduling methods.

Modeling Framework Construction

In order to perform the experiments, the first three steps of SHAPSO, as seen in Figure 23 on page 50, will be performed to construct a modeling framework representative of that built during an application of SHAPSO for design and evaluation of a hybrid concept. The system architecture, size, and technology levels will be chosen based on an existing hybrid aircraft study to ensure that it is representative. The optimization problem will then be defined conservatively to concentrate on the new hybrid operational freedoms without attempting to simultaneously optimize the flight path. With this done and modeling assumptions defined, a detailed model will be constructed to serve as a testbed for the experiments. These preliminary steps and the modeling effort are described in Chapter 4 before the experiments in Chapter 5.

Experimental Plan

The experimental plan is designed to address the five research questions and thereby determine if SHAPSO is a good methodology for determining the optimal operational schedules for hybrid electric architectures. Accordingly, the first step is to address Research Question #1: How important is it to use the optimal operational schedule? Hypothesis #1 states that the use of optimal power schedules over a mission should produce savings in fuel burn. If Hypothesis #1 is incorrect, and the choice of

power schedule does not affect fuel burn, SHAPSO is not needed. Experiment #1 will therefore be a simplified test problem, simulating flights consisting of a single cruise segment of varying length with different payloads and battery size. The power schedule for these flights is varied by trying several different parametric schedules and optimization methods. These shall include: running full motor power from the beginning of the mission until the battery is depleted, running full motor power from some time point until the end of the mission (inherited from the Chevrolet Volt[17]), selecting the starting point to deplete the battery (inherited from the Core Shutdown case from the SUGAR Phase II report[18]), and running at a constant motor power throughout the mission (inherited from the other cases in the SUGAR Phase II report[18]). Hypothesis #1 will be confirmed if there is a difference in the mission fuel burn between the different methods.

Experiment #1 will also shed some light on Research Questions #2-#4, by including several baseline schedules, Dynamic Programming, and Optimal Control in the set of power schedules and schedulers to be evaluated. It shall address Research Question #3 by finding which of the baseline schedules is the best for the cruise-only case. Determining which of these baseline schedules performs better may address Research Question #2 by identifying the dominant factor determining the optimal operational schedules. Research Question #4 will be addressed by comparing the performance of Dynamic Programming and Optimal control. However the answers to these three questions will not be fully determined by the partial mission analysis in Experiment #1. This is because the mission evaluated in Experiment #1 lacks the climb and descent

segments. The hypotheses of Research Questions #2-#4 are all proposed for a full mission.

Experiment #2 will expand on Experiment #1 by evaluating all these power schedules and schedulers on a full mission, which consists of a climb segment, cruise segment, and descent segment, with varying total mission distance, payload and battery weights. This evaluation will answer Research Questions #2-#4 and confirm or disprove Hypotheses #2-#4. The performance of the power schedules across the different missions will confirm or deny Hypothesis #3 which states that saving the battery power until the end of the mission is the best baseline schedule. The performance of Optimal Control relative to Dynamic Programming in terms of solution found and computational burden will confirm or deny Hypothesis #4 by finding whether Optimal Control is as effective in finding the optimum as Dynamic Programming and determining if Dynamic Programming is so slow that it would be difficult to select with SHAPSO. The optimal schedule found with Dynamic Programming along with the performance of the different baseline schedules should provide enough data to address Hypothesis #2 and find whether the weight of the fuel burned earlier in a mission rather than later in a mission is indeed the dominant factor determining the optimal power schedule.

These first two experiments will impact the fourth step of SHAPSO in which the power scheduler is actually chosen. Research Question #5 asks how the choice of optimal operational schedules affects the other problems in hybrid system design. This addresses the overall SHAPSO methodology and how it feeds back from the fifth step to the first to address design problems such as the battery pack sizing for the hybrid system. Experiment #3 addresses this research question by performing the battery sizing sweep-

57

finding fuel burn as a function of range with different installed battery packs- using the different power schedules tested in Experiments #1 and #2. If the different power schedules produce very similar performance than there would be no change in the choice of battery pack. At that point Hypothesis #5, which predicted an improvement in performance would change optimal battery pack sizing, would be disproven.

These three experiments address all five research questions as seen in Figure 25 below. Experiment #1 will answer Research Question #1 and shed some light on Research Questions #2-#4, but questions #2-#4 cannot be fully answered without testing the different power schedules on the entire mission. Experiment #2 will apply the different power schedules to the entire mission and fully address Research Questions #2-#4. Research Question #5 will be addressed by Experiment #3, which will apply the different power schedules to the problem of battery sizing.
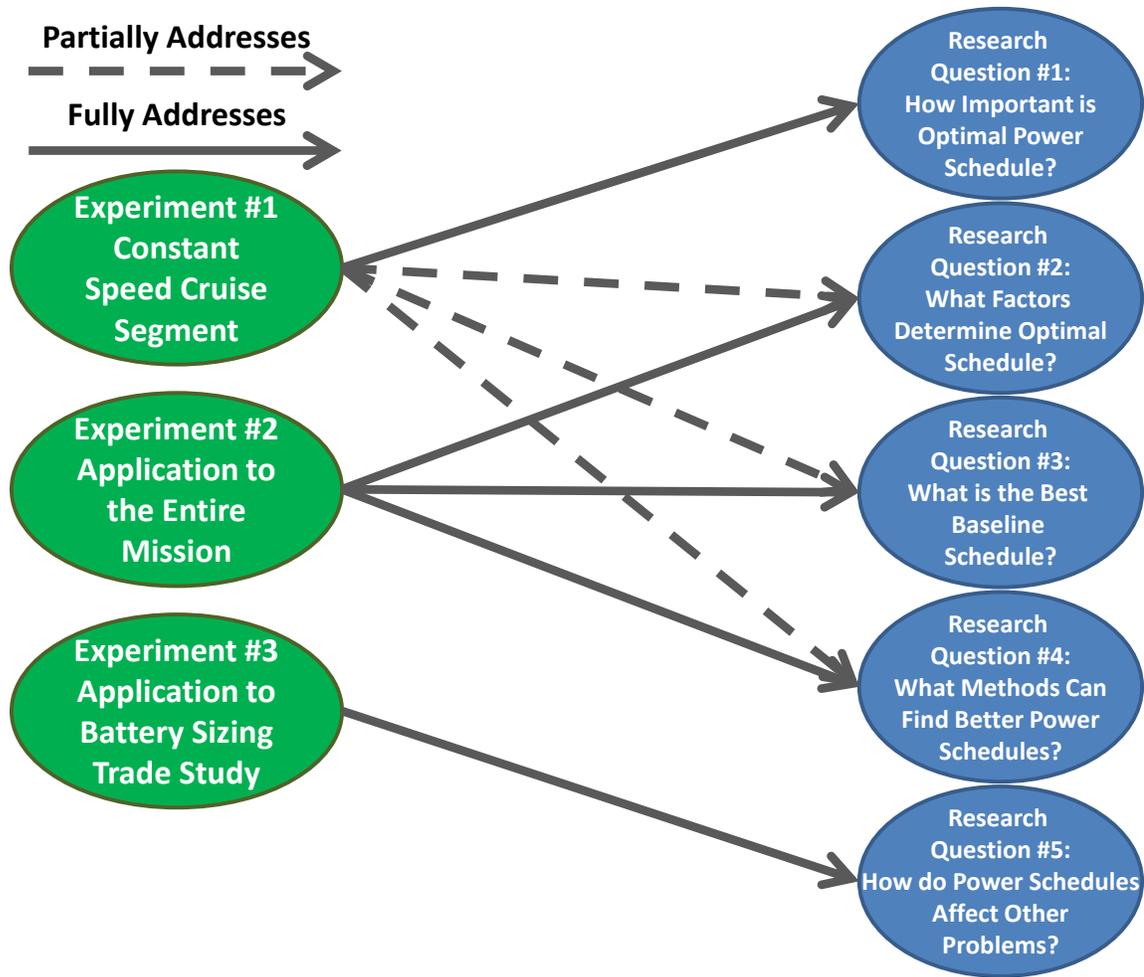
Figure 25: Applicability of Experiments to Research Questions

In order to perform each of these experiments, a modeling environment will be required to simulate a hybrid aircraft and its mission performance. This model will have to have a detailed enough propulsion system to capture the tradeoff between fuel and electric power at each time step and the influence this tradeoff has on the mission fuel burn. The rest of the aircraft model does not need to have the same level of detail but must be sufficiently described in order to give a representative profile of flight conditions and thrust requirements delivered to the engine. The model must also capture the change

in the thrust requirement and mission performance as a function of the aircraft weight, which changes as fuel is burned.

After the aircraft model is complete, Experiments #1 - $3 may be performed and Hypotheses #1-#5 can be evaluated. The experimental results should also show particular solutions for this particular aircraft architecture. An analysis of the experimental results should determine the merit of SHAPSO and identify any ways in which it could be improved. Chapter 4 will describe the modeling framework required to simulate the hybrid aircraft architecture and perform the experiments. Chapter 5 will discuss the implementation of the experimental plan, the results of the experiments themselves and the final answers to the Research Questions. The final conclusions from the experiments and any changes made to SHAPSO will be given in Chapter 6.

CHAPTER 4

FRAMEWORK FOR HYBRID ELECTRIC AIRCRAFT POWER SCHEDULE TESTING

The first three steps of SHAPSO, the hybrid power scheduling methodology proposed in Chapter 3, are to define the architecture, aircraft size, and assumptions, to define the optimization problem and to develop a detailed model of the system which can be used to address the optimization problem. Before the experimental plan can be applied to test the later steps and determine the overall utility of SHAPSO, the preliminary steps must be undertaken and a modeling environment must be constructed. This framework starts with the definition of the hybrid aircraft, its architecture, size, hybridization level, and the technology factors assumed. With these known, the optimization problem can be defined in terms of free variables and an objective function. After all these are defined, models of the aircraft and its propulsion system can be developed which are tailored to answer the optimization problem under the defined set of assumptions.

This chapter will develop the framework required for later testing of the experimental plan from Chapter 3. First, the hybrid aircraft, technology and operating assumptions will be selected and defined. Next, the optimization problem will be stated along with its associated assumptions. Finally, a modeling environment will be chosen and required models constructed which can capture the effects of the free variables in the optimization problem on the objective function.

Example Hybrid Electric Concept

The hybrid electric aircraft concept defined by an architecture and sizing point in the first step of SHAPSO was chosen to be a concept that has previously been studied, that is representative of a possible nearer-term hybrid civil transport and that did not have a fixed hybrid power schedule. The specific concept is a power split hybrid electric air transport, based on the aircraft described and sized by Perullo et al. in [27]. This concept, consists of an advanced truss braced wing airframe based on the Boeing TTBW X-plane seen in [75] and in Figure 26 below. It is equipped with two powersplit turbofan engines similar to the Rolls-Royce Electrically Variable Engine (EVE), in which an electric machine is mounted on the fan shaft and augments the gas turbine with electric power.

Figure 26: Boeing SUGAR Volt, a Concept With Similar Configuration[76]

This concept carries with it some operational assumptions. The electrical power augmenting the gas turbine is sourced from batteries which are fully charged on the ground, discharged fully or as much as possible during the mission and carried for the entire mission. The engine is sized to be capable of flying the entire mission using no battery power, only fuel, but the addition of batteries allows for fuel to be offset with electric energy[45]. This conservative approach represents an early hybrid concept, possibly easier to certify but also capable of operating from airports without recharging facilities if necessary.

The technology assumptions for this concept were also drawn from Perullo et al. who assumed a 750 Wh/kg battery energy density and an electric propulsion system power density (including the motors, power converters, and power cables) of 5 hp/lb, drawing these assumptions from the earlier Boeing SUGAR reports. The gas turbine technology levels were set to represent TRL 6 advancements by the year 2025, with the Rolls-Royce Ultrafan as a guide. It anticipates 25% improvement in fuel burn and emissions over the current state of the art. [27]

This particular aircraft is sized to carry a 150 passenger payload, with a MTOW of 152,000 lbs and an empty weight of 83,684 lbs. as shown in Table 2. Since 150 passengers corresponds to 35,000 lbs, this leaves over 30,000 lbs. for the fuel and the battery packs which is not included in the empty weight. The hybrid power system was sized by Perullo et. al. to have 3500 Hp. motors assisting each engine, however the size of the batteries, while fixed for any particular mission, has not been finally determined and can only be selected after a trade study has been performed evaluating the different options[46]. This is a motivation for using SHAPSO to find the best algorithm for

controlling the power schedules of the candidate batteries and allow a comparison of optimal battery pack performance.

Table 2: Modeled Aircraft Properties[45]

Property	Value	Units
Empty Weight	83683.9	Lbs.
Max Payload Weight	35000	Lbs.
MTOW	152398	Lbs.
Takeoff Thrust (Total)	47504	Lbs.
Cruise L/D	22.75	

The aggressive cruise Lift to Drag ratio (L/D) seen in Table 2 is achieved both through the application of advanced aerodynamics, for example the truss-braced wing's high aspect ratio, and also through a lower cruise speed. In an effort to achieve NASA's far term goals for fuel burn, the aircraft was designed to cruise at 37700 ft. at Mach .7. This reduction in speed increases the mission time. In addition, designing the wing to take advantage of the lower speed makes it impossible to fly at Mach .8 due to the different wing sweep, wave drag considerations and the change in required engine size. SHAPSO is intended to work for hybrid architectures regardless of cruise speed. However it may be expected that faster aircraft, which have a lower percentage of their drag coming from lift induced drag, should see a smaller reduction in required thrust over a mission as the fuel weight diminishes. This change in lift induced drag would impact the answer to Research Question #3, which asked which of the baseline schedules would give the most fuel burn savings, as the diminished importance of weight would make

Constant Power a better power schedule compared to End Power, which is based on the changing thrust requirements due to weight change.

This particular aircraft architecture was selected for use in the experiments for several reasons. First, it is a relatively well developed concept, with publications on designs similar to this one going back to 2011 detailing the assumptions and technology factors necessary to make it work. Second, it has a power schedule unconstrained by mission requirements, not needing electric power to climb but having a 3,500 HP electric motor, capable of draining the battery in all but the shortest missions with the largest batteries. This requires some power schedule decisions to be made and could therefore see great benefit from SHAPSO. Third, it has a deeply interconnected propulsion system architecture. This architecture should demonstrate the effects of all the factors that could shape the ideal power schedule discussed regarding Research Question #2. Finally there seems to be interest in carrying a similar concept forward to a technology demonstrator, which makes the ideal usage schedule and algorithms of significant interest[28].

Optimization Problem Definition

The second step in SHAPSO is to define the optimization problem in the operation of the hybrid architecture. This includes defining the objective function and identifying the free variables that can be chosen to optimize the function. In the case of this hybrid architecture, the battery is fully discharged or discharged as much as possible during every mission and recharged on the ground from grid power. This follows from assumptions that grid power will be preferred over jet fuel due to cost or emissions and that it is detrimental to carry battery capacity which is unused. If the first assumption was

incorrect, the feedback loop of SHAPSO used for battery sizing would size down the battery. Since the electricity consumption is fixed, any objective of minimizing emissions or energy costs can be accomplished minimizing mission fuel burn.

The independent variable of primary interest is the hybrid power setting which for this hybrid concept, sized to be capable of operating without power, can be set very freely. The power setting can be any value between zero and the lesser of 3500 Hp (the size of the electric motors) or the amount of power that the gas turbine can accept. The electric motor limit is active during climb and cruise, but when the engine thrust is reduced to idle during descent, the engine cannot accept hybrid power. Additional independent variables could be introduced by varying the flight condition, either changing the climb schedule, the cruise point, or allowing step cruise or cruise climb operations. In addition to greatly increasing the computational burden, Attempting to optimize on these variables would potentially bring the aircraft into conflict with air traffic control rules. These rules typically assign altitudes based on traffic needs rather than aircraft efficiency. If air traffic control rules were ignored, aircraft would climb to the highest altitude they could reach while maintaining required excess power in order to take advantage of the lower air density. This might drive the outer loop battery selection process further towards smaller batteries that would enable a higher cruise. For the purposes of this SHAPSO demonstration, the aircrafts intended cruise conditions will be maintained, a constant Mach .7 cruise at 37,700 ft.

With the independent variables defined, stating the objective function to be minimized is the next step. The objective function can be stated as seen in Equation 11 below: to find the power schedule $P_e(t)$ which minimizes W_f, the mission fuel burn,

equals the integral of the instantaneous fuel burn w_f which is an instantaneous function varying with time through the mission and with the electric power added.

$$Find\ P_e(t)\ to\ Minimize\ W_f = \int_{t_{start}}^{t_{finish}} \dot{w}_f(P_e(t), t)dt \qquad (12)$$

Modeling the Hybrid Electric Architecture

The third step of SHAPSO is to build a model of the hybrid architecture with sufficient detail to allow the evaluation of the objective function identified in step two. This means the model needs to be at a higher fidelity in the areas affected by the independent variables, such as the propulsion system, than it does in the areas which are not affected by the independent variables, such as the model of the aircraft structure. In addition, the choice of modeling tool and the design of the models will reflect any assumptions that have been made, both about the performance of the architecture and its components and also about the fidelity required to make the models.

Modeling Assumptions

Many of the key modeling assumptions have already been mentioned when describing the hybrid architecture and technology level in step one of SHAPSO: the gas turbine and the airframe technologies being set at a 2025 TRL 6 level, the truss braced wing and cruise conditions of Mach .7 at 37700 f, and the step two assumption of a fixed climb and cruise profile. The primary technology assumptions are those which affect the electrical components, specifically that the electric powertrain exclusive of batteries has a power density of 5 hp/lb, and that the battery has an effective energy density of 750 Wh/kg. The chemistry of such a battery is unknown, as is the efficiency curve of future

power electronics. Therefore the efficiency of the battery will be estimated with a simple resistance and the power electronics will be modeled with a single bulk efficiency.

A change in most of these assumptions would result in a change in the empty weight of the aircraft. For example, if the battery energy density is less than 750 Wh/kg, or if 20 % of the battery must remain unused for battery life, safety, or reserve power reasons, a larger battery with the required available energy must be carried giving a corresponding change in the aircraft weight. Similar calculations would be required for changes to either the power density of the electrical system or the structural weight assumptions. If the payload is decreased to match the increase in empty weight, the optimal power schedule can be expected to have no net change. However, if instead the payload weight is not decreased, the power schedule may be slightly more sensitive to the weight of the aircraft because the induced drag will be a larger component of the required cruise power. If the gas turbine assumptions are too optimistic, and the specific fuel burn is higher than expected, this may have a stronger effect on the power schedules, again causing more fuel burn early and battery usage later. On the other hand, if the cruise conditions are changed to a higher speed, this will reduce the impact of the weight change by producing more parasitic drag and less induced drag by proportion.

In addition to these technical and operational assumptions, there are assumptions particular to a modeling effort itself. In particular, there is an assumption to be made as to which transients are important and which can be neglected. Modeling a mission for any aircraft is inherently a transient problem, as the flight conditions, required power settings, and weight change throughout the mission. However many of the transients in the aircraft can be neglected due to their short duration with respect to the mission and their small

effect on cumulative power and fuel consumption. These include inertia of the gas turbine components and electric machines, voltage transients in the power converters, and the maneuvering required to change flight conditions such as the transition from climb to cruise. Therefore the airframe, engine, and hybrid components can be modeled with steady state models, with the steady state updated at each time step with the current vehicle weight, flight condition, and battery state of charge.

Modeling of Electric Components

The electrical systems can be modeled as a set of components which pass electrical power around as a voltage, current and frequency. Each component can be captured as a set of equations relating the inputs to the outputs and including any losses. In addition, an estimate of the mass of each component as a function of peak system power is required to compute the total system weight.

Motors/Generators

All motors and generators, collectively called electric machines, can be modeled as ideal machines with added losses [77]. Significant losses include resistive losses (resistivity of the copper windings), windage losses (due to air resistance on the rotor), and backiron losses (losses from induced currents in the magnetic material, typically iron, used to focus the magnetic field). Bearing losses can also be included in total losses; however, some designs escape this by including bearing losses in losses attributed to the gas turbine[45].

To compute the specific losses applicable to the motor in this architecture, a motor type has to be selected. Based on the existing literature[18], the Switched

Reluctance Motor was selected as the appropriate type to use in the high temperature environment on the inside of a gas turbine[78]. Examples of the Switched Reluctance Motor have been tested as early as 2005 by Brown et al.[79], although other more recent work is exploring the potential of Permanent Magnet Synchronous Motors[80], despite their greater sensitivity to temperature.

The ideal motor behavior and the losses inherent to switched reluctance motors can be computed as follows: The resistance loss is given by Equation 13 below.

$$P_{resistive} = RI^2 \tag{13}$$

The resistance R is computed from the number of motor phases, stator area, and the number of wire turns per motor phase and wire gauge as detailed in Perullo et al. [81] The windage power loss, due to aerodynamic drag as a function of the mechanical speed ω is given by Equation 14 below.

$$P_{windage} = c_d \pi \omega^2 \left(P_{max}^{.3} \frac{Diameter}{2} \right)^3 \tag{14}$$

c_d is a drag coefficient estimated based on Vrancik[82] and the diameter is computed using the drawings from the h-fan included in the Boeing SUGAR reports[19]. Similarly the backiron losses can be calculated from Equation 15 from Huynh et al.[81, 83]

$$P_{backiron} = \left(K_h B_p^2 f + K_c (B_p f)^2 + K_e (B_p f)^{1.5} \right) \left(\frac{Motor\ Weight}{176} \right) \tag{15}$$

In this equation, B_p is the peak magnetic field intensity, K_h K_c and K_e are magnetic constants for the backiron material, and f is the electrical frequency (in Hz), found with Equation 16, where n_{poles} is the number of magnetic poles in the motor.

$$f = \frac{\omega}{\pi n_{poles}} \qquad (16)$$

These losses are subtracted from the ideal power such that for a motor the efficiency (η_{motor}) is given by Equation 17.

$$\eta_{motor} = \frac{P_{mech}}{P_{mech} + P_{resistive} + P_{windage} + P_{backiron}} \qquad (17)$$

Thus the motor is modeled as having a mechanical power equal to the electric power input minus the losses. Generators can be modeled in the same manner with care taken to ensure that the electrical power is equal to the mechanical power minus the losses.

Power Converters (Rectifiers, Inverters, DC transformers)

Power converters are required to connect each electric machine and each battery to the high voltage DC power distribution system. These converters come in different types: an inverter generates AC to drive each motor, a rectifier is used to make DC from a machine used only as a generator and DC-DC converters are used to connect batteries to the high voltage distribution cables. Each of these has its own electric topology of switching and passive components oscillating at hundreds of Hz. With our assumptions about timescales, this means each is represented as a bulk efficiency and a power density. For higher fidelity modeling the efficiency can be a function of the input and output voltages and frequencies or simply the power if an efficiency map is available. In order to model the hybrid architecture chosen, an inverter efficiency map and a DC-DC converter efficiency map were required, and were found at [59, 84] and shown in Figure 27 and

Figure 28. These were normalized such that 100% power corresponds to the design power of the hybrid power system.
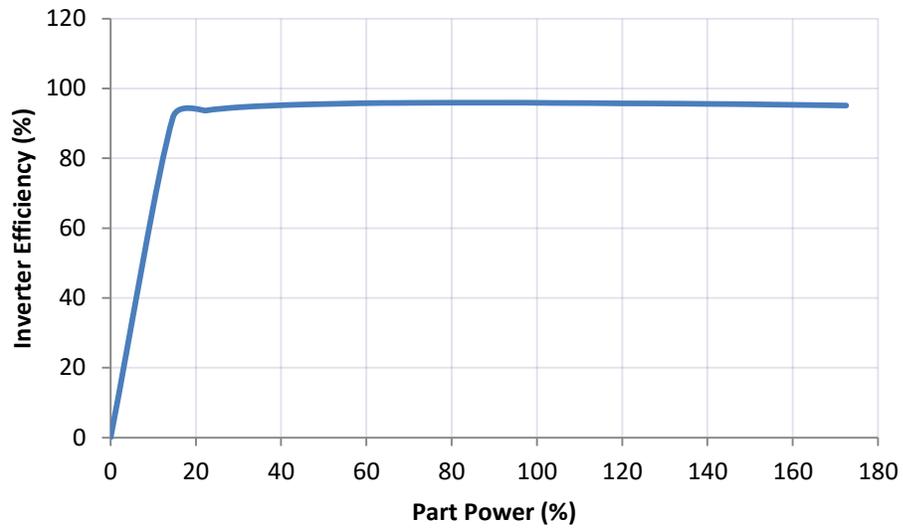
Figure 27: Inverter Efficiency Map[84]
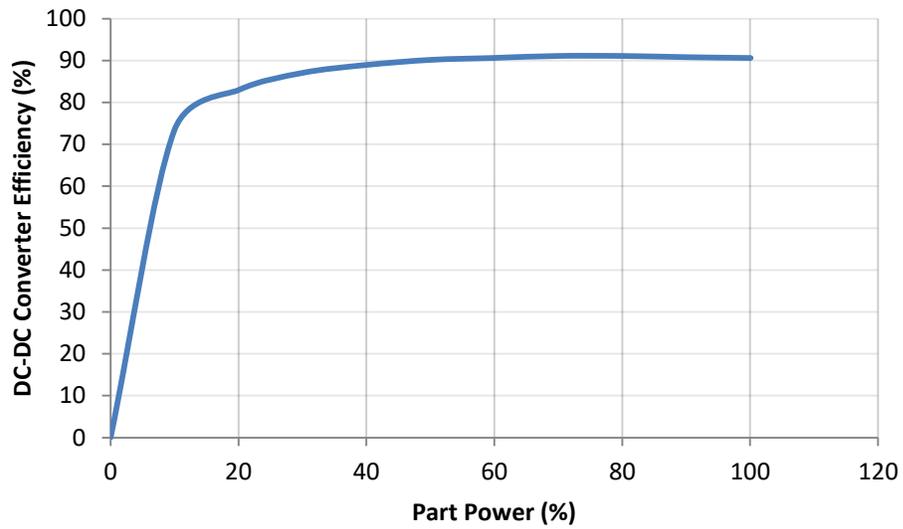
Figure 28: DC-DC Converter Efficiency Map[59]

Cables

Having assumed that cables between the power electronics and the motors and batteries are very short, the only cables of significant length are those between the bus and the power electronics. These carry high voltage DC power. The cables can be captured as a resistive loss using Equations 18 and 19 as dictated by Ohm's Law, where V is voltage, I is current, and R is the cable's resistance.

$$V_{out} = V_{in} - I_{in}R_{cable} \tag{18}$$

$$I_{out} = I_{in} \tag{19}$$

Bus

The Bus is a mathematical construct intended for use in multi-input/multi-output systems in which there are forks in the flow of power from source to use. Even in the single-input/single-output case, the bus can be captured by Equations 20 and 21, where V_i and I_i are defined such that I_i is positive into the bus, and i = 1, 2, 3… is each input.

$$V_i = V_{bus} \ \forall i \tag{20}$$

$$\sum_i I_i = 0 \tag{21}$$

Thus all current into the bus flows out, and the bus is the point where the system voltage is enforced. Other points in the system have voltages which are slightly higher or lower than the stated system voltage depending on the current and resistance through each cable.

Batteries

Unlike the other electric components, the batteries used in Far Term hybrid modeling do not yet exist. The motors and power electronics would be sized and shaped during detailed design, but the batteries will have to use a chemistry that hasn't yet been used commercially in order to reach 750 Wh/kg. Battery performance can be portrayed on Ragone charts such as that in Figure 29, which depicts state of the art Lithium Ion batteries from 2010 [85]. Ragone charts show a battery's power density and energy density as a trade-off, both within a single battery, and in a family of batteries. Each of the five battery curves represent capability of individual battery types, while intersecting lines indicate the time it takes to discharge a given amount of energy at the rated power. Because the battery performing the best between one and eight hours is the High Energy Lithium Ion, this is the best conventional battery for aircraft using electric assist during cruise. The existing High Energy Lithium Ion battery can be captured with an exact curve fit, however the proposed Far Term batteries cannot. Therefore a Thévenin Equivalent Circuit model of the batteries will be needed. In addition the size of individual cells of future batteries is unknown, so for convenience the battery will be made up of 1 kg cells arranged in series and parallel.
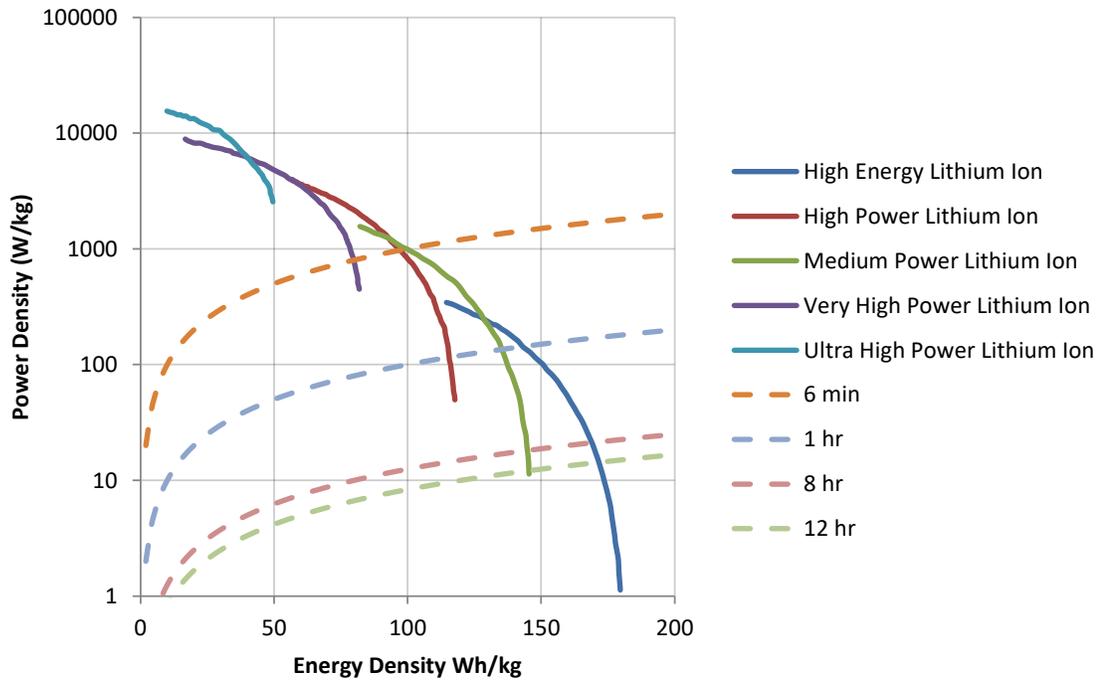
Figure 29: Lithium-Ion Ragone Chart (digitized from [85])

The Thévenin equivalent circuit model of a battery, seen in Figure 30, treats the battery as an ideal battery in series with a resistor and can be described with three parameters: the open circuit voltage (V_{th}), the resistance (R_{th}), and the ampacity of the battery (the amount of current that can be drawn from the circuit before it shuts off). These parameters can be extracted from a battery's Ragone chart through the following equations.
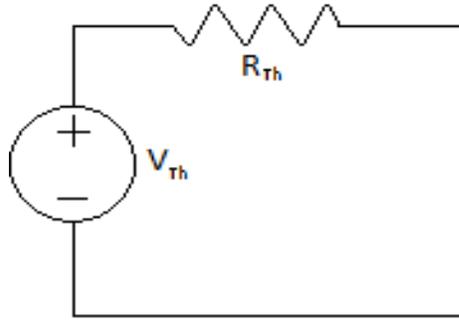
Figure 30: Thévenin Equivalent Circuit Battery Model

$$I = \frac{Ampacity}{Endurance} \tag{22}$$

$$PowerDensity = VI = (V_{oc} - IR)I \tag{23}$$

$$EnergyDensity = Endurance * PowerDensity$$

$$= (V_{oc} - IR)I * Endurance \tag{24}$$

Sweeping the value of endurance in these equations gives the entire Ragone curve. This can be used to fit existing Ragone curves, demonstrated below using some of the Li-Ion curves in Figure 31. The requisite values of ampacity, resistance, and voltage used to match each of the three curves in Figure 31 are shown in Table 3.
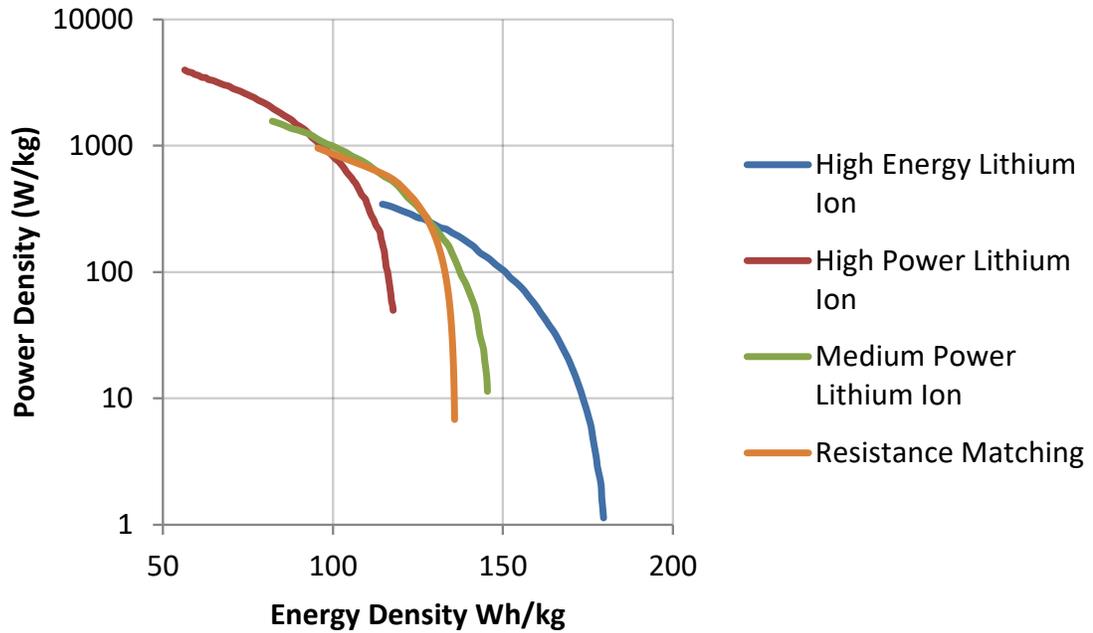
Figure 31: Ragone Chart with Thévenin Fit of Medium Power Li-Ion Battery

Table 3: Parameters to Match Li-Ion Batteries

	High Energy	Medium Power	High Power
Ampacity (Ah/kg)	40	34	29
R (Ohms/ 1kg cell)	0.01	0.0035	0.002
Open Circuit Voltage (Volts)	4	4	4

This approach can be used to match any battery with available Ragone information. However many future battery technologies are not developed sufficiently for Ragone curves to be available, and only have anticipated power density and energy density numbers such as those in Table 4.

Table 4: Future Battery Performance Parameters

Chemistry	Info	Energy Density (Wh/kg)	Power Density (W/kg)	Source
Li-S	Claimed in 2017	400	1800	[86]
Li-Air	2030's	2000	640	[87]

Mapping these battery performance estimates to the Thévenin equivalent circuit parameters requires some assumptions as to their location on the Ragone chart. If the numbers given are for peak energy density and peak power density, which occur at each end of the Ragone curve, the battery could have any amount of internal resistance losses at peak power, as shown in Figure 32. Scaled curves from the medium power and high energy lithium ion batteries are shown for comparison. Because these scaled curves are close to the 50% loss curve, the 50% loss curve can be used to estimate the performance of future batteries in absence of higher fidelity data.
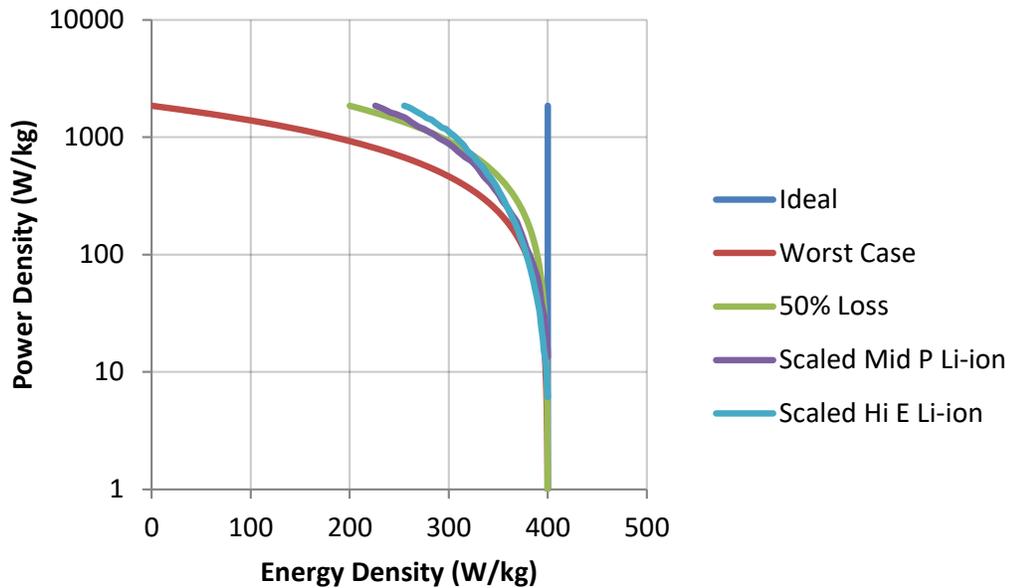
Figure 32: Alternative Ragone Curves for Lithium-Sulfur Batteries

78

The SUGAR Volt modeling effort assumed 750 Wh/kg batteries with no limit on power density. That effort used mission profiles which consumed battery power over long periods instead of in short bursts where power limits would be significant[18, 19]. For the purpose of these experiments, and in the absence of actual cell chemistry from 2030, 750 Wh/kg cells will be approximated by retaining the power density/energy density ratio of a lithium ion cell while scaling the mass of the battery to match the 750 Wh/kg metric.

Modeling of Hybrid Engines

In order to capture the effects of the hybrid components on the gas turbine, the gas turbine needs to be modeled with a sufficient level of fidelity that the impact of the electric motor's torque on the fan shaft will be reflected in the fuel efficiency of the gas turbine core. In lieu of a dedicated hybrid gas turbine modeling tool, a component based gas turbine modeling tool can be used which examines the performance of conventional gas turbine components when attached to an unconventional system. This can be accomplished by modeling the system in the Numerical Propulsion System Simulation (NPSS) tool, an industry standard gas turbine modeling tool viewed by NASA to serve as a virtual wind tunnel during the development of advanced propulsion systems[88].

NPSS can be considered as consisting of three different parts. First it is an object oriented modeling environment. This modeling environment utilizes a c like syntax with which different models can be constructed and different functions and scripts can be written and run to command the models to operate while recording their output. Second,

NPSS includes a solver. When properly configured to move a model's independent variables and track the dependent equations, this solver can solve systems of nonlinear equations and thereby cause the model to converge on a solution. Thirdly, NPSS includes a library of standard gas turbine component models which can be used to construct engine models. These models can be used as is, modified to include known efficiencies or efficiency maps to match experimental data, or replaced component by component with higher fidelity models depending on the availability of maps and calibration data and on the desired fidelity of the model[89].

The conventional gas turbine components in the hybrid architecture were modeled in this fashion, using standard NPSS library components for the inlets, shafts, burner, and nozzles, and using elements with modified performance maps for the fan, compressors, turbines, and gearbox required for this two spooled, geared hybrid turbofan. Along with the component weight models, the efficiency maps of these components were tuned to match trusted data from the literature, such as previous hybrid engine studies by GE or NASA studies describing the meeting of the Far Term goals. Matching the efficiency maps to trusted data was necessary because untuned component models can cause the system efficiency to be in error by as much as 20%[90].

In addition to modeling the conventional gas turbine components, NPSS was used to model the electric components of the hybrid. This was done by creating custom NPSS components for each of the hybrid components which captured the hybrid components' performance as described in the previous section. Because NPSS did not have a native interface for electrical connections between components that would match the mechanical and fluid connections, the electric components were built around the NPSS DataPort. The

DataPort was used then to send arrays containing the electrical values between the different electric components. The electric motor was connected to the low speed shaft using a standard shaft port, allowing it to drive the fan alongside the low speed turbine [62].

The model constructed using these standard and custom components was sufficient to model a hybrid electric propulsion system. However the system so modeled was found to have trouble in certain states of operation. Specifically, under conditions of less than maximum thrust with a high level of electric assist, the low pressure compressor would sometimes stall. That was because it was spinning faster than usual when compared to the high pressure compressor due to its sharing a shaft with the electric motor. This meant the low pressure compressor was trying to force more air through the core than the high pressure compressor could accept and so caused the low pressure compressor to stall. This problem was solved by adding an operability bleed to vent some of this air between the two compressors out into the bypass stream. This strategy recovered some of the work from compressing the air by augmenting the bypass stream but still traded some efficiency for stability. To prevent bleeding more air than required for stability, a duplicate engine model called a shadow engine was run simultaneously. This shadow engine was a model of an identical engine producing the same amount of thrust, but with the hybrid power set to zero. The operability bleed in the main model was then set such that the stall margin in the low pressure compressor of the main model was the same as that in the shadow engine. This allowed the engine model to converge at the flight conditions expected for the hybrid aircraft mission [90].

In anticipation of the fourth step of SHAPSO, determining the appropriate hybrid power scheduling method, the speed of the NPSS model was considered. For every flight condition, power setting, and hybrid assist setting at which the fuel burn, thrust, and power draw are desired, the NPSS model must solve all of the continuity equations inherent in the operation of a gas turbine such as ensuring that the net torque on every shaft is zero. Depending on the fidelity of the model and the available computational resources, this may take an unacceptably long amount of time. This is particularly true if the model is to be queried very many times as in the case of a Dynamic Programming simulation. Instead of querying the high fidelity model at each step of the simulation, a precomputed engine deck can be used, computed before the mission is simulated by stepping the engine through the entire flight envelope and saving the engine performance data. This reduces an engine call to a table lookup of the form seen in Equation 25.

$$[thrust, fuel\ burn] = EngineDeck(Altitude, Mach, Power\ Code) \qquad (25)$$

The power code used in Equation 25 is a standard for normalizing the throttle command, such that a power code of 50 is maximum power and 21 is minimum power at the current flight condition. In practice the engine deck can be an interpolation between a set of points which are sampled only as finely as necessary to achieve the desired precision.

Incorporating hybrid components and the inherent additional degree of propulsive freedom into the engine requires increasing the engine deck to have the form given in Equation 26 below.

$$[thrust, fuel\ burn, electric\ power]$$

$$= EngineDeck(Altitude, Mach, Power\ Code, Electric\ Power\ Code)$$

(26)

The electric power code is defined such that 0 is no battery power in use and 50 is the maximum battery power usable under current conditions, constrained by the electric system size or by the maximum power the gas turbine can accept at the current flight condition without violating some engine constraint. The increase to four dimensions for the table lengthens the time it takes to generate the engine deck, which can change its usefulness in speeding up mission analysis.

Modeling of Airframe

For the purposes of a hybrid propulsion system study, the airframe must be modeled to a degree that will allow the thrust requirements of the aircraft to be calculated for every phase of flight. The airframe can be captured with a wing area, an empty weight, and a drag polar. No short term effects such as control surface deflections or gusts need to be considered. For the Boeing SUGAR Volt, the wing area, empty weight and drag polar derived from the Boeing SUGAR High concept can be found in the Boeing SUGAR Phase 1 report[19]. This concept included an extremely high aspect ratio wing in order to reduce the induced drag. This high aspect ratio wing used a truss to reduce the bending stress and therefore the weight of the required structure and was referred to as a Truss Braced Wing (TBW). The wing design also took advantage of a reduction in aircraft cruise speed to reduce the wing sweep, further decreasing the structural weight and increasing the L/D ratio, but limiting the aircrafts maximum speed.

Different assumptions about the amount of battery to be carried resulted in different proposed airframes by the time the SUGAR Phase 2 Volume 2 report[18] was completed. This report contains different aircraft concepts with differing weight and wing area, but the same drag polar. This drag polar can be digitized and used to model similar aircraft including the hybrid concept selected for Experiments #1 thru #3. With a drag polar in hand it was only necessary to size the wing to handle the specific aircraft gross weight.

Mission Modeling

To model an aircraft mission, the equations of motion and the aircraft performance must be integrated through all the mission phases from takeoff to touchdown. Each phase can be broken up into segments within which the forces on the aircraft, including weight, are assumed constant. At the end of each segment the forces are computed and the change in distance, energy height, battery charge, and fuel are recorded.

The cruise phase of the mission, which has a constant altitude and Mach number is broken into N segments of equal distance with length ds given by Equation 27 below.

$$ds = \frac{Phase\ Distance}{N_{segments}} \tag{27}$$

At the beginning of each segment, the required thrust is computed from the weight of the aircraft and the flight condition (specified by an altitude (alt) and Mach number (Mn)) by the airframe model as specified in Equation 28 below.

$$Thrust_{required} = Drag\left(\left(W_e + W_{batt} + W_{payload} + W_{fuel}\right), alt, Mn\right) \tag{28}$$

From the required thrust and a chosen hybrid strategy (which sets the Electric Power Code (EPC)) the fuel burn and battery consumption can be computed by varying the power code (PC) until the engine deck gives the required thrust as shown in Equation 29 below.

$$[Thrust_{required}, \dot{w}_f, P_e] = EngineDeck(alt, Mn, PC_{required}, EPC_{chosen}) \quad (29)$$

The time required to complete each segment, dt, can be calculated from the airspeed and the distance of each segment through Equation 30.

$$dt = \frac{ds}{airspeed(alt, Mn)} \quad (30)$$

At the end of the segment the fuel and battery consumed can be calculated using dt and Equation 31. The process can repeat with a new thrust required computed from the new w_f and any change in the hybrid strategy.

$$w_{f,n+1} = w_{f,n} - \dot{w}_f dt, \; Batt_{n+1} = Batt_n - P_e dt \quad (31)$$

Mission phases with a change in altitude are discretized by energy height, He, adding the kinetic energy to the altitude to find the height that corresponds to the aircraft's mechanical energy through Equation 32, where g is the acceleration due to gravity.

$$H_e = alt + \frac{\left(airspeed(alt, Mn)\right)^2}{g} \quad (32)$$

The energy height change, dh, in each segment is given by Equation 33.

$$dh = \frac{H_{e,end} - H_{e,start}}{n_{segments}} \quad (33)$$

For climb dh will be positive and for descent it will be negative. The throttle setting is fixed during these segments, typically at full power during climb and idle power

during descent. The difference between thrust and drag determines the change in energy height through the specific excess power computed in Equation 36, with the change in energy height given by Equation 37.

$$[Thrust, \dot{w}_f, P_e] = EngineDeck(alt, Mn, PC_{climb/descent}, EPC_{chosen}) \qquad (34)$$

$$Drag = Drag\left((W_e + W_{batt} + W_{payload} + W_{fuel}), alt, Mn\right) \qquad (35)$$

$$P_s = \frac{(Thrust - Drag)airspeed(alt, Mn)}{W_e + W_{batt} + W_{payload} + W_{fuel}} \qquad (36)$$

$$dH_e/dt = \frac{P_s}{g} \qquad (37)$$

These equations allow the time for each segment to be calculated and the fuel burn and battery depletion to be calculated as before. As the aircraft climbs or descends, the split in the energy height between altitude and airspeed must be defined by a climb schedule, which specifies both for any value of the energy height. The distance travelled during these each mission phase is computed by integrating the airspeed and used when computing the length of the mission and the required length of the cruise segment.

The fuel burn, battery and distance are integrated over the mission and compared to the fuel and battery carried and the total mission length desired. If they do not match, the mission must be resimulated with a new guess for the length of the cruise segment, the starting w_f and potentially a change in the hybrid schedule.

The mission can also be simulated in reverse by reversing the integration of distance, energy height, energy, and fuel usage. This should produce the same result for total fuel consumption, cruise length and battery usage, but should allow some changes in the mission setup by. For example, simulating the mission in reverse would allow

computing the fuel burn in one pass instead of guessing a starting weight and finding if it is consumed by the end. Instead, a guess and check method could be applied to the distance travelled during the climb segment. The choice of integration order is driven by an attempt to reduce the number of guess and check loops within the requirements of the optimization method used.

With models of sufficient fidelity to address the optimization problem under consideration, the third step of SHAPSO is completed. It is now possible to begin to address the three research questions by following the experimental plan. In Chapter 5 the fourth and fifth steps of SHAPSO will be applied to the test hybrid architecture as a means to answer the research questions and find the importance of the hybrid power schedule, the factors determining the ideal hybrid power schedule, the best baseline hybrid power schedules and optimization methods and to determine how the ideal hybrid power schedule can affect the other choices in hybrid aircraft design.

CHAPTER 5

IMPLEMENTATION AND RESULTS OF EXPERIMENTS

The experiments laid out at the end of Chapter 3 establish how to address the research questions and prove or disprove the value of SHAPSO. The first experiment is designed to answer Research Question #1: How important is it to use the optimal power schedule. The first experiment will answer this question by testing the impact of different power schedules on fuel burn over a simple cruise segment. It also examines the effectiveness of different optimization methods in finding more efficient power schedules, providing some insight into Research Questions #2-#4. The second experiment is intended to answer these three Research Questions: Question #2: What factors determine the optimal power schedule, Question #3: What is the appropriate baseline schedule and Question #4: What methods can be used to find better hybrid power schedules. Experiment #2 will do this by testing each of these methods on an entire mission, including climb, cruise and descent, and comparing their performances. Finally, the third experiment sweeps through many ranges and battery sizes to answer Research Question #5: How does the choice of optimal schedules affect other problems in hybrid system design. It will do this by using the different power schedules and optimization methods developed in Experiments #1 and #2 during the battery sizing process. This chapter details the implementation of these experiments utilizing the framework discussed in Chapter 4, as well as the results of the experiments and the answers to the research questions.

Experimental Setup

In order to perform each of the experiments, it was first necessary to devise not only the different control strategies to be tested but also a common testing environment capable of simulating a hybrid electric aircraft being controlled in different ways. This simulation tool had to be able to simulate a fixed aircraft, to which each of the methods could be applied in turn, each method attempting to find the ideal solution to the same problem so that their results could be compared. There is precedent for extending the gas turbine simulation tool NPSS beyond the simulation of the engine and the hybrid components to the performance of the mission simulation[91, 92]. Many of the schedules and methods are compatible with this approach. However but the global optimizer of interest, Dynamic Programming, requires many parallel calculations instead of a single integrated execution order and is difficult to implement in NPSS. Although NPSS therefore was not suitable for the entire simulation, NPSS could still be used to generate an engine deck as discussed in Chapter 4. This engine deck was portable and could be translated into multiple modeling environments.

An engine deck based model could be constructed using any programming language. These languages include a new effort in NPSS or more common programming languages such as MATLAB or Java. MATLAB was chosen primarily because of its built in parallel computing toolbox which was expected to shorten the execution time of the Dynamic Programming method significantly. In addition MATLAB is relatively easy to debug and was available on all of the computers used for development. MATLAB's other features, particularly the MATLAB Coder toolbox, were found to be very helpful

when conducting Experiments #2 and #3. The mission modeling equations from Chapter 4 were therefore implemented in MATLAB.

Study Aircraft and Propulsion System Model

As described in Chapter 4, the aircraft used for this study is a 150 passenger air transport resembling the Boeing SUGAR Volt concept. It has truss braced wings which provide a high aspect ratio and low drag and 3,500 HP electric motors mounted to the low speed spool on each of its turbofan engines. It was based on the final aircraft model from Armstrong et al. [45, 93] and has the characteristics listed in Table 5 below.

Table 5: Modeled Aircraft Properties[45]

Property	Value	Units
Empty Weight	83683.9	Lbs.
Max Payload Weight	35000	Lbs.
MTOW	152398	Lbs.
Takeoff Thrust (Total)	47504	Lbs.
Cruise L/D	22.75	

The aircraft's properties were derived from Armstrong et al., and the drag polar was derived from the Boeing SUGAR reports as also done by Armstrong et al.[18, 45] The engine performance was captured by creating an NPSS model using the hybrid components discussed in Chapter 4. An engine deck was then created by running the model at a sweep of flight conditions, thrust and electric assist settings while recording the net thrust, fuel consumption and expended battery power. Of note is that the electric power commands to the engine were indexed in shaft horsepower, up to the motors' maximum power of 3,500 HP, while the power draw was logged as the battery terminal

power in watts. In addition the battery terminal power included the losses between the motor and the battery. These losses included the inverter and battery controller loss models whose efficiency curves were given in Chapter 4. Due to these losses the electrical power in watts was not a simple conversion of the shaft power in HP. This was because the total efficiency of the power transmission system was <90% across the envelope when the inverter and DC transformer maps were combined.

The electric power was recorded at the battery terminals when generating the engine deck. This required the battery model to be implemented separately in MATLAB using the same Thévenin equivalent circuit equations discussed in Chapter 4. So unlike the other hybrid components, whose performance was baked into the engine deck, the battery could be resized to be larger or smaller or it could have its internal resistance changed without regenerating the entire engine deck.

Along with the aircraft and engine model, some technology assumptions were inherited from Armstrong et al. [45]. In particular the battery energy density was assumed to be 750 Wh/kg, and the engine was assumed to be incapable of recharging the battery in flight and to be unable to accept electric boost at thrusts lower than cruise thrust. These assumptions confined all battery power scheduling to the climb and cruise segments of a mission, with the descent segment flown conventionally with the engine at idle and no electric assist.

The initial attempt to convert the NPSS results into an engine model for use in MATLAB was to create a four dimensional table (Mach, Alt, Throttle, and Electric Boost) and use linear interpolation to find any intermediate values of output variables needed. However the results of the linear interpolation were found inadequately smooth

91

as described later in the discussion of Optimal Control. The data was instead used to fit a surrogate model for each of the output variables (thrust, fuel burn, electricity usage). These models were treated as a truth model for the duration of the experiments, and were used by all of the MATLAB models.

Experiment #1: Constant Speed Cruise Segment

Research Question #1 asks: "How important is it to use the optimal power schedule?" Although different factors are identified in Chapter 3 which may affect the mission performance as a function of the power schedule, the actual impact of these factors is not certain until an experiment is conducted. Hypothesis #1 states that the use of optimal power schedules over a typical aircraft mission will yield significant savings in fuel burn. Experiment #1 is intended to address this hypothesis over an even simpler mission than typical, by testing different baseline power schedules and optimization methods over only an aircraft mission's cruise segment. If there is a significant difference in aircraft fuel burn between the different power schedules, Hypothesis #1 will be confirmed. Different baseline power schedules and optimization methods will be tested for different payloads and ranges to capture the cruise segment of a typical aircraft mission.

In addition to answering Research Question #1, Experiment #1 will also shed light on Research Questions #2-#4. Research Question #2 asks what factors determine the optimal power schedule, and the related Research Question #3 asks what the appropriate baseline power schedule is for hybrid aircraft. Both of these questions will be addressed somewhat by Experiment #1 as specified, as the relative performance of the different

power schedules will show which is appropriate for a cruise segment and shed light on the factors which determine the optimal power schedule. Similarly Research Question #4, which asks what methods can be used to find better hybrid power schedules than these baseline schedules, will be addressed by the application of Optimal Control and Dynamic Programming to the cruise segment's power schedules. However none of Research Questions #2-#4 can be definitively answered without including the entire aircraft mission and the additional complications involved in the climb and descent segments. Final answers to these research questions will have to wait until Experiment #2.

Implementation

The first step in implementing Experiment #1 was to code the engine deck equations and the drag polar into MATLAB functions that could then be called by the main simulation code. In addition the battery resistance model was coded into functions allowing the state of charge change to be determined as a function of battery power, battery size, and time step. The reverse process was also coded which calculated the power required to cause a given state of charge change. This done, the mission could be simulated by following the basic steps laid out in Figure 33.

As shown in the figure, the first step is to initialize all the variables to their starting values. These variables include the amount of fuel and battery state of charge. After logging these variables in the time history, the aircraft weight and drag can be computed by adding the current fuel weight to the no fuel weight and using the drag polar to calculate the current drag from the current flight condition and weight. For a cruise segment this drag is the required thrust, which corresponds to an engine power setting

that can be looked up using the engine deck. With the power setting defined, the hybrid power setting is chosen based on whichever power schedule or scheduling method is being simulated. The engine deck is then called to find the current fuel burn and battery consumption. These values for this fuel burn and battery consumption, along with the aircraft speed, are integrated over the time step and added or subtracted as required from the fuel weight, battery state of charge, and distance from start. If the mission is complete the simulation ends, otherwise the time step is logged and the next weight and drag calculation is started. This simple procedure works for the methods other than Dynamic Programming by changing only the direction of integration and the section of code in which the power setting is actually chosen.
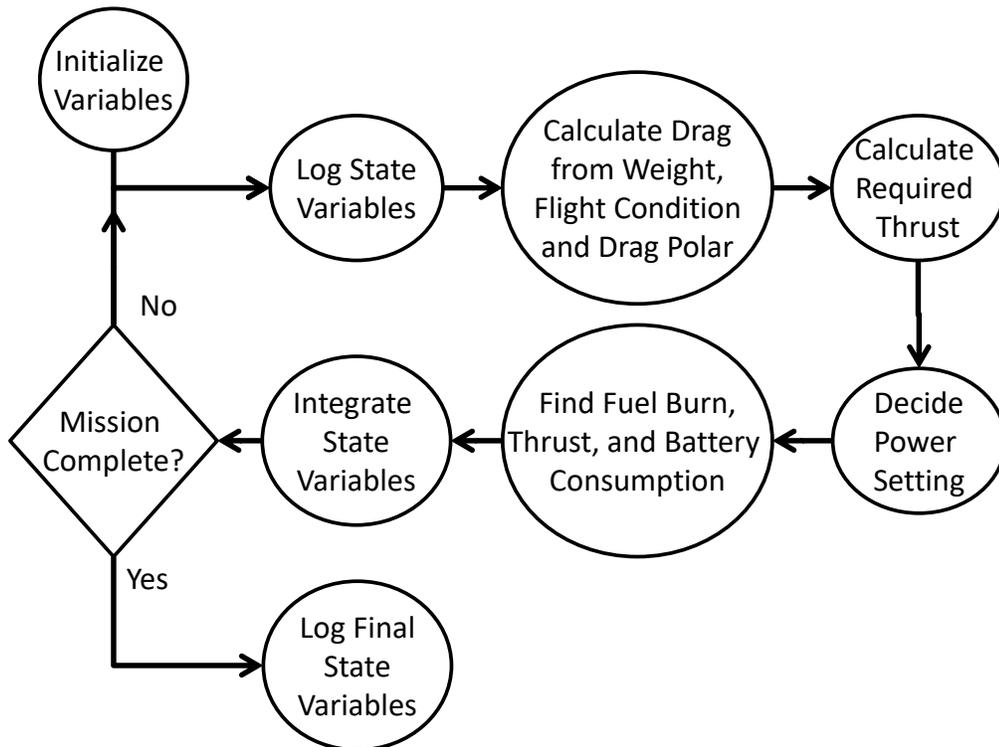
Figure 33: Mission Simulation Procedure

One remaining choice common to all the methods was the determination of the size of the simulation time step. Decreasing the size of the time step increases the simulation time for all methods but reduces the integration error. An early version of the Optimal Control code was used to measure the integration error as a function of time step and find the largest time step which had an acceptable error. The results of this study are shown in Figure 34 below.
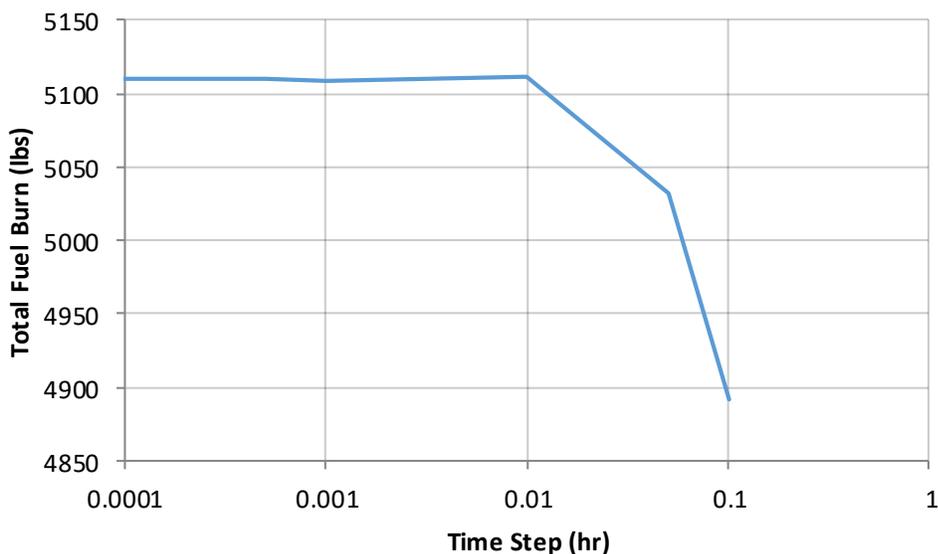
Figure 34: Experiment #1 Time step Study

Figure 34 shows a graph of total fuel burn over a cruise segment as a function of the time step used to integrate the simulation. It shows that in the limit where the time step is one ten thousandth of an hour, the total mission fuel burn is about 5110 lbs. If the time step is increased in size by a factor of ten, reducing the number of time steps and

hence the computation time by a factor of ten as well, the mission fuel burn computed remains the same. The knee of the curve comes after the time step is increased past .01 hr. A time step of .05 hr shows a fuel burn of about 5040 lbs. over the same mission which would represent an unacceptable 1% error in mission fuel burn. Based on this study .01 hr time steps were the largest time steps which could be used without significant error when compared to .0001 hr. time steps. .01 hour time steps were therefore used across all methods so that any integration errors would be consistent.

With this framework complete the different methods, Constant Power, End Power, Start Power, Optimal Control and Dynamic Programming, could be implemented. Each method was used in missions of different lengths, battery sizes, and payload weights to find the fuel required at the beginning of the cruise segment such that the fuel weight at the end of the cruise segment was zero.

Baseline Methods

For the purposes of Experiment #1, three different baseline power schedules were considered. In keeping with Hypothesis #3, one of these was to save the battery energy until as late in the mission as possible. This meant that the maximum power, 3,500 shaft HP on each engine, was implemented from some point in the mission until the end. This method was integrated in reverse for ease of control, allowing the motor power to be set solely as a function of the battery SOC. At the time step in which maintaining full power would cause the SOC to go above 100%, the power was instead set to exactly fill the battery.

The complement of this power schedule, the Chevrolet Volt strategy of using the maximum allowed battery power at the beginning of the mission until it runs out, was implemented as well. This was calculated in the same manner as the End Power method, but instead of simulating the mission in reverse, the simulation was run from the beginning until the battery reached 0% SOC instead. This required iterating to converge on the correct amount of fuel to start the mission, so that the tanks would be empty within 1 millionth of a pound of fuel when the mission was completed.

Running the mission at a Constant Power schedule was the third baseline method included. At the same point of the simulation at which the starting fuel weight was determined in the start power case, to make sure exactly none is left at the end, the motor power for the entire mission was also computed to ensure there was no charge left in the battery at the end of the mission, to within .000001%.

Optimal Control

Optimal Control is one of the methods that was used to optimized the battery and fuel use on these experimental missions. Optimal Control can be implemented as an instantaneous optimization strategy, in which the cost function J is minimized at each time step. Based on Kim et al. the cost function can be constant throughout the mission assuming that the efficiency of the battery is not a function of its charge, which is true for the Thévenin equivalent circuit model used in this model[71]. The resulting cost function is shown in Equation 38 below, where J is the cost, $\dot{w}_f$ is the fuel burn rate, P_e is the electric power, and λ is a weighting factor.

$$J = \dot{w}_f + \lambda P_e \tag{38}$$

Instead of varying the power level in order to zero the battery, as in Constant Power, in Optimal Control it is λ that is varied so that it converges on the battery SOC, which must be depleted at the end of the mission. In addition W_f and the range of the cruise segment are varied so that they converge on the mission fuel weight and the mission length respectively.

Accordingly, the Optimal Control equations were programmed into the Decide Power Setting step. This was implemented with an execution of the built in MATLAB function for finding a minimum on a bounded interval, fminbnd(). Power levels were varied between 0 and 3,500 HP to find the minimum value of the weighted sum of fuel burn and battery power. The weighting on fuel burn was fixed at 10,000 to handle the unit discrepancy between pounds of fuel per hour and watts. This caused the battery power weighting required to deplete the battery to be a number between 2.5 and 4 depending on the mission and the battery size. This battery weighting was then set at the mission level using MATLAB's nonlinear root finding function, fzero()[94].

The early runs of the optimal control code revealed a problem with using linear interpolation when the power schedules started to look like the one shown in Figure 35 below. This figure shows the electric power setting chosen by Optimal Control over the mission elapsed time. Ignoring a final time step at which the power is set to zero due to a depleted battery, the power chosen is exactly 1000 Hp. of electric power until about 1.35 hours of elapsed time at which it drops to exactly 900 Hp. of electric power. The schedules were also completely flat except for jumps as seen in this example. In addition the motor powers chosen by this method were exact multiples of 100 Hp. - the same points which had been sampled to create the engine deck. At some point through the

mission, the weight change (and resulting thrust change) caused the cost function value at one multiple of 100 Hp. electric assist to be better than the next, but the intermediate settings were never chosen. This was due to Optimal Control finding shortcomings in the engine deck.
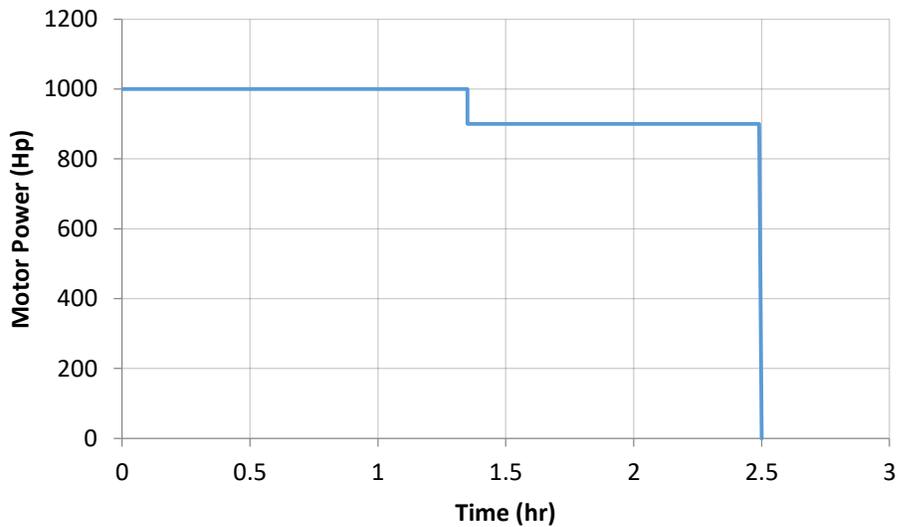
Figure 35: Optimal Control Power History Using Interpolated Engine Deck

Optimal Control works by using a minimizer to find the minimum of a weighted cost function at every time step. If that cost function is a linear interpolation, the minimum will typically occur at the vertices of this linear interpolation. This is demonstrated with a parabola as a notional example in Figure 36 below- the blue line depicts the true value of a parabola, and the red is a linear interpolation between sample points taken at every .01 of x. It can be seen from this notional example that the minimum of the linear interpolation is one of the sampled points. This will always be the case except for when two sample points share the minimum value, in which case a

minimizer may pick either one or any point in between. In all other cases, a minimizer will generally pick the vertex closest to the true minimum, but it will always choose a vertex.
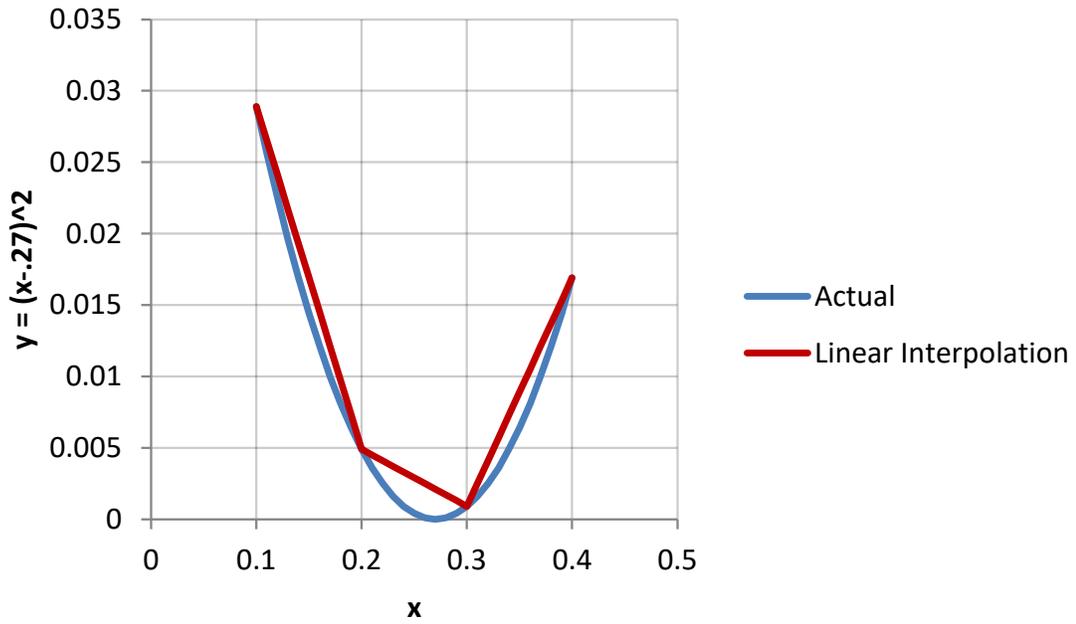
Figure 36: Linear Interpolation Notional Example

The purpose of the engine deck was to give the algorithms a model similar to an actual engine. However, engines typically do not have ideal points only at multiples of 100 HP, and so a smoother function was required. The engine deck can be considered to consist of two parts- first, a table of values generated from the operation of the NPSS model at many points covering the operating envelope, and second, the algorithm performing the linear interpolation. Some attempts were begun to improve the engine deck by attempting a higher order interpolation, based on the nearest three or four points in each axis instead of the nearest two. However these attempts either introduced discontinuities in the resulting engine performance, in which one point was exchanged

for another, or simply introduced a different set of artificial minima from the set derived by linear interpolation. The next attempt to improve the engine deck was to use the data table to fit a surrogate model. A set of neural network equations was fit to the same data table used with the interpolation method. This had the advantage of being guaranteed to be smooth enough to find a minimum in a continuous manner, but the disadvantage of not quite going through all the points which were sampled from NPSS. In order to create a tight fit and make sure all the sample points were included for Experiment #1, the neural networks were only fit for the cruise condition (Mach =.7, Altitude = 37700 ft.) which is assured during this experiment, and a very tight match was obtained. This surrogate model was used for Experiment #1, and a second surrogate model was made including all four dimensions to be used for the remaining two experiments.

Dynamic Programming

Because of its parallel nature, Dynamic Programming does not fit within the same experimental framework as the other methods, which use a sequential integration of time steps. The Dynamic Programming code starts by initializing the known, final state of the mission. From that point it evaluates every possible state transition to get there from the next to last time step. Each state is defined by the state of the battery, which for Experiment #1 could only have a state of charge that was a multiple of 1/100,000 of full at each time step of .01 hr. This set the minimum possible increment of shaft power at ~2.5 Hp., depending on the exact efficiency of the system at each point. For each time step each of these 100,001 states was evaluated in parallel, finding the fuel burn required to get one time step closer to the end of the mission, transitioning to any valid state of

charge. The fuel burn is a function of the fuel weight already accumulated at those valid states of charge, with invalid states identifiable by the invalid fuel weight with which they were seeded. Each point except the final empty battery state is initialized to have 100,000 lbs. of fuel. As mentioned in Chapter 3 and shown in Figure 37, the fuel burn required to traverse any valid edge of the battery state/ mission time step graph is computed, and the lowest sum of (fuel burn this step) + (fuel burn from next step to the end) is saved as the minimum fuel burn to the end from this step. The path from this state towards that minimum fuel state is then saved in a path matrix. The final mission schedule is found by looking at the path matrix- starting from the start of the mission at the 100% battery point, and following the matrix back to the end of the mission.
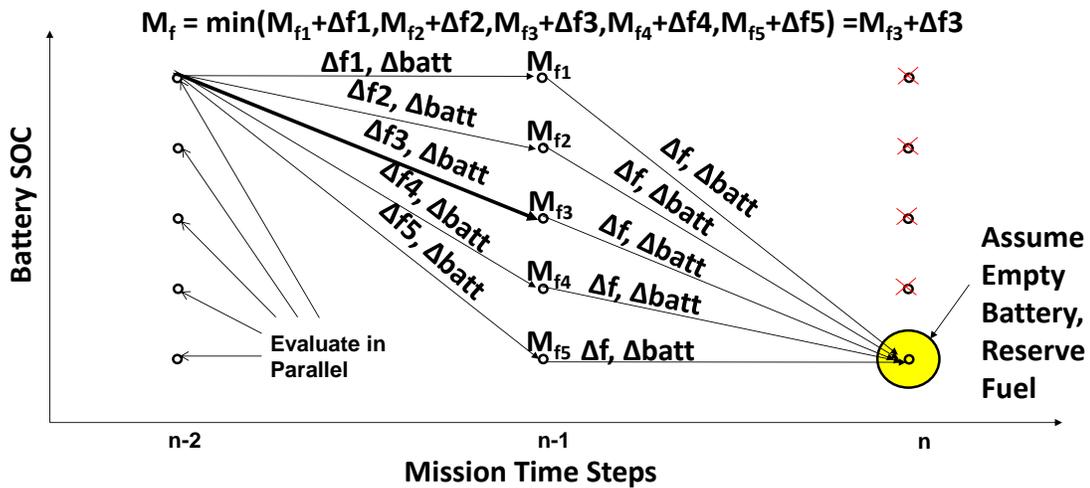
Figure 37: Parallelization in Dynamic Programming

Implementing this calculation in MATLAB involved some changes to the ideal procedure. With unlimited computing resources a matrix could be created for every

102

tracked variable (thrust history, fuel weight, etc.) showing the value at every state of charge/time history for the ideal path from that point to the end. This approach quickly hit a memory limit as each matrix would have ~20 million values. Instead of remembering these matrices, only column vectors containing the values for the previously evaluated time step were ever used, overwritten at each time step. The exception was for the path matrix which only contains the integer indexes of the next battery state.

This path matrix was then used to generate the time history of the optimal path by using a translation script that ran through the path matrix to extract the power used to drain the battery at each time step. This power history was then used in a version of the code used in other methods, running the motor power from a schedule instead of choosing it using Optimal Control. If this did not result in exactly consuming the battery due to some slight mismatch between the Dynamic Programming code and the other codes, the other methods were run to the exact same final battery state for consistency, whether this was slightly more or less than zero charge remaining. For Optimal Control in experiment #1 this was done by manipulating the first or last time steps, which caused discontinuities in the schedule.

Dynamic Programming was massively sped up by using the MATLAB's parallel computing toolbox. This evaluated each state in parallel during a time step as shown in Figure 37, using MATLAB's built in parallelized for loop, parfor[94]. The evaluation was also sped up by constraining the transitions examined to those which could be reached using a nonnegative motor power which was less than the maximum. This eliminated two parts of the path matrix as unreachable. Towards the end of the mission there is a maximum battery charge which can be drained by the mission's completion,

and at the beginning there is a minimum charge that can be reached by draining the battery at maximum rate. For the standard battery, sized such that at full power it will totally discharge in 250 nmi. when flying at cruise speed, this can eliminate a quarter of the path matrix for a 1000 nmi. mission as unreachable, thus speeding the evaluation.

Experiment #1 Results

The unknowns going into Experiment #1 were amount of the fuel burn for each method, the motor power schedules determined by Optimal Control and Dynamic Programming, and the length of time these methods would require to calculate their results. The experimental model was run with six different variations of payload, mission duration, and available battery. The results were found to be consistent across all these cases.

Optimal Power Schedules

The power schedules for a 1,000 nmi. mission carrying 25,000 lbs. of payload and equipped with a 10,457 lb. battery are shown in Figure 38 below. This shows the Dynamic Programming in blue, the Constant Power in yellow, and the Optimal Control in Grey and Orange for Reverse and Forward respectively. The two Optimal Control curves lie on top of each other for all but the first and last time steps. The instantaneous optimization schedules (Start Power and End Power) instantaneously minimized fuel burn by going to maximum power (3,500 Hp.) for the first or last quarter of the mission respectively when they ran out of power. Start and End power are not shown here in order to highlight the other schedules, which only vary from 860 to 1040 Hp.

104
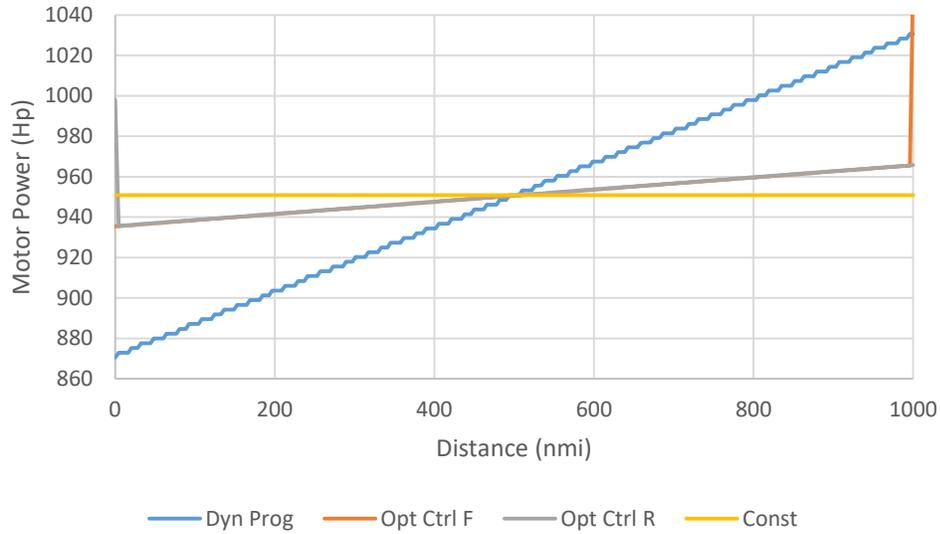
Figure 38: Experiment #1 1,000 nmi. 25,000 lb. Payload, 10,457 lb. Battery, .7 Mach, 37,700 ft.

Both Optimal Control and Dynamic Programming chose linear schedules, although Dynamic Programming chose one with a steeper slope. The stair step effect found with Dynamic Programming is a result of the resolution used- the minimum increment of motor power works out to 2.5 HP. Linear power schedules were chosen in all cases tested, as demonstrated in the two cases shown below in Figure 39 and Figure 40. Figure 39 shows a longer duration mission with the same battery and payload. Figure 40 shows a shorter mission with more payload and battery. As in Figure 38, the Constant Power, in yellow, is bisected in both cases by Optimal Control and Dynamic Programming. However, the average power and the slope chosen by Dynamic Programming and Optimal Control in each case is greater for the shorter ranges and lesser for the longer ranges. This reduction in power with increasing range is an expected consequence of having more distance of travel per kWh of energy in the battery in Figure 39 compared to Figure 40.

105
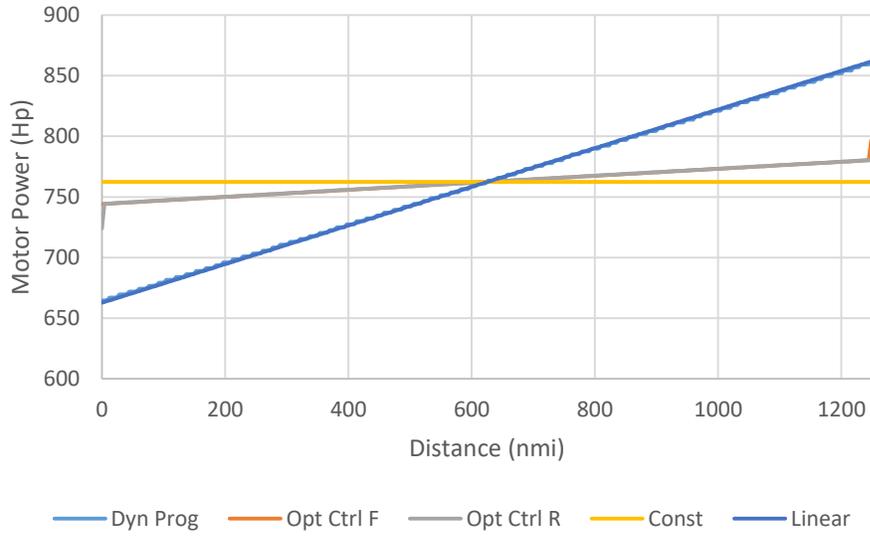
Figure 39: Experiment #1 1,250 nmi. 25,000 lb. Payload, 10,457 lb. Battery, .7 Mach, 37,700 ft.
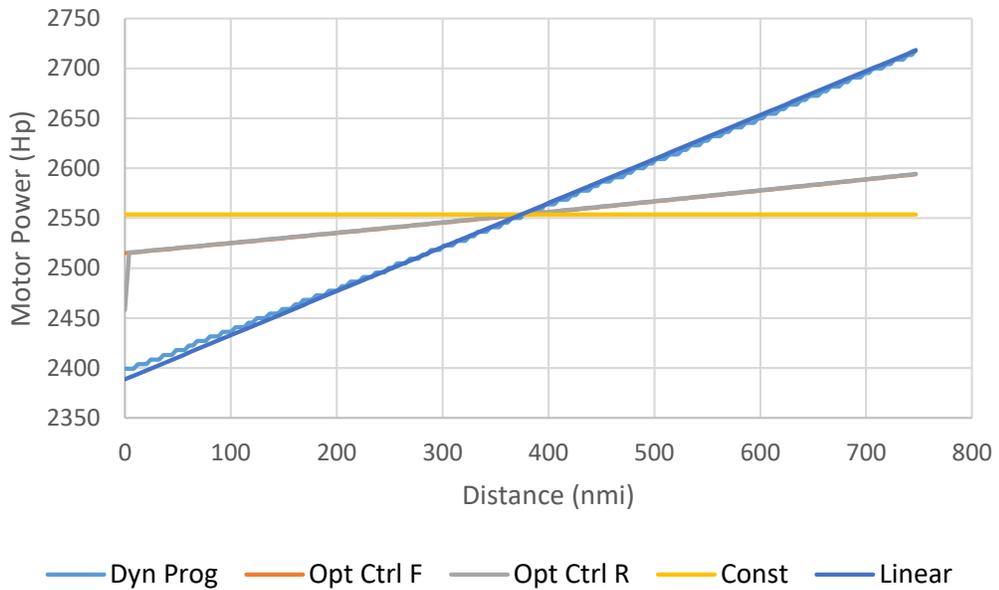
Figure 40: Experiment #1 750 nmi. 35,000 lb. Payload, 20,914 lb. Battery, .7 Mach, 37,700 ft.

An additional method is shown in the previous two figures: the ideal Linear Power schedule. This was calculated by setting the power to a basic line (given by

Equation 39 below) with slope m and intercept b, and varying b to consume the battery and varying m to find the minimum fuel burn.

$$y = mx + b \tag{39}$$

This Linear Power schedule can be seen to track the Dynamic Programming schedule nearly exactly, in many cases running right through the stair step schedule set by the resolution-limited Dynamic Programming. This suggests that in the case of the single cruise segment a linear power schedule may be the best baseline method, as it is a simple enough formula to be listed as such alongside Constant Power and Power at End. However, the performance of the schedules is determined not by the graph of the power setting but by the fuel burn results.

Fuel Burn Results

The fuel burn results from each of these methods and cases are given in Table 6 and Table 7 below. Dynamic Programming was expected to be the global optimum, so the percentage difference for each method compared to Dynamic Programming is given as well.

Table 6: Experiment #1 Results, 10,457 lb. Battery, 25,000 lb. Payload

	Range (nmi)	Dyn Prog	Opt Ctrl F	Opt Ctrl R	Const	Power at Start	Power at End	Linear
Fuel Burn (lbs.)	750	3543.15	3543.18	3543.19	3543.20	3719.02	3697.65	3543.15
	1000	5114.72	5114.86	5114.86	5114.93	5314.21	5295.48	5114.72
	1250	6681.10	6681.36	6681.36	6681.49	6893.24	6868.30	6681.10
% more than D.Prog	750	0%	.00071%	.00093%	.00147%	4.96%	4.36%	-0.0000014%
	1000	0%	.00262%	.00275%	.00397%	3.90%	3.53%	0.00003%
	1250	0%	.00392%	.00392%	.00587%	3.18%	2.80%	-0.000002%

(Row label: 10457 lb. Battery)

Table 7: Experiment #1 Results, 20,914 lb. Battery, 35,000 lb. Payload

		Range (nmi)	Dyn Prog	Opt Ctrl F	Opt Ctrl R	Const	Power at Start	Power at End	Linear
20914 lb. Battery	Fuel Burn (lbs.)	750	2660.33	2660.47	2660.47	2660.57	2741.86	2728.51	2660.33
		1000	4259.34	4259.67	4259.21	4259.81	4405.48	4376.82	4259.34
		1250	5864.34	5864.97	5864.96	5865.17	6053.84	6009.70	5864.34
	% more than D.Prog	750	0%	0.00528%	0.00522%	0.00914%	3.07%	2.56%	-0.00001%
		1000	0%	0.00791%	-0.00301%	0.0110%	3.43%	2.76%	-0.00001%
		1250	0%	0.0107%	0.0105%	0.0142%	3.23%	2.479%	-0.00001%

Considering the three baseline methods first; using the battery at the start of the mission was expected to be the worst of these cases based on Hypothesis #2, and it was. In each case it performed over 3% worse than the optimum and .5% worse than any other method. Less expected was that using constant motor power would outperform saving the battery energy until the end of the mission. The difference between saving the power until the end and using it all at the start, reflecting the Hypothesis #2 effect of burning fuel early rather than late, hovered around .5% to .75% of the mission fuel burn. The difference between either schedule and Constant Power was consistently 2-4%, indicating that one of the other effects was more dominant. The performance of the Linear Power schedule compared to the Constant Power schedule illustrates the small power schedule change that the weight change effect has on aircraft flying on as simple a mission as this constant speed cruise.

Integrating Optimal Control in the forward or reverse direction was found to give almost identical results, but as promised, Optimal Control performed nearly as well as Dynamic Programming. The Linear Power schedules with the form given in Equation 39 lie right over the Dynamic Programming schedules on the graphs and are an

improvement over Dynamic Programming due to the resolution limitations of the Dynamic Programming method.

However the most surprising result was that the overall difference between Constant Power and the optimal solution found by Dynamic Programming was very slight. This was judged to be due to the relatively invariant nature of the problem- the thrust required at the beginning and the end of cruise varied by no more than 3% over any of these cases. Therefore the ideal assist level for the engine should not vary by very much. The difference between using Constant Power and saving the battery for the end of the mission was found to be equal to the battery resistance. Even though each case used the same battery and depleted an identical fraction of the battery, the amount of electricity actually applied to the gas turbine was as much as 10% higher compared to Start Power or End Power when passed through the battery resistance at the lower power level used by Constant Power.

Execution Time

The execution time for each of the methods varied not only with the length of the mission but with stage of development, as slight improvements were made to speed up Dynamic Programming in particular. However by the end of Experiment #1, the execution time of the non-Dynamic Programming methods was down to a few minutes each per case on a standard workstation. Dynamic Programming took as much as 15 days to execute on an otherwise unoccupied workstation with 10 cores working in parallel at 4 GHz. This verified the hypothesis that only Dynamic Programming would take an

unreasonable amount of execution time. The magnitude of the difference in execution time exceeded expectations.

Experiment #1 Conclusion

The research questions were reevaluated upon the completion of Experiment #1. Research Question #1 asked "how important it is to use the Optimal Power Schedule", and Hypothesis #1 stated that "the use of optimal power schedules over a typical aircraft mission will yield significant savings in fuel burn." Looking at the results of Experiment #1 as detailed in Table 6 and Table 7, the difference in fuel burn for aircraft which varied only in power schedule was 3% or more between the most optimal and least optimal power schedules. Although this savings is only over a single segment of a typical aircraft mission, it is certainly significant, amounting to as much as a passenger's weight in fuel.

Research Question #2 asked "what factors determine the optimal power schedule," with Hypothesis #2 proposing that "the reduction in aircraft weight resulting from burning fuel early in a mission is the dominant factor determining the optimal power usage schedule." This hypothesis was disproven by the results of Experiment #1, as these results show clearly that the power schedule most favoring this factor, Power at End, performed the second worst of the power schedules tested. The results in Table 6 and Table 7 suggest instead that the battery resistance and other factors driving the optimal power schedule towards Constant Power must be the dominant factors. However Research Question #2 cannot be answered for certain until all the possible factors are evaluated. These factors would include the changes in an aircraft's thrust setting or the

influence of an aircraft's weight which would be included in a simulation which contains a climb segment.

Research Question #3 asked "what is the appropriate baseline schedule?", and Hypothesis #3 followed Hypothesis #2 and proposed that "the best baseline hybrid power schedule is to use the battery power as late in the mission as possible." This hypothesis was disproven by the results of Experiment #1, which show that the Constant Power schedule outperforms the Power at End schedule across every scenario tested. Based on the optimal power schedule found by Dynamic Programming, an additional baseline power schedule was identified in Linear Power. The Linear Power Schedule is the best performing schedule for this single cruise segment. However it is unlikely to be the best performing schedule over the complete aircraft mission. The Linear Power schedule will only need to be examined over the complete mission if the optimal power schedule determined by Dynamic Programming continues to be linear. The best baseline power schedule for the complete mission, and therefore the answer to Research Question #3, will have to be found with an additional experiment considering the entire aircraft mission.

Research Question #4 asked "what methods can be used to find better hybrid power schedules?" and Hypothesis #4 proposed "Dynamic Programming will prove effective in finding the global optimum hybrid power schedule but take too long to be practical in design. Optimal Control will find almost as good a solution quickly enough to be practical." The results of Experiment #1 show that Dynamic Programming, found the optimal solution limited only by the resolution implemented. Dynamic Programming also identified an additional promising baseline method. However, Dynamic Programming

111

took weeks to execute, showing it is not practical in design without a great change in implementation or available computing hardware. The solution calculated by Optimal Control was nearly as good as that found by Dynamic Programming and determined in a fraction of the time. Thus the speed and accuracy of Optimal Control would enable it to be used in a design study. Hypothesis #4 is therefore conditionally confirmed, conditional on the fact that this is a mission segment and not a complete mission simulation, which could make either method perform differently.

Besides answering the research questions themselves, Experiment #1 showed an unexpectedly good performance of Constant Power. This suggests that SHAPSO might be improved by modifying it to take advantage of baseline methods if they perform close enough to optimal. This modification will have to wait until the entire mission is tested to see if the performance of the baseline methods holds for the entire mission. That and the pending results of Research Questions #2-#4 confirm the need of Experiment #2 to be a test across the entire mission. The only change to the planned Experiment #2 comes from the results of the run time measurements of Dynamic Programming. These indicate that some improvement to the execution of that method may be warranted to allow the experiment to run faster.

Experiment #2: Application to Entire Mission

Using an experiment involving only the cruise segment of a Flight mission, Hypothesis #1 is now confirmed: "the use of optimal power schedules over a typical aircraft mission will yield significant savings in fuel burn". The next experiment, Experiment #2, is designed to answer Research Questions #2 thru #4. Research Question

#2 asks "what factors determine the optimal power schedule?" with Hypothesis #2 stating "the reduction in aircraft weight resulting from burning fuel early in a mission is the dominant factor determining the optimal power usage schedule." This hypothesis was shown to be incorrect in Experiment #1, but the true dominant factor in the complete mission could not be found without simulating the entire mission. Likewise Hypothesis #3 proposes that "the best baseline hybrid power schedule is to use the battery power as late in the mission as possible." This hypothesis was shown to be false for Experiment #1, but the best baseline schedule for a typical mission requires testing of a typical mission profile. Research Question #4 addresses optimization methods for the power schedule, and these methods will now have to deal with the complexities of climb and descent. To test these questions Experiment #2 was chosen to be a test of the different baseline methods and optimization methods over a complete air transport mission. The best performing baseline method will then be directly identified, answering Research Question #3, and the performance of Dynamic Programming and Optimal Control will be measured, proving or disproving Hypothesis #4. The shape of the optimal schedules will be found with Dynamic Programming and the performance of the different baseline schedules will shed enough light on the factors determining the optimal power schedule to answer Research Question #2.
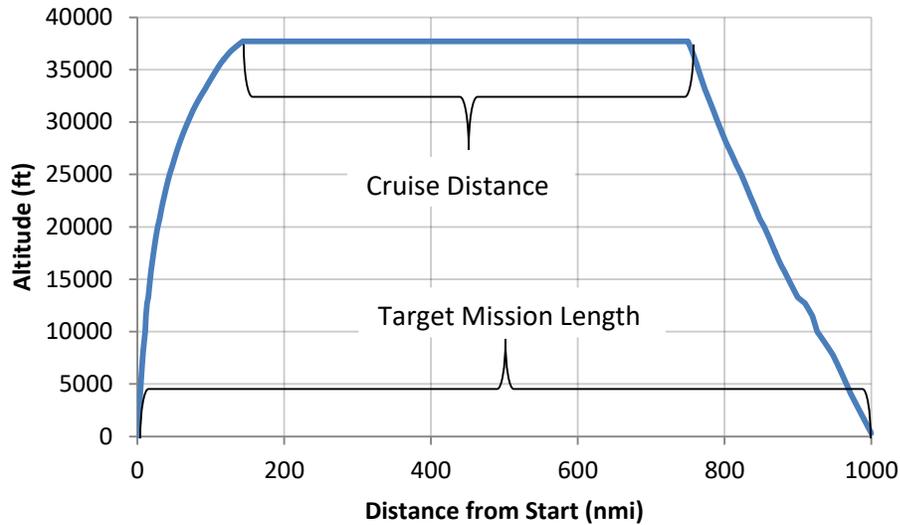
Figure 41: Typical Complete Mission Profile, 1000 nmi. Mission

The complete air transport mission, seen in Figure 41, is a more complex problem than a single cruise segment mission for multiple reasons. Not only does the flight condition and thrust vary greatly through the climb segment, at higher thrust than cruise, but the time and distance to climb is affected by the aircraft weight, and hence can be different for aircraft which use different schemes to reduce fuel weight. The cruise distance must be therefore varied in order to meet the targeted total mission range, as highlighted in Figure 41, for each payload/range/power schedule combination. Accounting for changes in these factors is expected to bring out differences between the different power scheduling methods and impact the answers to the research questions.

Even before modeling is started, the technical assumptions in the engine deck constrain the operation of the aircraft during climb and descent. The engine is modeled under the assumption that the engine cannot produce more thrust than the maximum non-hybrid thrust at any flight condition. This is because when an engine is at full thrust,

114

adding electric power causes the engine core to reduce fuel flow and maintain the same thrust. Therefore any climbing aircraft at full thrust will produce the same thrust at a given flight condition regardless of power scheme. In addition the engine cannot accept electric assist at low thrust levels, as the gas turbine has to remain lit under the operating assumptions. During descent, the gas turbine is at idle thrust and so electric assist cannot be used.

Before applying the methods to the complete mission, the framework had to be modified to handle climb and descent, the time step size had to be revisited, and each method had to be adapted to the different problem.

Modeling Framework Changes

To model a climb or a descent segment, the thrust is set to max or to idle respectively, and the change in energy height over each time step is calculated as explained in Chapter 4. This change in energy height could come from changing the altitude, the Mach number or both, so climb and descent schedules are required to translate an energy height into a Mach number and an altitude.

The ideal climb path for minimum fuel is an optimization problem in itself for conventionally fueled aircraft and was the problem which initially inspired the formulation of Dynamic Programming[64]. Besides the tradeoff between drag polars, engine performance, fuel to climb, and distance/time taken to climb, operational aircraft have air traffic regulations to consider when planning their ascents. There is potential for hybrid propulsion systems to change the optimum climb schedule depending on the use of battery power. Conventional gas turbine engines lapse in thrust with altitude as air

density increases, due to the reduced working fluid for the fan and the reduced oxygen to burn. But electric components only lose working fluid and are not dependent on oxygen, potentially improving their relative performance during climb. However for consistency it was decided to use a fixed climb schedule and descent schedule for all tests, using a procedure which did not utilize battery power.

The engine and airframe models, with hybrid power turned off, were entered into NASA's FLight OPtimzation System (FLOPS) software in order to actually calculate the optimal schedules[95]. FLOPS was configured to find the minimum fuel to distance climb for an air transport. It produced the schedules which are shown in Figure 42 and Figure 43 below. Each of these figures shows the altitude in blue and the Mach number in red as a function of the aircraft's energy height. While the altitude represents the greater part of the aircraft's potential energy, and increases nearly linearly with energy height, the increase in Mach number is not applied uniformly on either schedule. The wrinkles show strange behavior at 10,000 ft in order to comply with speed limits that occur beneath this altitude, and the Mach number of the Climb schedule hooks up at the high end as the final acceleration occurs at altitude as the aircraft departs its ideal climb condition and eases into cruise. The descent schedule generally is at a lower Mach number at any altitude, reflecting the reduced drag and increased glide distance that occurs at this lower speed. Although adjusting the climb schedule was found to affect the resulting power schedules, these original schedules were used for all of the experiments in this thesis.
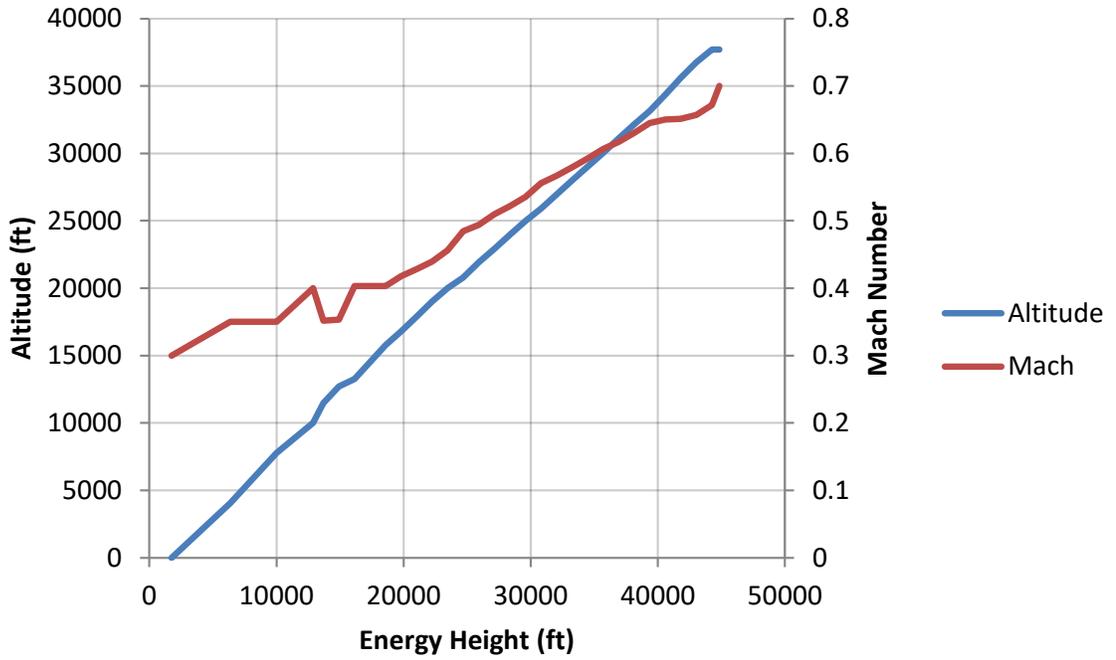
Figure 42: Climb Schedule
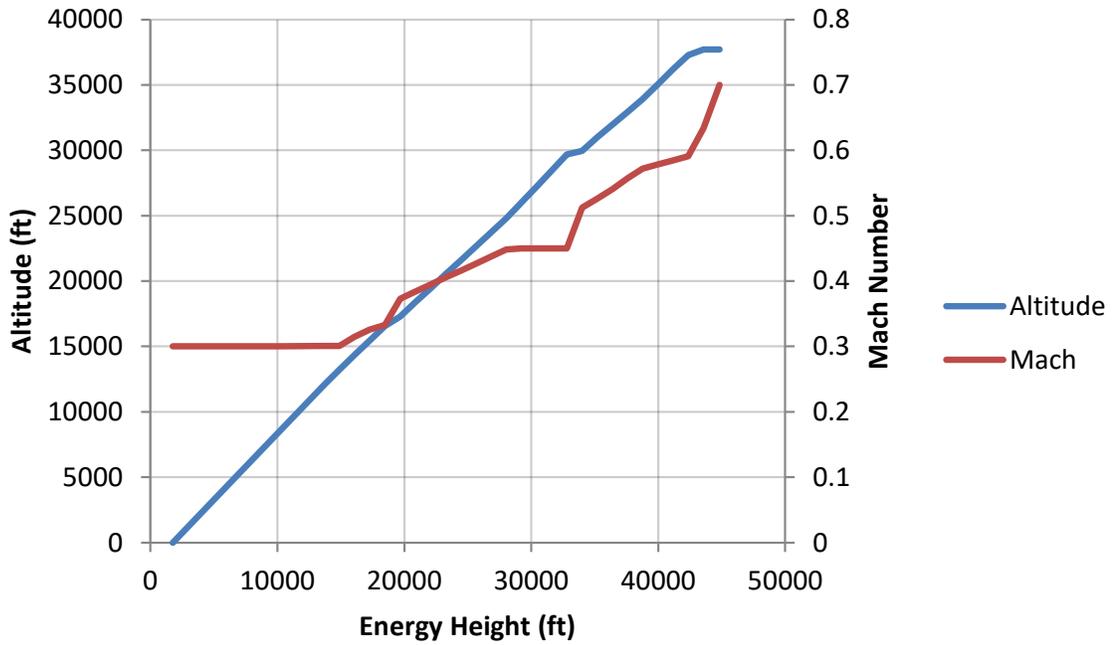
Figure 43: Descent Schedule

117

Integration errors during the cruise segment are caused by the fuel burn and power consumption being considered constant throughout a time step. However during climb and descent the climb and descent rates are also held constant within a time step and therefore also produce integration errors in energy height. These errors cause a more drastic impact than those in the cruise segment as the climb rate in particular lapses with altitude. To find the appropriate time step for simulating climb with minimal integration errors, a study was again performed. This study calculated time to climb, distance to climb and fuel burn on a mission without added power assist as a function of time step. The results are shown in Figure 44 below, and show the climb distance and climb time diverging faster than the fuel burn as the time step is increased from one ten thousandth of an hour to a hundredth. As the error at .01 or even .005 hour was too great, the time step of .001 hour was chosen for simulating the climb and descent segments, while the cruise segment was still simulated at .01 hour.
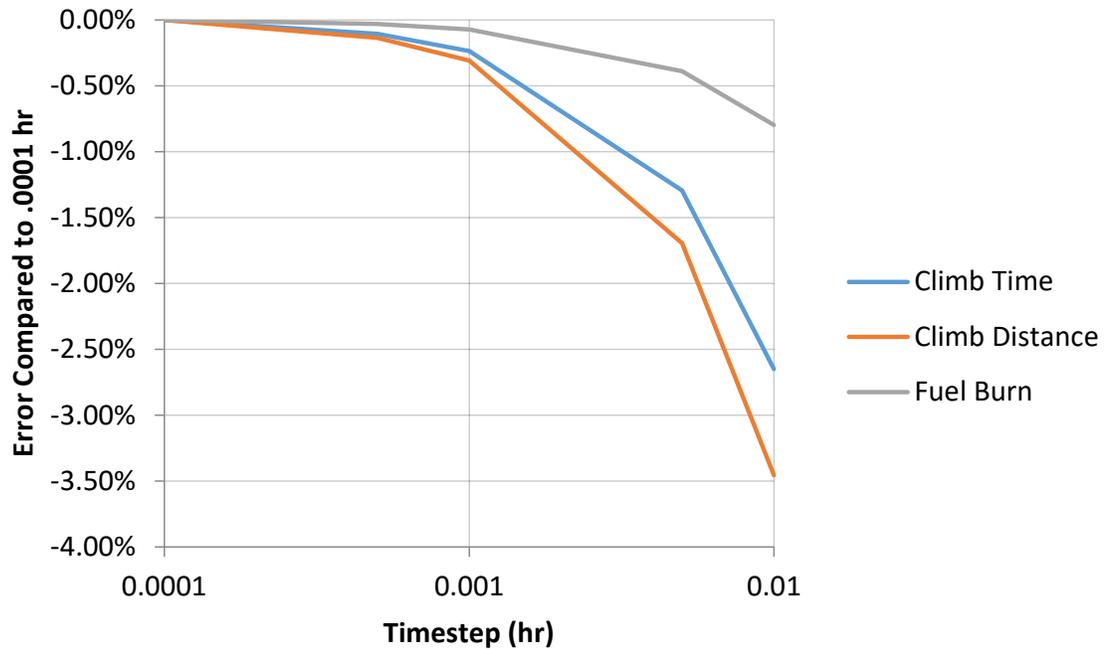
Figure 44: Experiment #2 Time Step Study

The small differences found in Experiment #1 motivated additional care in ensuring any errors were as small and as consistent as possible. For this reason all of the schedules and methods were integrated in reverse, starting at the end of the mission, to be consistent with Dynamic Programming, which operates in reverse by nature. In addition, to the greatest extent possible, identical code was used for different methods. The only differences between Optimal Control, Constant Power, and the other non-Dynamic Programming methods became the lines of code setting the electric power level at each time step and the wrapped around solvers which varied the power level, electric cost variable, or power start time to meet the battery constraint.

Implementation of Each Method

Dynamic Programming

With each method the two key tasks were to implement climb and to handle the climb-cruise transition. The descent segment is precomputed separately as it did not contain any battery usage. The climb segment poses some difficulty as the different parallel evaluations created by Dynamic Programming have different aircraft weights and therefore different climb rates. The parallel evaluations of the climb segment, starting at top of climb, diverge in altitude as they descend due to these weight differences. However the optimal path of interest, which uses the least fuel, also climbs the fastest, and therefore will be the first to complete the segment. Under this reasoning, the climb segment continues until one of the paths reaches the bottom of climb, and this first path is always the one which has completely consumed the battery and used the minimum amount of fuel.

The splice between cruise and climb is accomplished by changing the end of the cruise code and the starting point of the climb code, since the mission is executed in reverse. Instead of truncating the space at the end of the cruise code, as was done in Experiment #1, the cruise code progresses until the path matrix has the ideal path from any battery charge at the beginning of cruise to the end of cruise and the fuel weight vector has all the fuel levels corresponding to these states of charge. This fuel vector is then passed to the climb code at the point where the code is not truncated at the beginning and starts from all 100,001 levels with 100,001 different starting fuel levels. The path

which reaches the ground first is then traced back through both path matrices, and the power schedule extracted.

Instead of rerunning the power schedule time step for time step as in experiment #1, the energy height and power schedule are both saved during the original execution of Dynamic Programming and used to create an energy height based power schedule for climb and a distance based motor power schedule for cruise. These schedules are read during the "Decide Power Setting" block of the conventional simulation code used for the other methods, linearly interpolating the current power setting from these correlated vectors. This prevents a slight mismatch in time segments from causing the motor to turn on at altitudes other than that selected by Dynamic Programming during climb. Any small error left in the remaining battery power is eliminated by scaling the entire power schedule up or down slightly until the battery is exactly consumed.

Due to the increased number of time steps and the elimination of some space-truncation methods, the execution time of Dynamic Programming was prohibitively long when using the same execution methods as Experiment #1. So instead of using the parallel computing toolbox, the MATLAB Coder toolbox was used to compile the Dynamic Programming code into C functions which executed hundreds of times faster. Conflicting versions of MATLAB and the compilers prevented the compiled code from using parallelization. Despite this the execution time was brought down to about 24 hours on a standard workstation, depending on the length of the mission being simulated. If parallelization were used, the execution time could possibly be brought down to 6 hours or less. In comparison, the same Matlab compilers were used on the other methods and brought their execution time down to less than 5 seconds per case.

Because of the long execution time, the Dynamic Programming runs were only used as the baseline for the other methods, which ran to exactly the same point in distance and battery consumption. This enabled a fair comparison to be drawn between them.

Constant Power

The Constant Power case was run using the same power schedule testing script which was used to get the final Dynamic Programming results, but the assigned power schedule was a constant value over the mission. The battery power was varied by an outer loop solver in order to set the power schedule to be a constant value which exactly drained the battery over the course of the mission. In addition an outer loop solver was used to lengthen or shorten the cruise segment so that it would cover the same distance as the original Dynamic Programming run for each case.

Full Power During Climb

With the addition of the climb segment, a new baseline power schedule called Climb Power was used in place of the Start Power schedule used in Experiment #1. In the Climb Power schedule, the highest constant power possible is used during climb with the remainder of the battery used up at a constant power over the cruise segment. This change in power schedule was implemented by making a slight modification of the Constant Power code. The code was set to check if the battery is above the (precomputed) size required to run the entire climb segment at full power. If so, the code set power to full during climb and to the existing constant power level during cruise, using the same solver setup as Constant Power. If the battery is smaller than the minimum required for

122

climb at full power, the code sets the power during cruise to zero and varies the climb power using the Constant Power solver.

Save Power Until End

The original Hypothesis #3 method was carried forward into Experiment #2, despite its failure in Experiment #1, in order to see how well it performed in the full mission. Because the engine could not accept hybrid power during descent, this meant that the maximum power was used during the last part of the cruise segment. The battery power start point was chosen by a solver in order to empty the battery, with the very first time step turning the battery power on at an intermediate level calculated to exactly empty the battery despite the discrete time simulation.

Optimal Control

The Optimal Control implementation began with the same code as the Constant Power implementation in order to eliminate errors from different integration schemes or from handling the climb/cruise transition differently. The only two changes made to this code were located in the power selection step and in the outer loop. The power selection step was changed by minimizing the weighted sum of fuel burn and battery power at each time step. The outer loop was changed by varying the weighting of electrical power in the sum of electrical power and fuel burn in order to cause the battery to be exactly emptied, just as in Experiment #1. Unlike Experiment #1 the power schedules found during initial testing of Optimal Control were unexpected. An early example is in Figure 45 below.
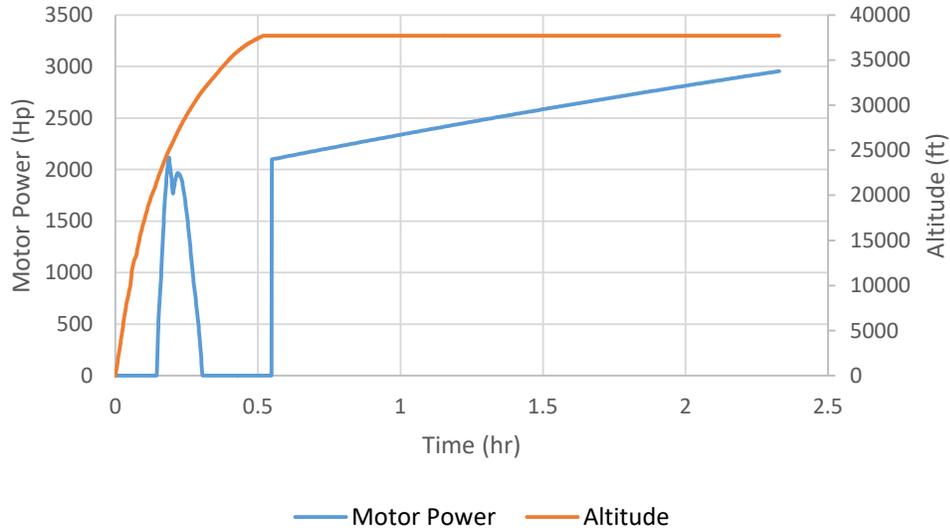
Figure 45: Optimal Control 900 nmi, 20,457 lb. Battery, 35,000 lb. Payload, Early Engine Surrogate

This unexpected hump in the blue Motor Power curve during climb became apparent whenever the cruise thrust was high (due to a heavy load) and the available battery power was above a certain level. Closer examination of the engine deck under the weightings used here revealed that Optimal Control had found an island in the engine deck, where added power causes the greatest reduction in fuel burn. This is shown in Figure 46 below, which shows the difference in fuel burn between a single engine run with zero motor power and an engine run with 1,500 HP of motor power across the climb schedule.
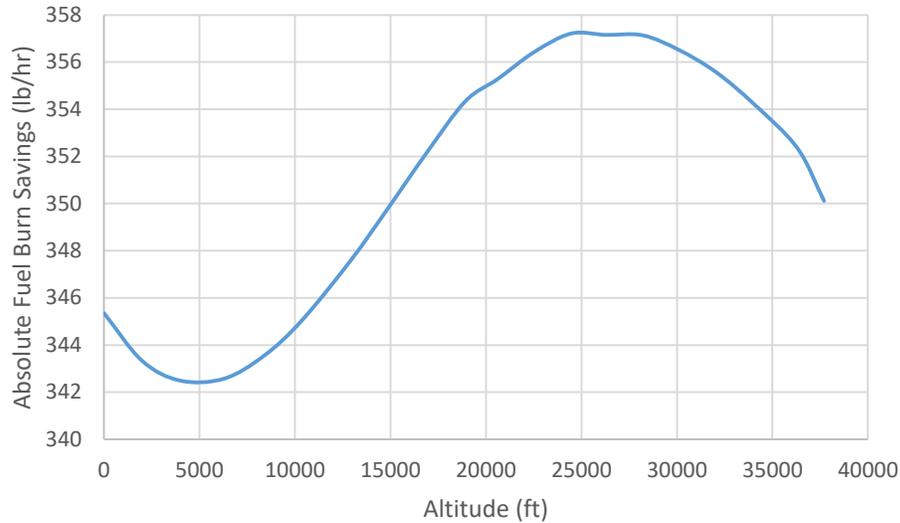
Figure 46: Fuel Savings from 1,500 HP of Assist at Full Thrust along Climb Schedule, One Engine

The peak in at 25,000 ft. showed up in the mission battery power histories only when there was not greater fuel savings to be had during cruise. The same delta between zero assist and 1,500 HP assist was graphed for cruise conditions, sweeping the power code from maximum thrust (power code of 50) to below the typical cruise thrust levels (between 42 and 44), as seen in Figure 47. For light missions the cruise thrust was low enough that Optimal Control used the entire battery during cruise. If the vehicle was heavy enough that the cruise power code was 44 or more, the Optimal Control solver would preferentially use the battery power during climb to take advantage of the efficiency curve seen in Figure 46, producing power histories like those seen in Figure 45.
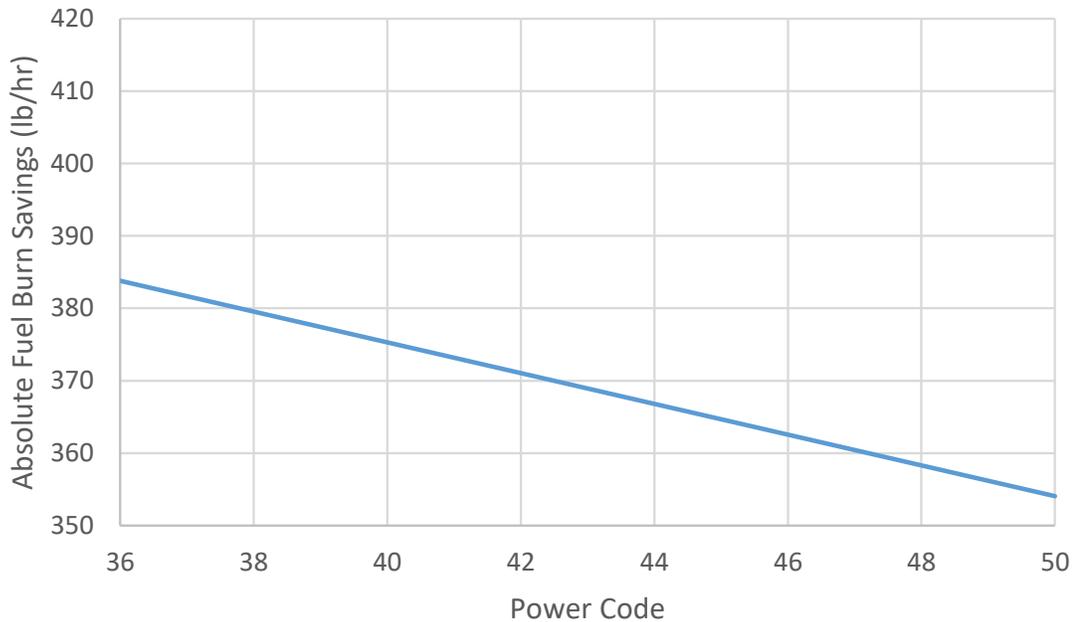
Figure 47: Fuel Savings from 1500 HP of Assist at Cruise Conditions, One Engine

Looking at the engine decks it became clear that the Optimal Control algorithm was working as intended, and finding a source of fuel savings that had not been previously found, although early runs of Dynamic Programming also found the same efficiency island at around 25,000 ft. during climb. What was less clear was the cause of this efficiency island in terms of the physical interaction between the hybrid components, the gas turbine engine, and the airframe as it climbed through this altitude. Testing found that the island moved slightly if the climb schedule was shifted but persisted as long as the cruise thrust level was high enough. The next thing to check was the surrogate model itself, comparing it to the source data table, which had to be done at a constant Mach climb due to the grid spacing of the data table. The results, shown in Figure 48 below, show that when the engine model is examined this closely, it does not match the original

data as well as required. The expected behavior would have the engine surrogate model tracing a line neatly through the engine data points, or nearly so. However Figure 45 shows an error of 20% or more, and a trend that reverses the actual trend, showing a maximum savings at 30000 ft instead of a minimum savings at 35000 ft.
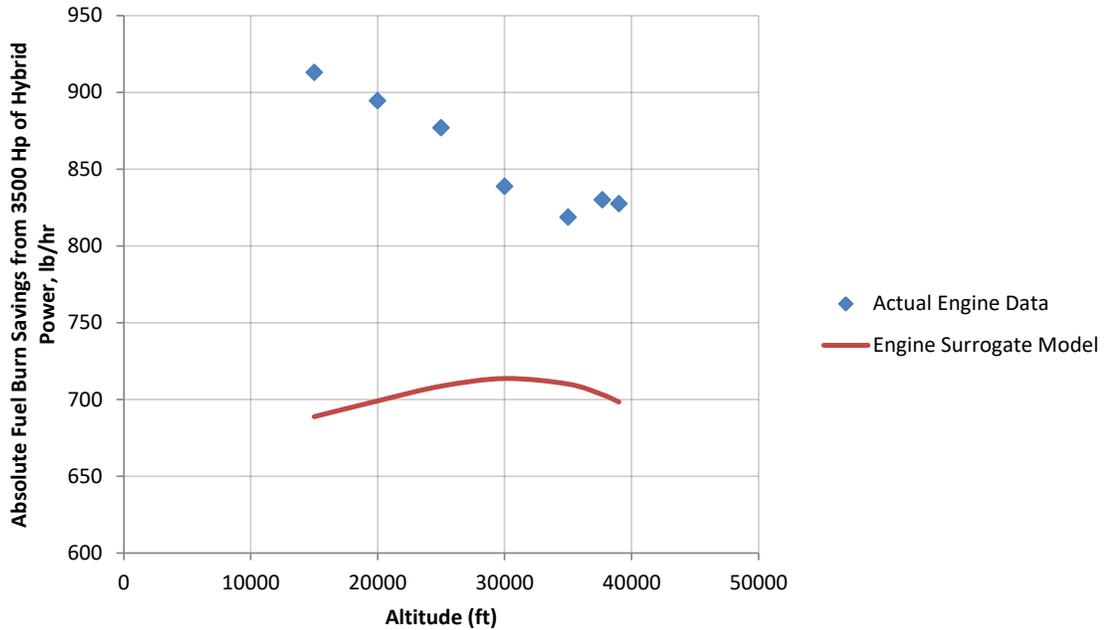
Figure 48: Comparison of Engine Model to Source Data at Mach .6, Full Thrust

Based on the results of this test, the engine surrogate model had to be regenerated with much tighter tolerances in order to capture the trends of the actual engine model when looked at differentially and at high resolution. The original engine surrogate used a single fit over the entire flight envelope and could produce any thrust at any altitude/Mach number with any level of electric assist. In contrast, the new surrogate was made in three pieces. One surrogate function was used to fit at the fixed cruise condition,

where only thrust and hybrid assist could change. Another was fit to descent, where thrust is at idle and hybrid power cannot be used. And a third was created for the climb segment, using data resampled from the NPSS model along the fixed climb schedule, with a tight fit exploiting the facts that thrust is always at maximum during climb and that each altitude has a corresponding Mach number. This climb engine deck remained the most difficult to fit, but the resulting statistics are shown in Table 8 below. They show a very small average error for all three response variables, small standard deviations, and R-squared values practically or actually equal to 1, indicating a very tight fit.

Table 8: Properties of Engine Surrogate Model During Climb

Property	Value
Fuel Burn R-Squared	.9999935
Fuel Burn Mean Error	.00105%
Fuel Burn Error Standard Deviation	. 18%
Net Thrust Error R-Squared	.999998
Net Thrust Mean Error	.00000863%
Net Thrust Error Standard Deviation	.00886%
Battery Power R-Squared	1
Battery Power Mean Error	-.00000376%
Battery Power Error Standard Deviation	.008863%

This tight fit was only made possible by fixing the cruise flight conditions and the climb and descent schedules. These restrictions prevent any studies on the impact of changing the cruise altitude or optimizing the climb. The resulting model was compared to the source data, which was also taken along the climb schedule, with the results seen in Figure 49 below. This shows a fit that very nearly follows the data. Of note, the additional data taken for this model along the climb schedule is more available for

comparisons of fit along the climb schedule than the data used for the model discussed in

Experiment #1. Importantly this surrogate model not only tracks the value of the points, it

shares the trends of the real data and can be expected to have maxima and minima in the

same places as the NPSS model if the NPSS model were run directly. This fit is still not

perfect, but it does capture the trends of the physics based model well enough that the

same general power schedules should be found by the different optimization methods.

Therefore it was used for the duration of Experiments #2 and #3.
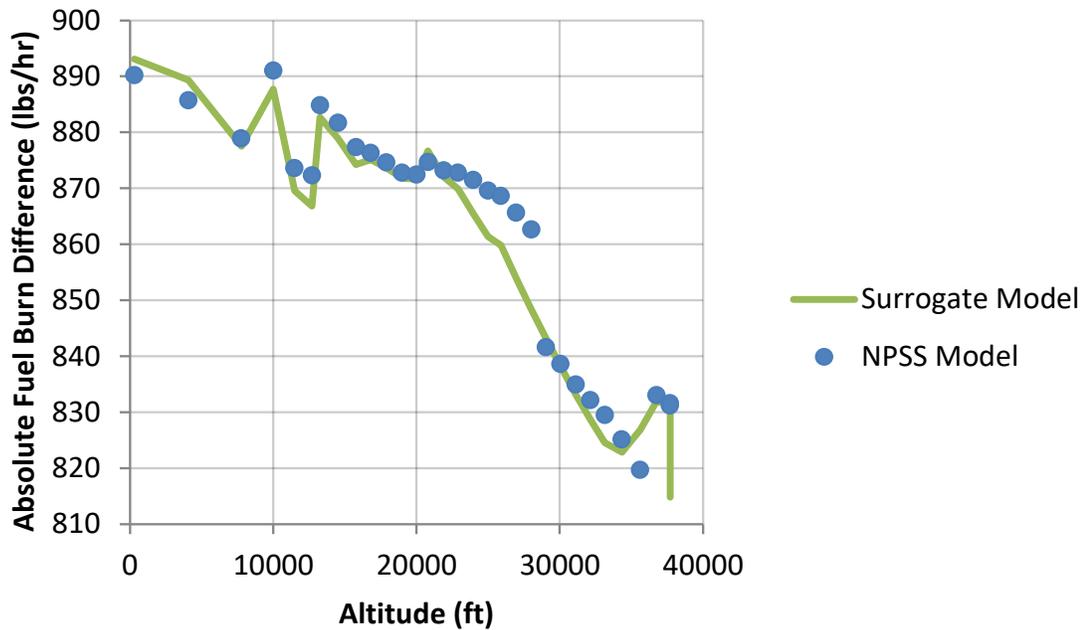
Figure 49: New Surrogate Model Fuel Savings from 3,500 HP Hybrid Power

In addition to the difficulties with the surrogate model, during the development of

Optimal Control an error in the assumptions was found which compromised the

performance until it was corrected. The Optimal Control code is fundamentally based on

a weighted function of electricity and fuel required to operate the engine, but the

measurement of electricity consumed was at the terminals of the battery. This measurement did not account for the losses within the battery-the battery resistance, which increases with the square of the power drawn and is a function of the size of the battery. To take this into account and properly disincentivize higher power levels, the cost function was augmented by including the efficiency of the battery in the Optimal Control score function. The efficiency equations from the battery model were based on the efficiency of one of the cells in the battery, having a nominal voltage, resistance, and size. The power through one nominal cell is given by Equation 40 below.

$$ScaledPower = Power * \frac{Capacity\ of\ Nominal\ Cell}{Capacity\ of\ Battery} \tag{40}$$

The current draw from that battery is greater than it would be for an ideal battery due to the voltage drop from the internal resistance. The resulting quadratic equation for the current through one cell is shown in Equation 41 below.

$$I_{cell} = \frac{\left(V_{cell,ideal} - \sqrt{V_{cell,ideal}^2 - 4R_{cell} * ScaledPower}\right)}{2R_{cell}} \tag{41}$$

The Voltage drop is therefore given by Equation 42, and the battery efficiency by Equation 43.

$$V_{drop} = I_{cell}R_{cell} \tag{42}$$

$$Eff_{batt} = \frac{V_{cell,ideal} - V_{drop}}{V_{cell,ideal}} \tag{43}$$

This makes the cost function being minimized by Optimal Control to be that given in Equation 44.

$$cost = \dot{w}_f + \lambda \frac{Power}{Eff_{batt}} \tag{44}$$

Experiment #2 Results

One question not directly listed in chapter 3 but related to Research Questions #2 and #3 is: "What actually is the global optimum power schedule?" The Dynamic Programming results show that the power schedules vary depending on the range and available battery but have a peak power during the lower part of climb and use a linear schedule during cruise as found in Experiment #1. This can be seen in Figure 50 and Figure 51 below which depict the motor power level vs. distance from start as determined by Dynamic Programming. Figure 50 shows that the aircraft carrying the larger battery at short range uses hybrid assist throughout the mission. In the case with a smaller battery at long range shown in Figure 51 the system instead turns it off during the latter part of climb to conserve power for cruise.
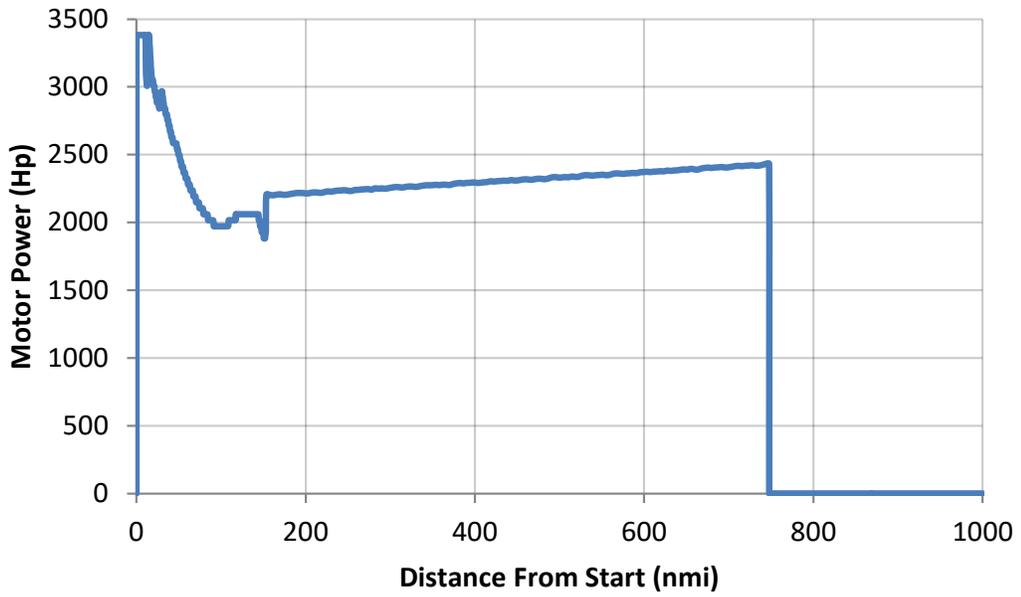
Figure 50: Dynamic Programming Power Schedule, 20,000 lb. Battery, 25,000 lb. Payload, 1,000 nmi. Mission
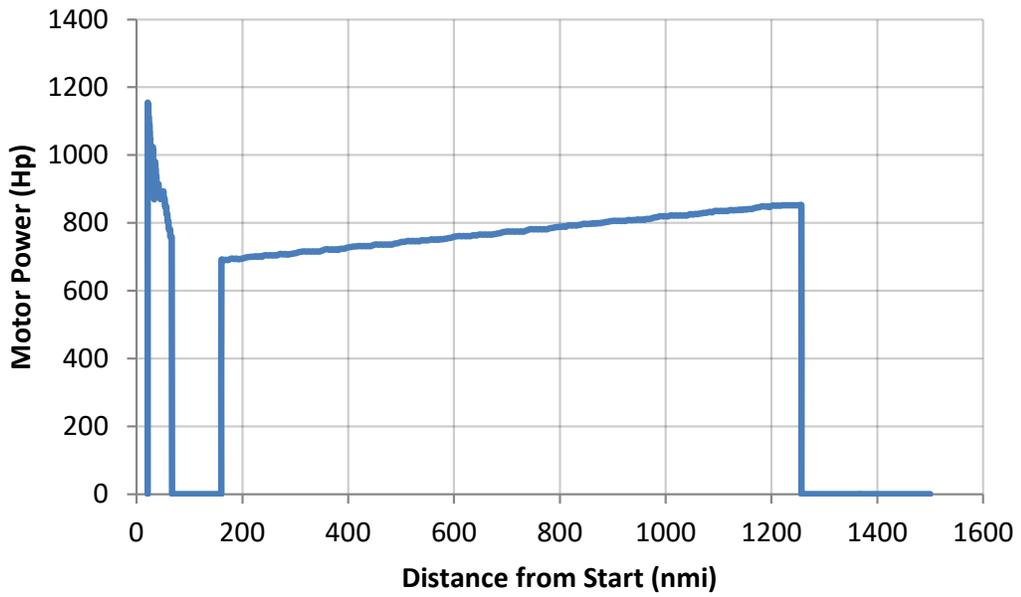
Figure 51: Dynamic Programming Power Schedule, 10,000 lb. Battery, 25,000 lb. Payload, 1,500 nmi. Mission

The baseline methods tested in accordance with Research Question #3 performed as seen below in Table 9. Because the numbers are still close together, the percent difference compared to the optimal performance found with Dynamic Programming is shown in Table 10. These tables show that Constant Power remains the best of the baseline schedules across the tests, and is therefore the answer to Research Question #3: "What is the best baseline power schedule" for this hybrid aircraft system. Instead of the Experiment #1 Start Power method, an alternative baseline schedule, Climb Power, was introduced in this experiment as described on page 122. This method uses full motor power during climb and a lower constant motor power, chosen to empty the battery, during cruise. This performed better against End Power than Start Power did in Experiment #1, which sheds light on Research Question #2 showing that the fuel burn savings effect of using power at the end of the mission is not as strong as anticipated.

Table 9: Fuel Burn (lbs.) of Baseline Schedules and Dynamic Programming

Range (nmi.)	Battery (lbs.)	Dynamic Programming	Constant	End Power	Climb Power
1500	20000	8251.302	8251.736	8393.431	8301.243
1479	10000	8837.758	8840.286	9019.024	9004.342
1000	20000	5012.323	5013.39	5089.516	5026.975
1000	10000	5803.615	5803.656	5964.37	5920.508

Table 10: % Increase in Fuel Burn of Baseline Schedules vs. Dynamic Programming

Range (nmi)	Battery (lbs)	Constant	End Power	Climb Power
1500	20000	0.005%	1.723%	0.605%
1479	10000	0.029%	2.051%	1.885%
1000	20000	0.021%	1.540%	0.292%
1000	10000	0.001%	2.770%	2.014%

In order to further explore Research Question #2 and the relative weights of the different influences on power schedule performance, these four power schedule choices were repeated using a battery with reduced resistance, setting the resistance to 50% and 0% of its original value. The complete set of these results is shown in Table 11 and Table 12 below, showing the absolute values and the percent difference from the Dynamic Programming results respectively.

Table 11: Fuel Burn (lbs.) of Baseline Schedules and Dynamic Programming With Reduced Battery Resistance

Resistance	Range (nmi.)	Battery (lbs.)	Dynamic Programming	Constant	End Power	Climb Power
50%	1500	20000	8216.237	8216.658	8304.123	8250.05
50%	1500	10000	8951.344	8955.944	9045.427	9047.864
50%	1000	20000	4906.793	4908.81	4951.507	4916.331
50%	1000	10000	5771.589	5771.592	5855.039	5830.682
0%	1500	20000	8177.491	8180.551	8220.555	8201.58
0%	1500	10000	8929.162	8938.118	8958.876	8984.579
0%	1000	20000	4896.577	4900.028	4918.289	4904.257
0%	1000	10000	5739.59	5742.307	5768.92	5768.275

Table 12: % Increase in Fuel Burn of Baseline Schedules vs. Dynamic Programming at Reduced Battery Resistances

Resistance	Range (nmi)	Battery (lbs)	Constant	End Power	Climb Power
50%	1500	20000	0.005%	1.070%	0.412%
50%	1500	10000	0.051%	1.051%	1.078%
50%	1000	20000	0.041%	0.911%	0.194%
50%	1000	10000	0.000%	1.446%	1.024%
0%	1500	20000	0.037%	0.527%	0.295%
0%	1500	10000	0.100%	0.333%	0.621%
0%	1000	20000	0.070%	0.443%	0.157%
0%	1000	10000	0.047%	0.511%	0.500%

The reduction in battery resistance improves the relative performance of the End Power and Climb Power schedules, and worsens the performance of Constant Power in almost every case when compared to the new global optimum schedules. However despite that, Constant Power still outperforms the other baseline methods in every case. The significant improvements in the other methods show that battery resistance is the dominant factor in the typical case, but the hybrid engine's performance alone is still enough to drive a preference for Constant Power over these methods. Notable too is that the Climb Power method does better than the End Power method except on the longer missions with the smaller batteries. On these missions, the fuel burned late in the mission must be carried the furthest.

Further insight into Research Question #2: "What factors determine the optimal power schedule?" and a more direct evaluation of Research Question #4: "What methods can be used to find better hybrid power schedules?" are given by the performance of Optimal Control when compared to Dynamic Programming, shown for all twelve of these cases in Table 13 and Table 14 below. These tables again show the mission fuel burn for the full mission with the range specified, a fixed payload of 25000 lbs, and the battery and battery resistance as shown. The differences in performance are better seen in Table 14 as a percentage difference, which show that both Constant Power and Optimal Control consume slightly more fuel than Dynamic Programming. Dynamic Programming continues to outperform Optimal Control and Constant Power as expected.

Table 13: Dynamic Programming, Constant Power, and Optimal Control Fuel Burn, lbs.

Resistance	Range (nmi.)	Battery (lbs.)	Dynamic Programming	Constant Power	Optimal Control
100%	1500	20000	8251.302	8251.736	8252.707
100%	1479	10000	8837.758	8840.286	8840.091
100%	1000	20000	5012.323	5013.39	5012.929
100%	1000	10000	5803.615	5803.656	5803.798
50%	1500	20000	8216.237	8216.658	8217.291
50%	1500	10000	8951.344	8955.944	8955.608
50%	1000	20000	4906.793	4908.81	4907.069
50%	1000	10000	5771.589	5771.592	5771.71
0%	1500	20000	8177.491	8180.551	8180.011
0%	1500	10000	8929.162	8938.118	8937.3
0%	1000	20000	4896.577	4900.028	4897.136
0%	1000	10000	5739.59	5742.307	5741.921

Table 14: Optimal Control and Constant Power % Increase in Fuel Burn Compared to Dynamic Programming

Resistance	Range (nmi)	Battery (lbs)	Constant Power	Optimal Control
100%	1500	20000	0.005%	0.017%
100%	1479	10000	0.029%	0.026%
100%	1000	20000	0.021%	0.012%
100%	1000	10000	0.001%	0.003%
50%	1500	20000	0.005%	0.013%
50%	1500	10000	0.051%	0.048%
50%	1000	20000	0.041%	0.006%
50%	1000	10000	0.000%	0.002%
0%	1500	20000	0.037%	0.031%
0%	1500	10000	0.100%	0.091%
0%	1000	20000	0.070%	0.011%
0%	1000	10000	0.047%	0.041%

Surprisingly, for most of these cases, Optimal Control actually performs worse than Constant Power as a power scheduling method. To look closer at the differences, the

136

power schedules for one case are shown in Figure 52 below. This figure shows the constant power in red being slightly more than the Optimal Control power level during cruise, while Dynamic Programming strikes a linear schedule in cruise reminiscent of Experiment #1. During climb both Optimal Control and Dynamic Programming use maximum power at low altitudes but drop to lower power levels at the end of climb. Optimal Control is using more power than Dynamic Programming at the beginning of the mission but less at the end and lacks the slope during cruise that Dynamic Programming consistently applies. It was realized that the Optimal Control equations never directly evaluate applying power at one end of the mission to applying it the other. Thus it neglects the effect of changing fuel weight on the power schedules. This inspired improvements to Optimal Control.
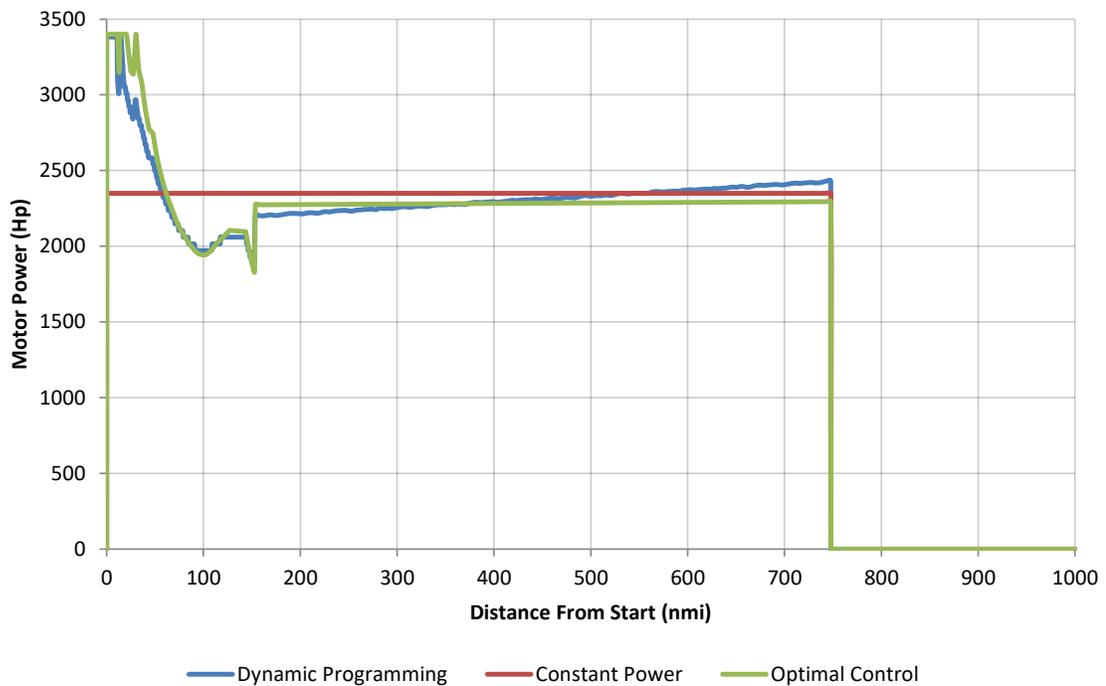
Figure 52: Power Schedules at 100% Battery Resistance, 20,000 lb. Battery, 1,000 nmi. Mission

137

Improvements to Optimal Control

As became evident in the Experiment #2 results, a fundamental weakness of Optimal Control is that it does not directly evaluate the effect of burning more fuel in one part of the mission on the thrust required in another part of the mission. Instead it simply finds the instances at which applied battery power could most reduce fuel burn instantaneously. This is reflected in the cost function optimized in each time step of Optimal Control, shown in Equation 45 below.

$$J = A\dot{w}_f + \lambda P_e \tag{45}$$

The factor A was fixed in the Optimal Control runs to this point. Its value was set at a constant value of 10000 which chosen to handle the difference in units, as $\dot{w}_f$ is in pounds of fuel per hour and P_e is in watts. The factor on the electrical power, λ, is varied by the mission level solver for each case. It is set to the value which when used at every time step in the mission causes the total mission electric power consumption to exactly consume the battery. If λ is calculated and left alone to continue ensuring the battery is fully utilized, changing the weighting factor on the fuel, A, over the course of the mission becomes a simple way to make Optimal Control account for the amount of energy used to carry fuel to a certain point in the mission and encourage burning fuel earlier rather than later. The question was how much to vary the fuel weighting, and according to what schedule.

Instead of trying to invent a penalty schedule for fuel from scratch, the amount of fuel required to carry weight to a certain point was measured. A version of the Optimal

Control code was created which carried an additional penalty weight for part of the mission. The distance that the weight was carried before being dropped was then varied from the start of the mission to the end. The total mission fuel burn as a function of the distance the penalty weight was carried is shown in Figure 53 for a 100 lb. penalty weight carried to different points in the first 800 nmi. of a 1,000 nmi. mission. Descent was excluded since no electrical power can be used in descent. The mission fuel burn increases most rapidly as the payload is carried through climb, with the taper off of the curve roughly corresponding to the decrease in climb rate with altitude, indicating the increase in work simply to lift the extra 100 lb. weight to altitude. However it still costs a pound of fuel to carry the 100 lb. penalty weight through the cruise segment.
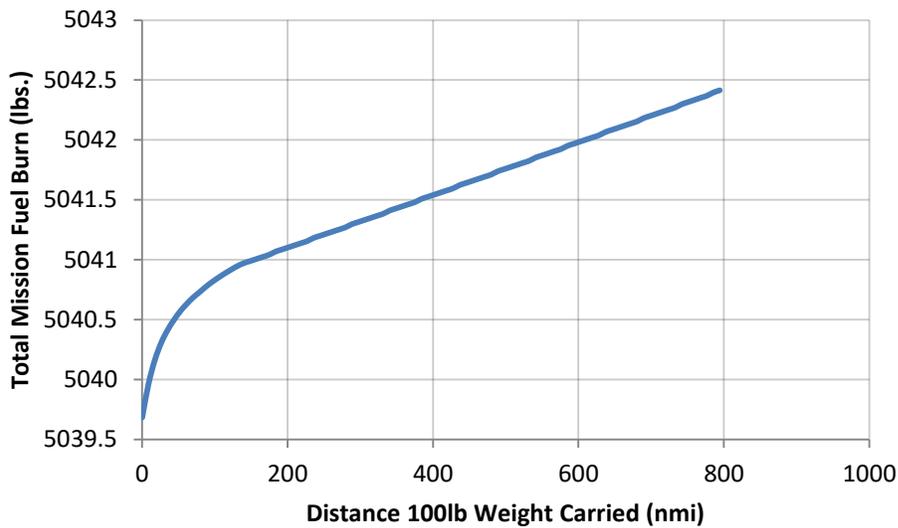
Figure 53: Mission Fuel Burn vs. Distance Penalty Weight Carried

Repeating this for different battery sizes and mission distances revealed similar curves differing in magnitude but still showing the steeper increase during climb and the

gradual increase in fuel burn as the payload is carried through cruise. Instead of trying to find a general form of this penalty function for all missions, the curve was generated for each mission and adapted into a penalty function. First this fuel burn number was normalized by the mean of the curve, and then scaled to change the magnitude of the cost variation using Equation 46 below, where FuelBurn(x) is the mission fuel burn having carried a 100lb. payload x nmi. as in Figure 53, and Mean(FuelBurn) is the average of the same curve over all distances in the mission.

$$FuelCost(x) = 1000 \left(1 + ScaleFactor \left(\frac{FuelBurn(x)}{Mean(FuelBurn)} - 1 \right) \right) \qquad (46)$$

The scale factor determining the magnitude of the effect to minimize fuel burn was sought experimentally and found to be different for different payload/range combinations. Rather than fixing it at some compromise point, the minimization procedure was included in the final method, called Weighted Optimal Control. The resulting power schedules are in many cases significantly closer to Dynamic Programming than the original Optimal Control is as shown in Figure 54. This figure shows the purple Weighted Optimal Control line tracking the blue Dynamic Programming line nearly exactly for the bottom half of climb and the first half of cruise, differing slightly by using less power in the second half of climb and more in the second half of cruise.
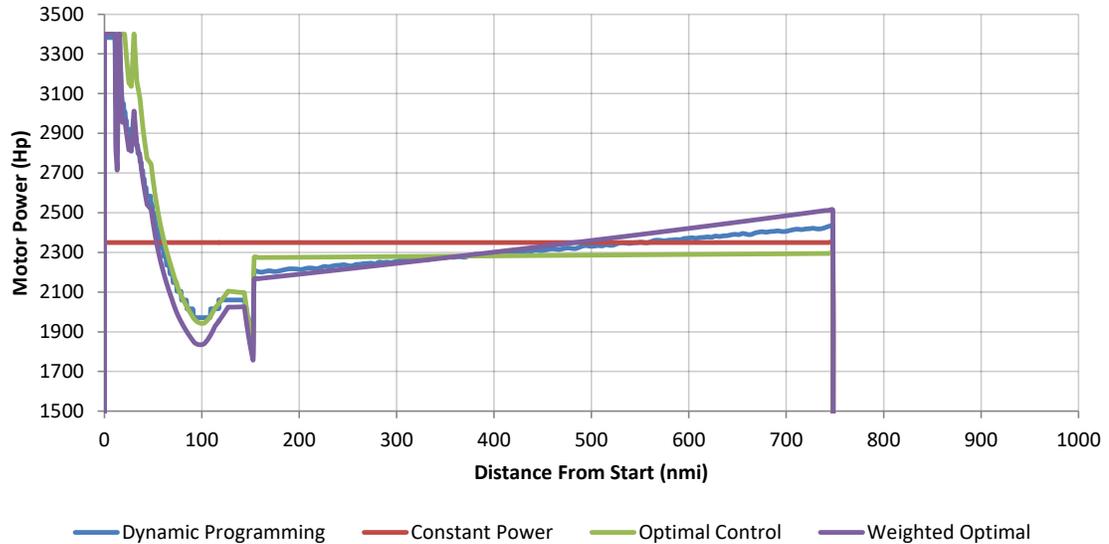
Figure 54: Power Schedules for 1,000 nmi. Mission, 25,000 lb. Payload, 20,000 lb. Battery 100% Resistance

Although this method does find a better answer than Optimal Control, and can find one closer to the Dynamic Programming answer, it does so at the risk of a drastic increase in execution time. Each run of the model requires first generating the weighting function by performing 100 runs of the original Optimal Control method carrying the extra weight and then running a minimizer on the mission which takes another 20 or so Optimal Control runs depending on the convergence criteria and initial guess. In addition after examining the different cases, it appeared that the main factor driving the scale factor selection was the amount of power used during climb vs. cruise. The cruise segment itself was always a slightly increasing but near constant value. This inspired a compromise method which only optimized the climb vs. cruise use problem, seen below in Figure 55.
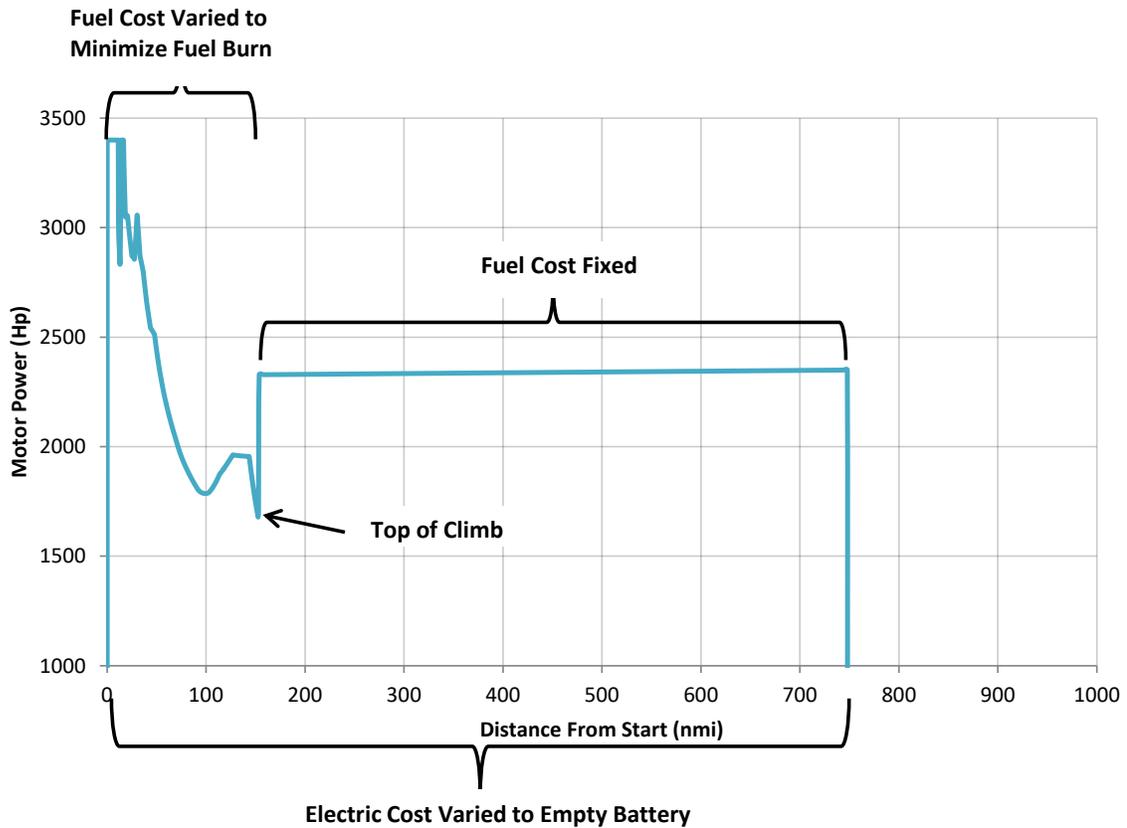
Figure 55: Two Level Optimal Control

This compromise method, called Two Level Optimal Control, uses the cruise segment flag inside the mission simulator to switch between two different weightings on the fuel. As shown in Figure 55, the fuel cost during cruise is left at its standard value, while the cost during climb is varied by an outer loop to find the level which minimizes fuel burn. The weighting on electric power usage is still fixed throughout the mission and varied by the outer loop to empty the battery. The power schedules found using this method were compared to the other methods as seen below in Figure 56.

142
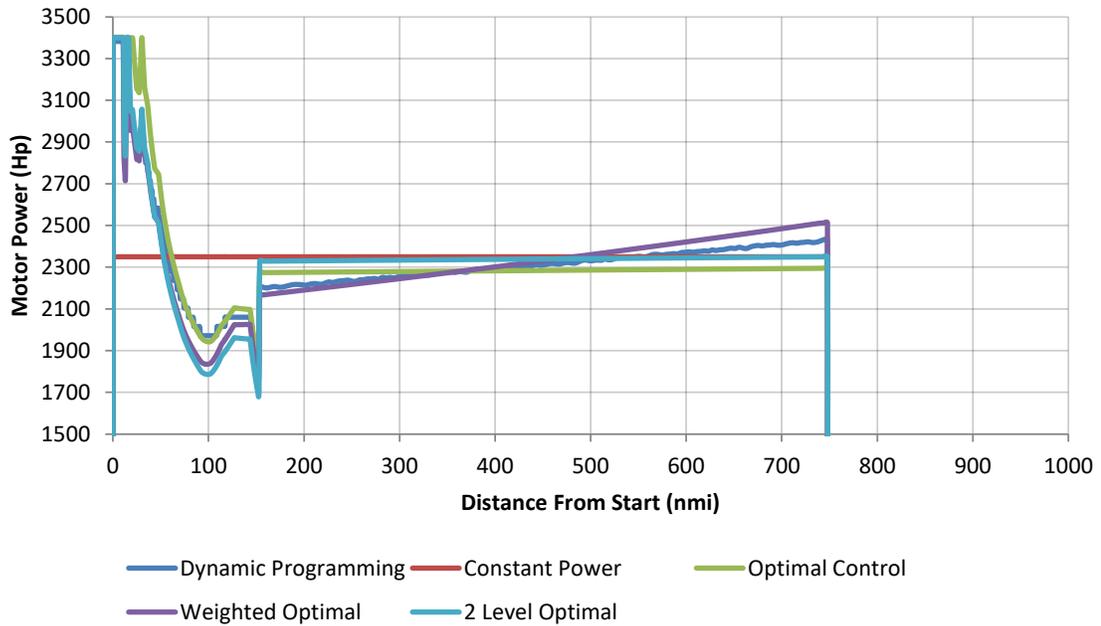
Figure 56: Comparison of Different Power Scheduling Methods, 1,000 nmi. Mission, 25,000 lb. Payload, 20,000 lb. Battery 100% Resistance

Figure 56 above shows that for this case Two Level Optimal Control tracks Weighed Optimal Control fairly closely during the climb segment. During cruise the light blue Two Level Optimal Control line is much flatter than Dynamic Programming and Weighted Optimal Control as expected from its constant weighting factors during that segment. It tracks instead very well with Constant Power during cruise, intercepting the linear cruise power schedule of Dynamic Programming at nearly the midpoint of cruise.

These two methods only improve on the fuel burn found by Optimal Control, as they both reduce to the original Optimal Control if the Weighted Optimal Control scale factor is zero or the Two Level Optimal control climb fuel cost is the same as the cruise fuel cost. These climb fuel cost and scale factor values would be chosen by the optimizer

if the original Optimal Control had the lowest fuel burn. Weighted Optimal Control and Two Level Optimal Control can be seen to have a better fuel burn than the original Optimal Control in Table 15 below. In fact they surpass Dynamic Programming in a few of the cases. As the Linear schedule demonstrated in Experiment #1, it is possible to do slightly better than Dynamic Programming due to Dynamic Programming's resolution limits which limit power choices to ~26 HP increments during the climb segment

Table 15: Experiment 2: % Fuel Burn Savings Compared to Dynamic Programming

Resistance	Range (nmi)	Battery (lbs)	Baseline Schedules			Optimal Control		
			End Power	Climb Power	Constant	Original	Weighted	Two Level
100%	1500	20000	1.723%	0.605%	0.005%	0.017%	-0.005%	0.002%
100%	1479	10000	2.051%	1.885%	0.029%	0.026%	0.022%	0.018%
100%	1000	20000	1.540%	0.292%	0.021%	0.012%	0.000%	0.004%
100%	1000	10000	2.770%	2.014%	0.001%	0.003%	-0.002%	0.000%
50%	1500	20000	1.070%	0.412%	0.005%	0.013%	-0.010%	0.000%
50%	1500	10000	1.051%	1.078%	0.051%	0.048%	0.040%	-0.013%
50%	1000	20000	0.911%	0.194%	0.041%	0.006%	-0.001%	0.003%
50%	1000	10000	1.446%	1.024%	0.000%	0.002%	-0.005%	-0.003%
0%	1500	20000	0.527%	0.295%	0.037%	0.031%	0.009%	0.021%
0%	1500	10000	0.333%	0.621%	0.100%	0.091%	0.043%	0.005%
0%	1000	20000	0.443%	0.157%	0.070%	0.011%	-0.021%	0.008%
0%	1000	10000	0.511%	0.500%	0.047%	0.041%	0.032%	0.036%

Execution Times

The increase in complexity in Experiment #2, in particular the increase in the number of time steps due to the .001hr step used during climb, increased the runtime of every method significantly. Dynamic Programming, as done in Experiment #1, became infeasible with the available hardware when the number of required steps as much as tripled for the long, heavy cases with many climb time steps. Fortunately MATLAB

includes a coder toolbox (called MATLAB coder) which enables MATLAB functions to be compiled into C or C++ code with only slight modifications. Certain built in functions are not compatible with this toolbox (such as the MATLAB standard atmosphere reference function, which had to be replaced by a custom version). Other functions require specific combinations of available compilers and versions of MATLAB, such as the parallel computing toolbox. Even with the loss of parallel computing the execution time for Dynamic Programming was reduced by a factor of over 100 by converting from the interpreted MATLAB script to this precompiled C code. If the compiled code could have been parallelized, execution times may have gotten even lower. However the required software was not available.

Between the increased number of time steps, changed space-truncation methods from the addition of climb, and the implementation of compiled code, the final Dynamic Programming code executed a case in approximately 12 hrs., depending on the length of the mission. This was on a single desktop less powerful than the one used in Experiment #1. The same Matlab Coder toolbox was also used to bring down the runtime of the Optimal Control and Constant Power codes, bringing their execution times down to approximately 2 seconds per case when executed in a batch mode. Optimal Control and Constant Power are therefore much more suited for use in a trade study scenario in which many runs are required. The improved versions of Optimal Control took a little longer to execute, typically under 1 minute for 2 Level Optimal Control and up to 5 minutes for Weighted Optimal Control.

Experiment #2 Conclusions

With the completion of Experiment #2 the answers to Research Questions #2 thru #4 can be assessed in the light of complete mission simulations. Research Question #2 was "What factors determine the optimal power schedule?" For these particular hybrid propulsion system, sized aircraft, and technology/operational assumptions, the resistance of the battery can be identified as the primary driver of the optimal power schedule, firmly disproving Hypothesis #2 which stated "The reduction in aircraft weight resulting from burning fuel early in a mission is the dominant factor determining the optimal power usage schedule." Research Question #3 asked the related question: "What is the appropriate baseline schedule?" The baseline power schedule which minimizes the effect of battery resistance, Constant Power, is the best of the baseline schedules tested under these circumstances, disproving Hypothesis #3 as well, since it predicted that "The best baseline hybrid power schedule is to use the battery power as late in the mission as possible." However the battery resistance is not the only effect driving the selection of Constant Power for this combination, as seen in the performance in the reduced battery resistance cases. These cases show that the combination of the hybrid component efficiencies along with the gas turbine's response to shaft power inputs is sufficient to favor a constant power input.

The originally hypothesized dominant effect, the change in weight as fuel is burned, does have a noticeable effect on the operation of Optimal Control. When Optimal Control is enhanced to take this into account, it performs closer to Dynamic Programming while still running many times faster than that method. Even the original Optimal Control performs nearly as well as Dynamic Programming depending on the

acceptable tolerances. Taking this into account, the answer to Research Question #4: "What methods could be used to find better hybrid power schedules?" can now be determined. Hypothesis #4 predicted "Dynamic Programming will prove effective in finding the global optimum hybrid power schedule but take too long to be practical in design. Optimal Control will find almost as good a solution quickly enough to be practical." This is now conditionally confirmed, with at least a modified Optimal Control performing as well or better than Dynamic Programming in a fraction of the time, and even the original Optimal Control never finding a solution more than .1% greater in total fuel burn than Dynamic Programming.

However the most impressive result of Experiment #2, if less surprising after the results of Experiment #1, is that Constant Power achieved very nearly the same fuel burn as the optimal methods. This is only necessarily true for this particular engine model operating under the operational assumptions, for example requiring the gas turbine core to always be lit, but it still holds true even if the battery is replaced with an ideal battery. Based on this result it may be necessary to modify the proposed methodology to enable utilization of baseline methods if their performance is close enough to the optimum. This will be considered in Chapter 6 after the conclusion of the experiments.

Confidence in Small Results

The optimization of operational schedules is inherently a quest to make small improvements to a system without changing the hardware or mission. This is in contrast to the selection of different architectures or sizing of hybrid power systems themselves, which can make great strides towards achieving NASA's Far Term goals by making large

changes to the system hardware. Even considering this modest expectation, the power savings from optimizing schedules in this case were smaller than expected; with the difference in fuel burn between Constant Power and the best power schedule found being less than a pound in some cases. As the results of these experiments are intended to shape the final methodology, it is important to take a moment to examine the potential sources of error and assess the confidence that can be taken in these small savings found in Experiments #1 and #2 before continuing with Experiment #3.

The largest sources of error in these results when compared to a physical hybrid architecture are the NPSS engine model and the surrogate model used to find the fuel burn at every time step. The NPSS model captures the interaction between the hybrid and the conventional gas turbine components but does not contain the advanced proprietary component maps that an engine design company would have available to capture the performance of each part of the engine with highest accuracy. The data the NPSS model produced was a challenge to fit, as has been described, and was finally captured with a three part fit which still shows discrepancies with the original data when examined as closely as Optimal Control requires, as seen in Figure 57 below. However this engine surrogate model was used in every method in Experiments #2 and #3, and can therefore be considered a truth model for the purpose of comparing these power scheduling methods.
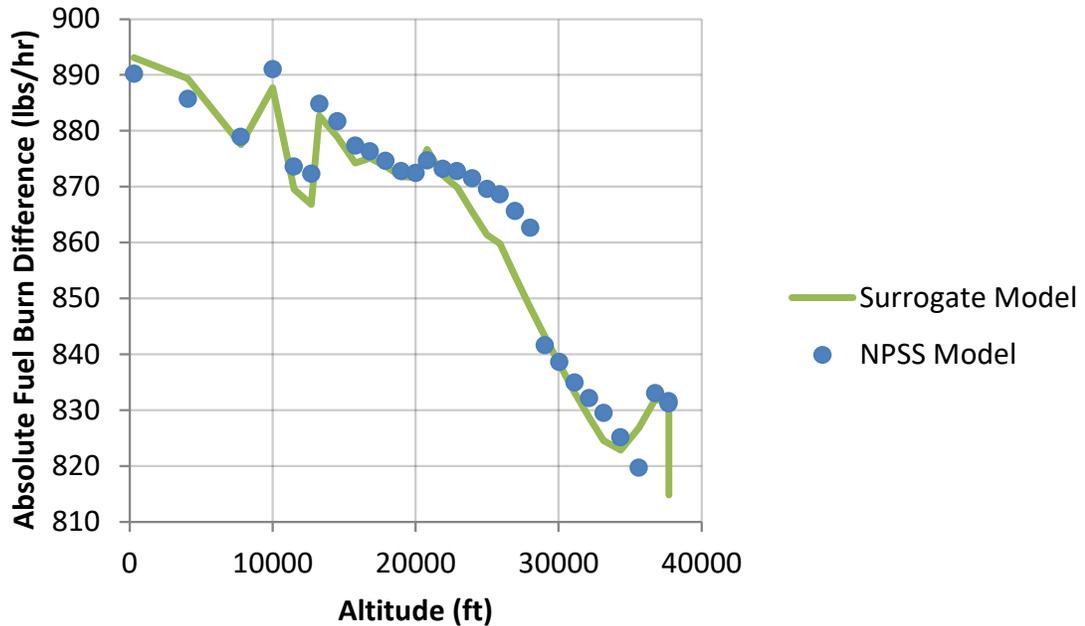
Figure 57: Example Fit Error of Final Surrogate; Fuel Burn Savings from 3,500 Hp Assist During Climb

Another significant source of error is the integration error inherent to discrete time simulations. The time steps were chosen as shown at the beginnings of Experiment #1 and #2 in order to bring this error down to an acceptable level, keeping the climb rate and fuel burn errors to a minimum. Any remaining error was minimized by integrating every method in the same manner, running each with time reversed from landing to takeoff in order to be consistent with Dynamic Programming. A similar approach of keeping any errors consistent was adopted by creating a single mission simulation code for each experiment and then modifying only the parts of that code which choose the power to simulate each method. This resulted in every method being run using nearly identical code; even including the final runs of the power schedules identified using Dynamic Programming.

Another potential source of error is the convergence criteria used in every simulation to select free variables. Even in the simple Constant Power method, it is necessary to guess and converge on not only the amount of power which exactly empties the battery but also on the exact length of the cruise segment which will cause the total mission length to exactly match the other methods. The choice to run the mission in reverse eliminates the required guessing for the starting weight of the fuel, but the length of the climb segment is different for each optimization method depending on the instantaneous weight of the aircraft. Due to its execution time, Dynamic Programming is not run with a convergence on mission length. Instead it uses a starting guess computed from Constant Power and utilizes whatever mission length falls out. The other methods converge to this new mission length to within 1 part in 10^8. In addition the same tolerance is used for the battery SOC for each method which ensures that all methods are solving the exact same problem.

One final consideration is the methods themselves and the reliability of determining their best answer. The baseline methods only have one free variable, which is set based on the available battery energy in a well behaved manner. Dynamic Programming is an exhaustive search which evaluates every schedule achievable within its discretization scheme in a systematic manner, finding the global optimum every time.

The Optimal Control variants are also deterministic. However unlike the other methods their performance depends on finding the minimum of continuous functions. The cost function of the instantaneous fuel burn and battery power minimized at the heart of Optimal Control is relatively well behaved, due to the surrogate model. However the outer loop which varies the weighting factor in Weighted Optimal Control and which is

150

also used to vary the cost of the fuel during climb for the Two Level Optimal Control is not guaranteed to be free of local optima. The results obtained by these two methods may be a function of the starting points of the minimizer if the minimizer is susceptible to local optima. If the wrong minimum is chosen a method would find a valid but slightly less optimal schedule. This does not seem to have been an issue in the Experiment #2 results and the near optimal schedules found by these methods.

With confidence in the results, Research Question #5 can now be considered, bringing the methods tested in Experiment #2 to bear on an actual hybrid system design study.

Experiment #3: Application to Battery Sizing Trade Study

Research Question #5 asks "How does the choice of optimal schedules affect other problems in hybrid system design?" These problems would include the trade studies required to size different parts of the hybrid architecture. The best way to demonstrate the effectiveness of these methods when performing conceptual design trade studies is to perform one such study and examine the results using different methods. An example of one problem that must be solved in the implementation of hybrid aircraft is sizing the battery which can be done without changing any other part of the aircraft design. The same aircraft can be used with different size batteries which displace fuel at the cost of carrying the battery weight. If batteries were as fluid as jet fuel this would lead to a different ideal battery weight being used on each mission. In order to select a single fixed battery or small set of batteries, a trade study can be performed to find the impact of the non-ideal sized battery. Hypothesis #5 posits that "Using the proper power schedule will

improve performance when the system is battery capacity limited." A proper power schedule should allow more capability to be extracted from smaller batteries in such a study. To perform the study for a fixed payload the battery size is set to each of the different prospective values and run for every range of interest, resulting in a family of curves showing energy or fuel savings vs range for each battery size as seen in Figure 58 below from a study of the Rolls-Royce EVE. Fuel savings is plotted as a function of battery size and range in the large chart and energy savings is shown in the inset. Depending on the power schedule adopted, these curves will be slightly different, demonstrating the merits of the different methods.
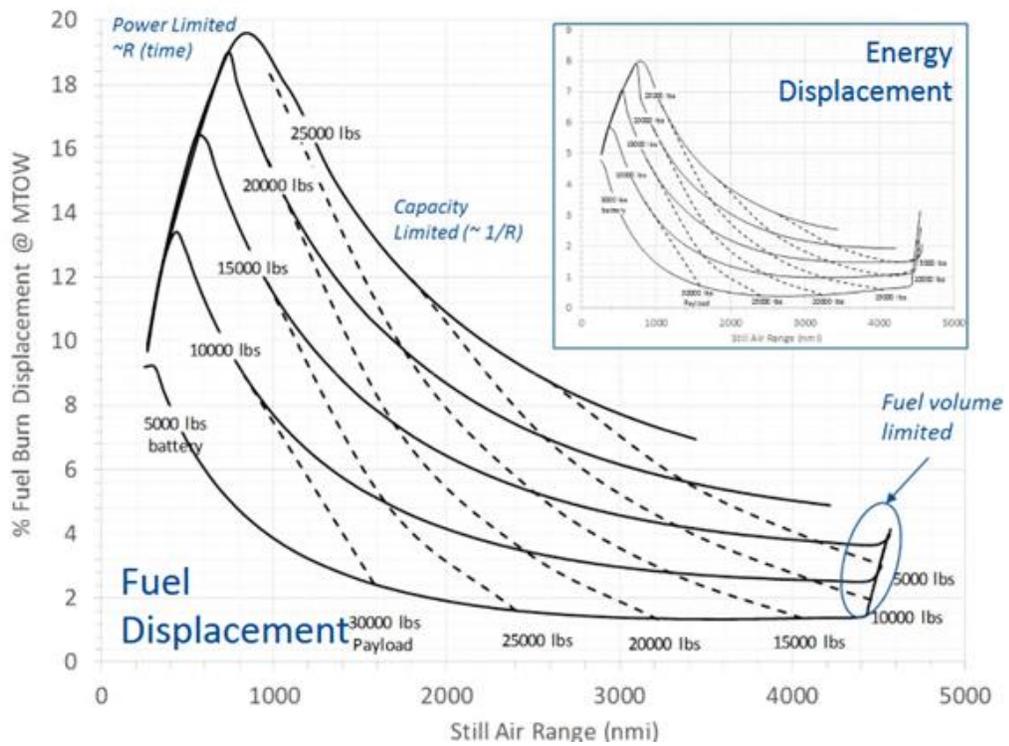

Figure 58: Battery Sizing Trade for Rolls-Royce's Electrically Variable Engine (EVE)[46]

To implement this analysis the Experiment #2 methods can be called as functions by a master script performing the sweep. Attempting to use Dynamic Programming on such a sweep of cases would take impractically long, so the sweeping comparison was only done with Constant Power and the Optimal Control variants. Dynamic Programming was only used to spot check and demonstrate how close these results are to the global optimum. In addition to these methods, the conventional case, using no battery power, had to be modeled at each range. The power limited case also had to be detected and simulated over ranges too short for Optimal Control to have any effect.

Power Limited Cases

Some conditions of battery and range do not lend themselves to optimization. Many cases at lower ranges with larger batteries will be unable to empty the entire battery before landing, even running the motor at maximum power throughout climb and cruise. These cases' power schedules cannot be further optimized through Optimal Control or Dynamic Programming and instead must be run at maximum power with the final amount of electricity used tracked and accounted for in the energy savings calculations. Longer distance missions can simply use up the maximum capacity of the battery.

Calculations for these cases were performed using the same code used for simulating constant power missions. However, instead of setting the power to exactly empty the battery, the mission was run at full power and at the end of the mission the amount of unused battery power was recorded. If the value of unused battery power was negative, the result was discarded and the other methods were used instead. The same

code was used to run the conventional case for comparison, setting both the battery weight and the power used to zero but leaving the electrical system weight included in the empty weight to simulate what the exact same aircraft could do if the battery alone were removed.

Trade Study Implementation

The battery trade study implementation was performed by systematically sweeping through battery sizes and ranges with each of the above codes. First the baseline was established using zero battery power and zero battery weight at each range to find the conventional fuel burn. Then for each of the battery sizes tested the range was increased from a minimum of 500 nmi. by 50 nmi. increments, and the power limited case was run, saving the amount of electricity used and the fuel burned in each case to the results matrices for every optimization method. When the power limited case returned a negative battery energy remaining, that case was rerun using each optimization method, and all longer ranges with that battery were run with the optimization methods without retrying the power limited code.

Unlike the earlier experiments, not every case used the entire battery; therefore comparisons strictly of fuel burn would not capture the difference in energy consumption of the different methods and the no hybrid baseline. Instead the total energy was used for comparison, using the heating value of the fuel burned and the amount of energy removed from the battery. The total energy was therefore given by Equation 47, shown below.

154

$$TotalEnergy \ (MJ)$$

$$= \left(FuelBurn \ (lbs)\right) \frac{43.5 \left(\frac{MJ}{kg}\right)}{2.2 \left(\frac{lbs}{kg}\right)}$$

$$+ \left(BattWeight \ (lbs)\right)(\%BattUsed) \left(EnergyDensity \left(\frac{Wh}{kg}\right)\right) \left(\frac{3600 \frac{J}{Wh}}{10^6 \frac{J}{MJ}}\right) \tag{47}$$

To enable the use of a 5,000 lb. battery, some modifications to the baseline power scheduling algorithms were necessary due to the battery's limited energy capacity and its higher cell resistance (for the 100% battery resistance case). The limited energy available meant that the Climb Power method could not run full power during the entire climb segment. Instead in this method and at this battery size the power was set to zero during cruise and to whatever constant value during climb which would empty the battery. In addition the cell resistance limits the maximum power that can be drawn from a battery, which is not a limiting factor for 10,000 lb. and greater battery sizes. However the reduced cell count of a 5,000 lb. battery brought down this limit enough that for that battery size the maximum power for all methods was reduced to 2,500 Hp.

Baseline Method Results

The energy savings for different battery sizes and ranges with 25,000 lbs. of payload and standard battery resistance are shown in Figure 59 below for each of the baseline methods. Figure 59 shows the savings as a percentage reduction in total energy use compared to the all fuel case at the same range and payload, carrying no battery. For the larger battery sizes, the figure shows no difference between the different methods left of the peak. This is expected because the cases left of peak are the power limited cases

where the battery cannot be drained before the mission ends. All of the methods tested reduce to full power at these power limited ranges. At longer ranges, the figure shows that Constant Power outperforms the others, with end power consistently doing worse than climb power as could be expected from the Experiment #2 results. In fact as the ranges increase only Constant Power continues to provide a fuel savings, as End Power and Climb Full Power have negative savings for all batteries at the 2000 nmi. mission.
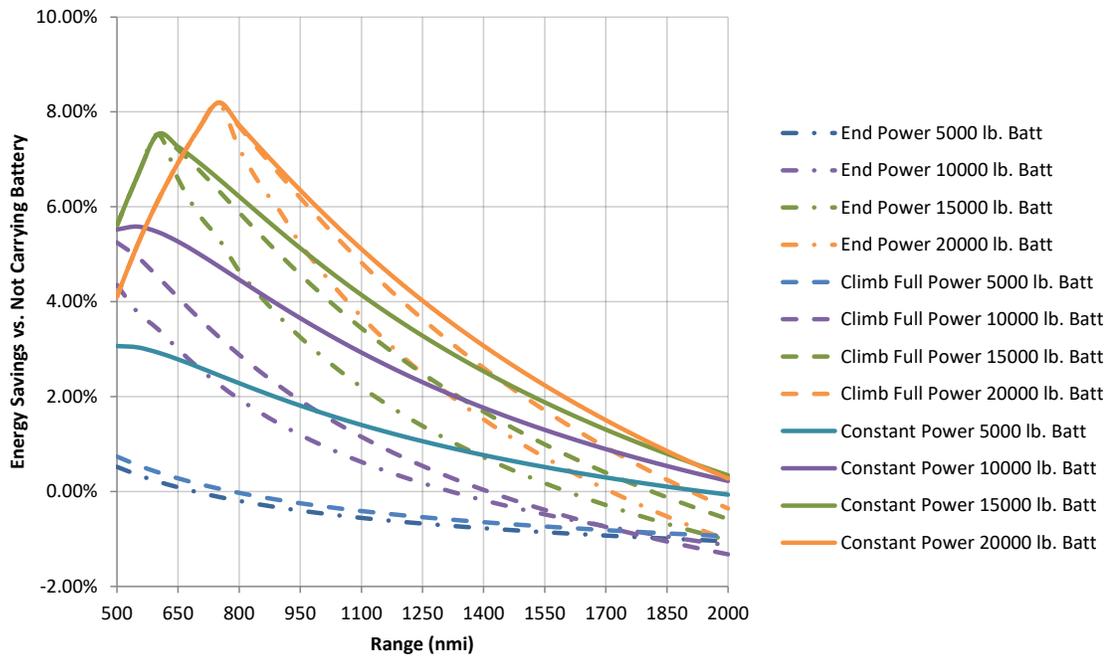
Figure 59: Energy Savings Carrying 25,000 lb. Payload with Different Battery Sizes and Baseline Schedules

Examining Figure 59 reveals that the difference between the different baseline schedules for a single battery weight can be as much as 2% of the total energy of the vehicle. This is reduced slightly from the peak fuel burn savings seen in Experiments #1 and #2 due to the inclusion of the battery energy. The difference is largest for smaller

156

batteries, which have a higher resistance due to their size. The non-constant schedules even have a net energy loss at ranges as low as 800 nmi., while the Constant Power schedule remains in the black at all ranges. The actual battery which an airframer would select based on this chart depends on the range the aircraft is expected to fly, but in all energy limited cases Constant Power outperforms the other baseline methods.

The same battery size and range study was performed using the baseline methods with the 50% resistance and ideal batteries as well. The results are seen in Figure 60 and Figure 61 below. These figures show that the absolute energy savings increases as the battery is made more ideal and as more energy becomes available to offset fuel. In addition, the difference between the three baseline methods gets quite small with an ideal battery.
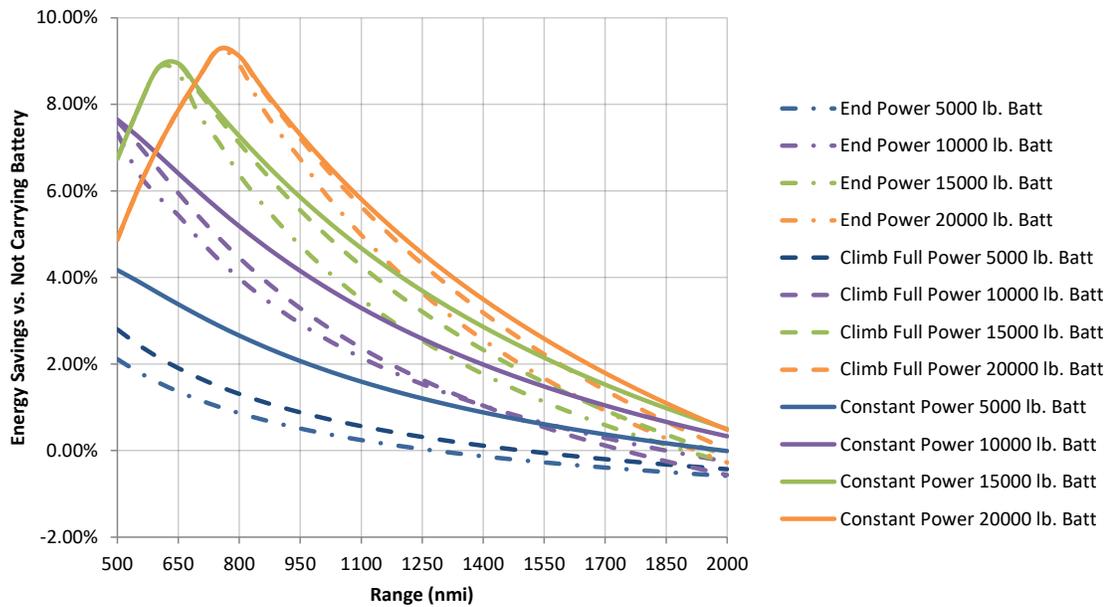
Figure 60: Energy Savings with 50% Battery Resistance, Baseline Schedules, 25,000 lb. Payload

157
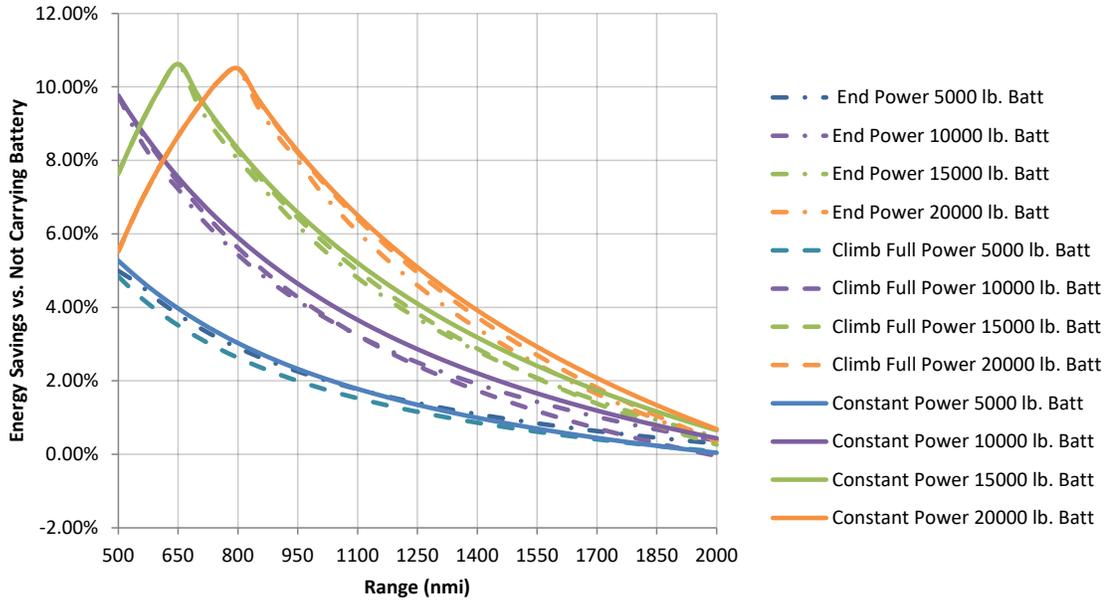
Figure 61: Energy Savings with Ideal Battery, Baseline Schedules, 25,000 lb. Payload

Optimal Control Results

The difference between each of the Optimal Control variants and Constant Power is very small and would be hard to see on a chart such as Figure 59. Instead the results can be graphed as a difference between each of them and Constant Power at the same range and battery size and shown in Figure 62. The Dynamic Programming points from Experiment #2 were also included for comparison, but Dynamic Programming's execution time precluded its use in such a study. For clarity each battery size is given on a separate plot, as the lines were almost superimposed.
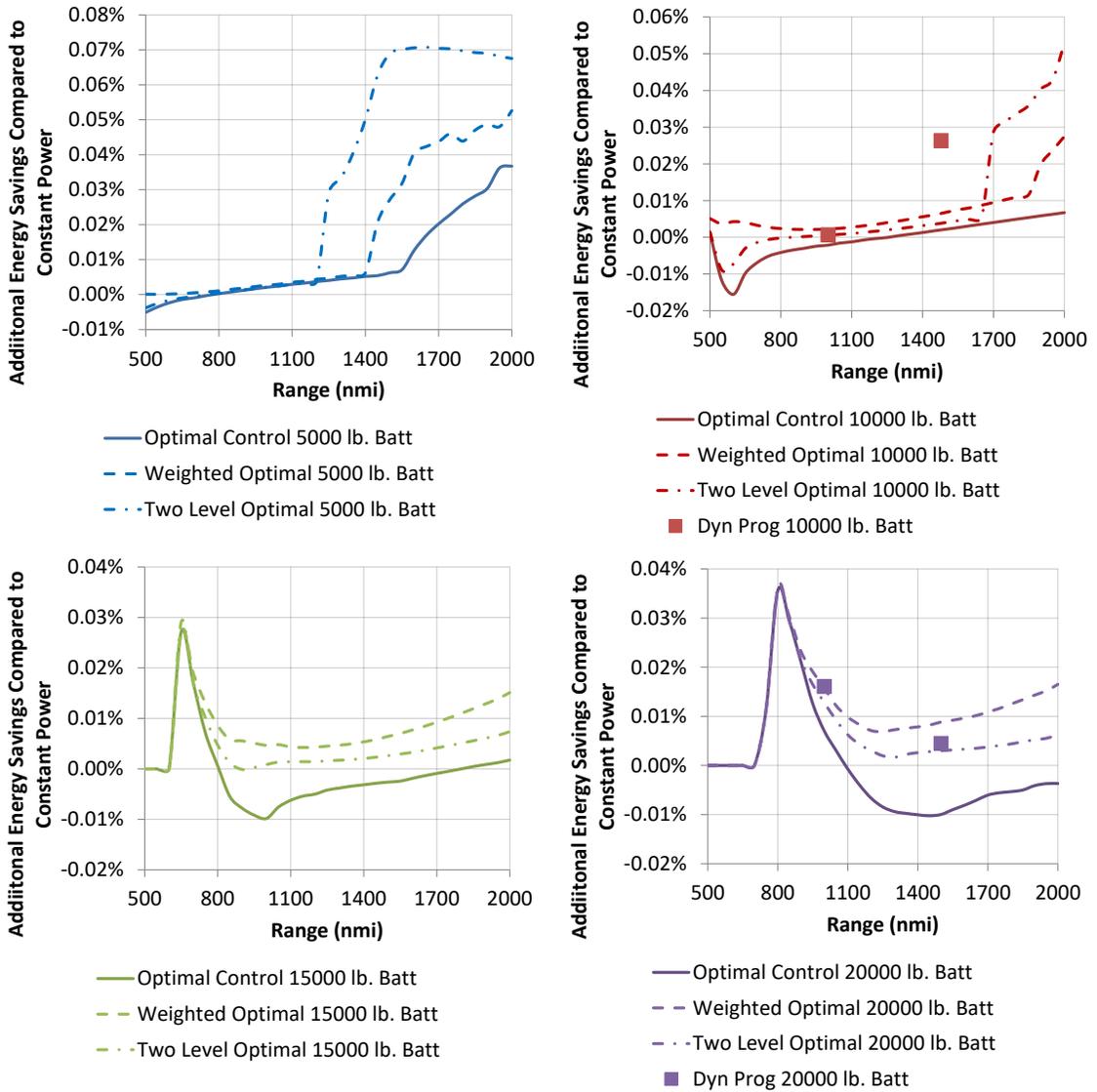
Figure 62: Optimal Control Variants' Energy Savings Compared to Constant Power, 100% Battery Resistance

Figure 62 shows that the performance of the Optimal Control variants is never very different from that of Constant Power. The largest percent difference is around .07% at longer ranges with the 5,000 lb. battery in this 100% battery resistance case. The bottom two charts in Figure 62 show a region where there is no difference at all, the power limited regions of the figure. The Dynamic Programming check points on the left

two subfigures show that the Optimal Control methods come very close to the global optimum, sometimes doing better than Dynamic Programming but never more than .02% worse. Similar plots were made for the 50% resistance and ideal battery cases, showing similar trends but a slightly higher maximum difference. These are shown on the following pages as Figure 63 and Figure 64. These show a maximum improvement over constant power of .16% in the 0% resistance 5000 lb. battery case at 2000 nmi. However, the absolute energy savings compared to no battery in these figures are at a minimum as was seen before in Figure 61.
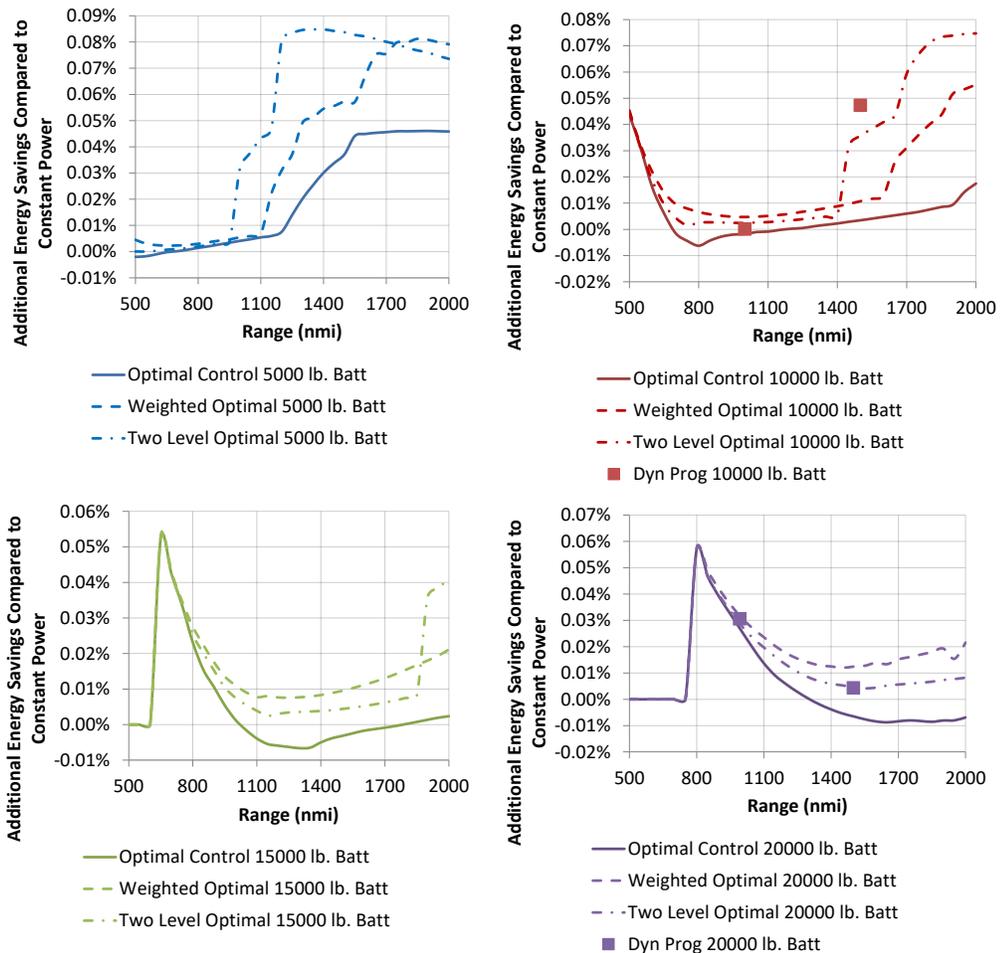
Figure 63: Optimal Control Variants' Energy Savings Compared to Constant Power, 50% Battery Resistance
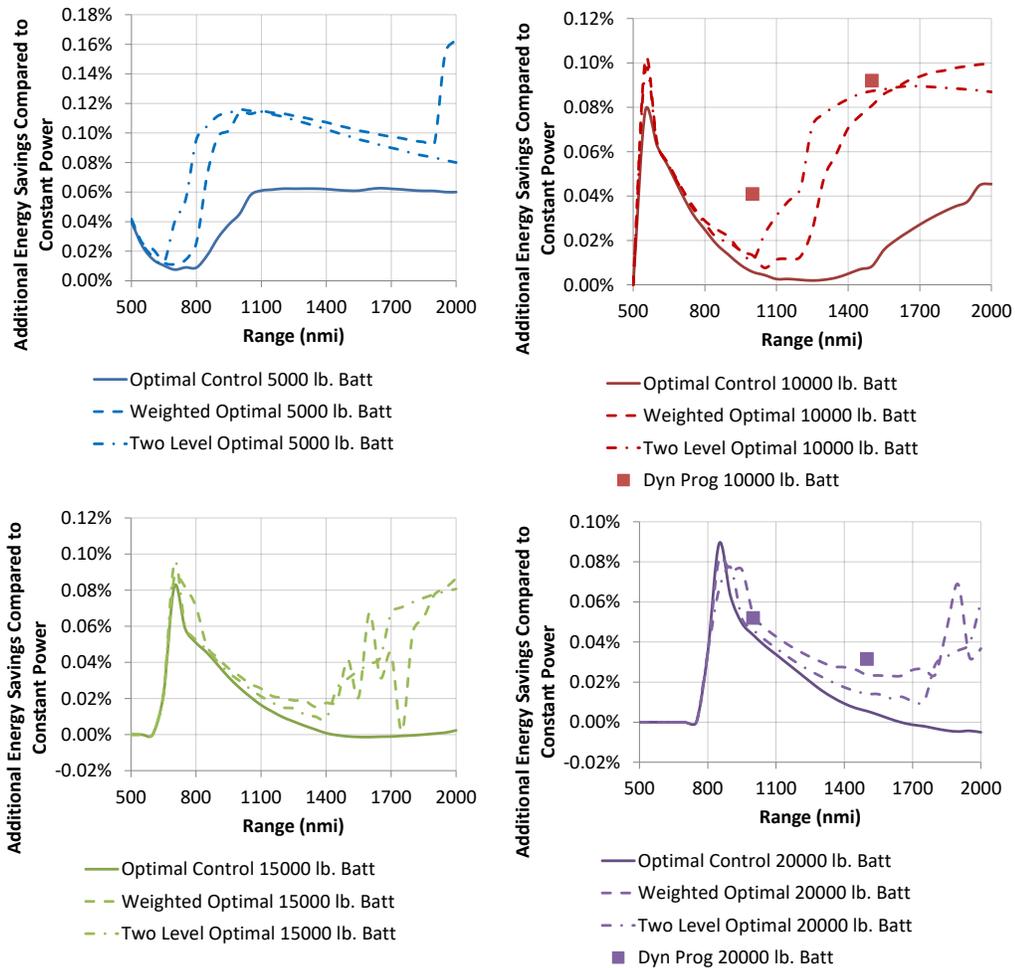
Figure 64: Optimal Control Variants' Energy Savings Compared to Constant Power, 0% Battery Resistance

The noise seen in these figures, particularly in the bottom two graphs in Figure 64, show the convergence trouble that Weighted Optimal Control and Two Level Optimal Control can have. The outer loop solver, setting the weighting factor for Weighted Optimal Control or the climb fuel cost in Two Level Optimal Control is trying to find the global optimum. Sometimes it finds a local minimum instead, costing .02% more of the total fuel burn but still performing better than the original Optimal Control shown in solid colors.

Experiment #3 Execution Time

Each of the original Optimal Control runs continues to execute in under 2 seconds, but the improved Optimal Control methods call the Optimal Control code many times per run and take significantly longer. The Two Level Optimal Control takes approximately 80 seconds per run, and the Weighted Optimal Control can take 3 minutes, although all times are a function of the mission length. The sweeps performed in Figure 59 and Figure 62 were performed in the same run of code and took approximately 6 hours to execute for the 4 batteries converging at 31 distances, with the power limited cases running faster than the others. The Dynamic Programming cases shown each took 12-18 hours to execute during Experiment #2, depending on mission length, making them unsuitable for such sweeps.

Experiment #3 Conclusions

The results of the trade study clearly illustrate that there is a significant difference in performance between a good power schedule and a poor one. For energy limited cases, the performance of Constant Power compared to the other baseline methods was significantly better. Research Question #5, which asked "How does the choice of optimal schedules affect other problems in hybrid system design?" is answered with a confirmation of Hypothesis #5: "Using the proper power schedule will improve performance when the system is battery capacity limited." This analysis would enable some systems to use smaller batteries, which are typically not only lighter, but less expensive. The dominance of the battery resistance's influence on the power schedules

can also be seen by observing the disappearance of performance differences in the ideal battery case.

The small magnitude of even the greatest difference between the best Optimal Control variant and Constant Power confirms that changes need to be made to SHAPSO. There must be some evaluation of whether the optimal methods provide an increase in performance over baseline methods that is significant and worth the additional computational burden of using an advanced method over a simple baseline method.

Exploring the Technology Assumptions

The technology and aircraft size assumptions set before the start of Experiment #1 and maintained through the subsequent experiments predict great improvement over the state of the art by the Far Term timeframe of this design. To show that SHAPSO is not dependent on these specific assumptions, some of the assumptions were changed and the battery sizing study from Experiment #3 was repeated. Within the modeling environment some assumptions are hard to change, for example the engine deck is only valid along the climb schedule used to generate it. Therefore the climb schedule was kept fixed. Instead the most ambitious of the technology assumptions, the 750 Wh/kg effective battery energy density, was reduced to 550 or even 400 Wh/kg. The effects of this change can be seen in Figure 65 and Figure 66 below. These figures show the performance of the different baseline schedules, with 550 Wh/kg and 400 Wh/kg batteries respectively, as a percentage fuel burn savings compared to carrying no battery at all. These can be compared to Figure 59, which used 750 Wh/kg batteries. For these tests the battery

resistance per cell was left at the original level, but each pack contained fewer cells due to their decreased energy density, resulting in less energy to be used to offset fuel.
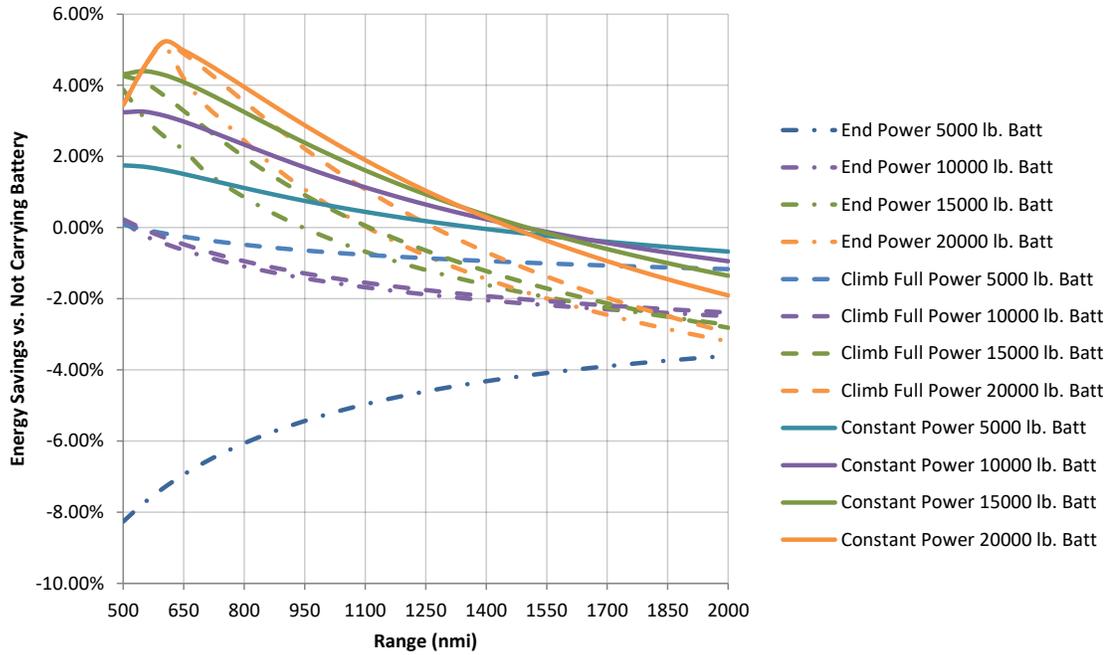
Figure 65: Energy Savings Carrying 25,000 lb. Payload with Different Battery Sizes and Baseline Schedules, 550 Wh/kg
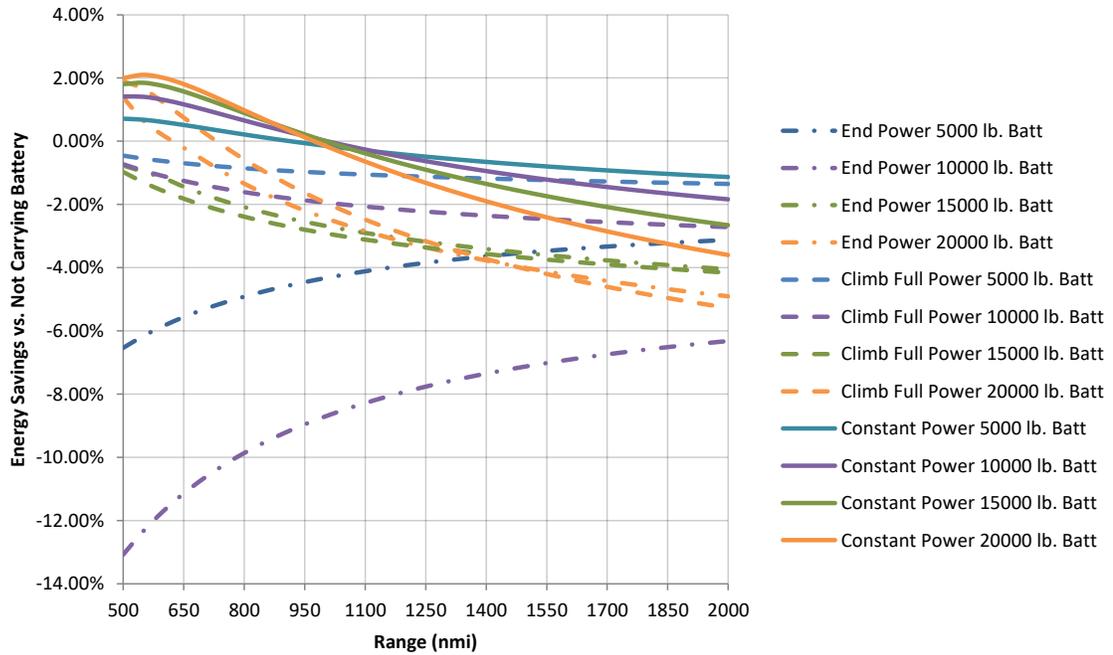
Figure 66: Energy Savings Carrying 25,000 lb. Payload with Different Battery Sizes and Baseline Schedules, 400 Wh/kg

These two cases with reduced battery energy capacity show a stronger deviation between the different power schedules than was seen by the 750 Wh/kg case in Figure 59. The 400 Wh/kg case shows even more deviation between power schedules than the 550 Wh/kg case. This is to be expected because the primary factor driving the difference in performance, battery resistance, is even more of a factor when the battery cell count is decreased due to increased cell weight. These fewer, heavier cells have more power drawn from each cell than was previously drawn from each of the more numerous, lighter cells did for the same mass battery pack and battery pack power. Constant Power is the only method that even provides a positive benefit for missions longer than 750 nmi. in the 400 Wh/kg case, or at any distance tested with a 5000 lb. battery pack of either energy

165

density. Based on this it is even more crucial for the proper power schedules to be used for battery energy densities less than 750 Wh/kg.

A second assumption that was tested was a design assumption. The hybrid architecture tested in Experiments #1-#3 was equipped with a 3500 Hp electric motor augmenting each of its turbofan engines. Many of the power schedules found never reached 3500 Hp of use, raising the question of how the results would change if the motor power was reduced to a maximum of 2500 Hp or 2000 Hp. This reduction in motor power reduces the freedom of the different algorithms to use a fixed battery at different times, but would also reduce the weight of the system. This study is shown in Figure 67 and Figure 68, which show the fuel savings of 2500 Hp and 2000 Hp motor equipped engines compared to flying the same aircraft without a battery. These figures can be compared to Figure 59 for the 3500 Hp case, and like Figure 59 these figures were generated with 750 Wh/kg batteries with 100% of the original estimated pack resistances.
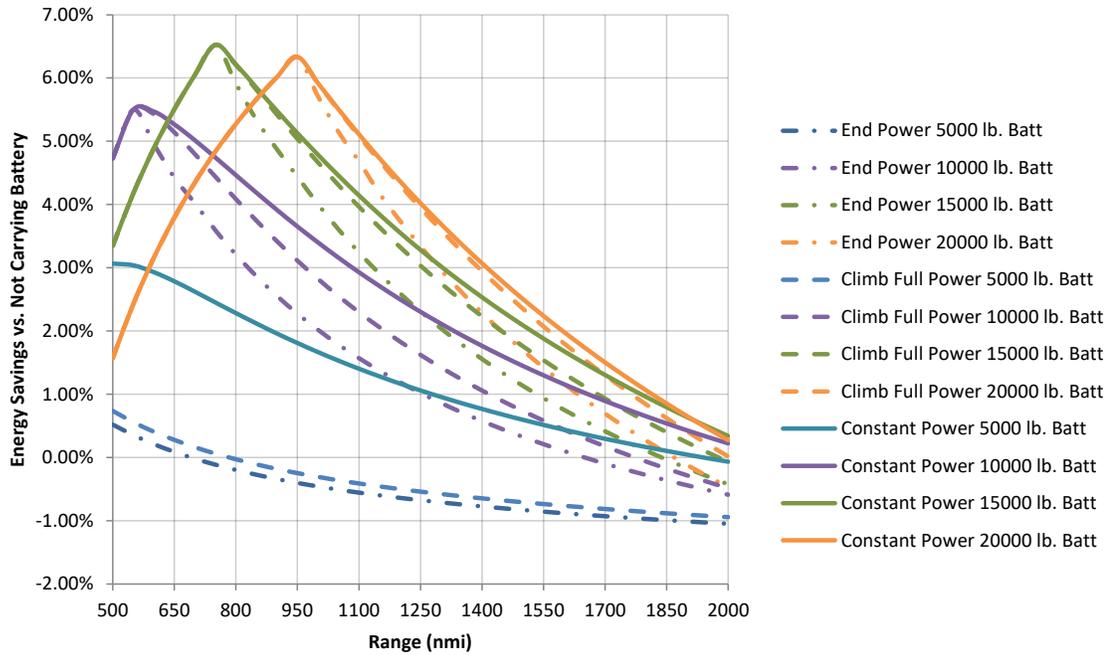
Figure 67: Energy Savings Carrying 25,000 lb. Payload with Different Battery Sizes and Baseline Schedules, 2500 Hp Motor
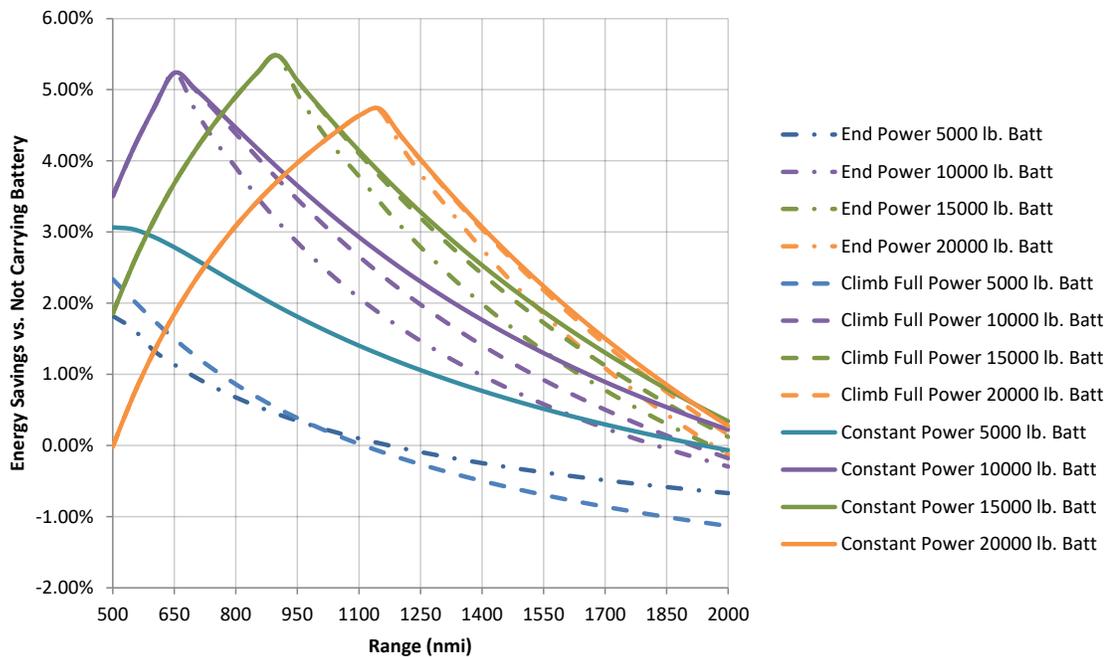
**Figure 68: Energy Savings Carrying 25,000 lb. Payload with Different Battery Sizes and Baseline Schedules, 2000 Hp Motor**

167

As expected each of these figures show that the power limited case extends much further into the mission and has a lower fuel savings value due to the tighter power limits. These power limits reduce the amount of the tested mission envelope in which the baseline schedules can show any differences and start their curves off from a lower peak. The curves do not diverge as much as they do in Figure 59 because End Power and Climb Power cannot reach the high power levels they could in the 3500 Hp case and therefore cannot sustain as great as a resistance loss. The restrictions on power level and resistance loss are seen even more in the 2000 Hp case than in the 2500 Hp, showing that tightening the allowed motor power does cause all power schedules to converge. Despite this, Constant Power is still outperforming the other baseline methods by enough to improve the performance of any of these battery packs for selection in a battery sizing study. Therefore, determining that the proper power schedule is still of importance when flying at greater than the power limited ranges.

Revisiting the Research Questions

With the experiments complete, the final answers to the research questions can be determined. Each of the five research questions shall be considered before the answers are used to update the methodology.

1. How important is it to use the optimal power schedule?

   Hypothesis: The use of optimal power schedules over a typical aircraft mission will yield significant savings in fuel burn.

Hypothesis #1 was found to be correct. In all three experiments the difference between the optimal power schedule and some of the baseline schedules was as much as 3%, despite discharging an identical battery to displace fuel.

2. What factors determine the optimal power schedule?

    Hypothesis: The reduction in aircraft weight from burning fuel early is the dominant effect determining the optimal power usage schedule.

    Hypothesis #2 was found to be incorrect for the hybrid aircraft tested under these assumptions. The impact of battery resistance was seen to be the largest factor in shaping the optimal power schedule, driving the answer towards Constant Power. When the battery resistance was eliminated the engine model itself also contributed to the Constant Power schedule through the drop in turbine efficiency with increased motor power. The effect of burning fuel early rather than late was seen to have an impact of around .5% of the fuel burn when comparing Start Power to End Power in Experiment #1. While that contributed to the effectiveness of Weighted Optimal Control, its impact was dwarfed by the 2% impact of battery resistance.

3. What is the appropriate baseline schedule?

    Hypothesis: The best baseline hybrid power schedule is to use the battery power as late in the mission as possible.

    Hypothesis #3 followed naturally from Hypothesis #2, and was also found to be incorrect. Of the baseline methods tested, Constant Power performed the best across all three missions, although an additional baseline method, Linear Power, was added to Experiment #1 after seeing the linear answer found by Dynamic Programming. Linear Power was practically the optimal schedule. No such method applicable to the entire

mission was identified in Experiment #2, although another method may be discovered for other systems.

4. What methods can be used to find better hybrid power schedules?

Hypothesis: Dynamic Programming will prove effective in finding the global optimum hybrid power schedule but take too long to be practical in design. Optimal Control will find almost as good a solution quickly enough to be practical.

Hypothesis #4 was confirmed in Experiments #1 and #2, as Optimal Control executed much faster than Dynamic Programming and found a fuel burn within .1% of Dynamic Programming in every case. However the performance of Optimal Control was worse than that of Constant Power until it was augmented. The original Optimal Control method was not equipped to detect savings from burning fuel earlier in the mission. However modified Optimal Control methods were developed that not only consistently outperformed Constant Power but in some cases also found a lower fuel burn than the resolution limited Dynamic Programming.

5. How does the choice of optimal schedules affect other problems in hybrid system design?

Hypothesis: Using the proper power schedule will improve performance when the system is battery capacity limited.

Hypothesis #5 was confirmed by a comparison of using the different baseline methods of optimization to calculate the fuel displacement of different battery sizes at the beginning of Experiment #3. There is no optimization of power schedules to be done when the system is power limited, seen left of the peaks in the Experiment #3 graphs, but

a significant savings was seen in the battery capacity limited parts of the curves, seen to the right of the peaks. In these sections the Constant Power schedule and the Optimal Control variants outperformed End Power and Climb Power by 1-2% over many ranges. This improvement could make the difference between choosing one battery or another depending on the set of ranges an aircraft is intended to fly. The improvement in performance of the Constant Power and Optimal Control variant schedules was still present even if the assumptions on battery energy density or the design motor power level were changed.

With the research questions answered, the conclusion in Chapter 6 will consider how the results reflect on SHAPSO and its utility in the hybrid architecture design process. The results will also be used to improve SHAPSO, and future work will be identified which could utilize or improve SHAPSO for continued research.

CHAPTER 6

CONCLUSIONS AND FUTURE WORK

This thesis set out to create a methodology for determining optimal operational schedules for hybrid electric architectures. These aircraft propulsion architectures use the energy carried in a finite battery to reduce the fuel required to carry out a mission. Use of an optimal operational schedule would allow such a system to minimize the fuel burn without changing any of the hardware or mission parameters and thus extract more performance out of a fixed system with only an increased computational cost.

In Chapter 2 the current literature on hybrid aircraft was surveyed to determine the types of hybrid electric systems which have been considered for aircraft. From these a hybrid turbofan similar to the Boeing SUGAR Volt was selected as a representative hybrid system to use to develop the methodology. In Chapter 3 a series of research questions were posed. These asked what impact the operational schedule has on the fuel burn, what factors affect the ideal operational schedule, what the best baseline schedules are, what optimization algorithms can be used with the hybrid architectures and what impact the choice of operational schedule has on the battery sizing and other hybrid sizing problems. Hypotheses were made for each of these questions based on the available literature on hybrid aircraft and hybrid electric cars, and a methodology, SHAPSO, was proposed based on these hypotheses. A series of experiments was then proposed to settle the research questions and determine the value of the methodology. Chapter 4 described the modeling process which was used to create a hybrid turbofan

model sufficient to carry out these experiments. The implementation and results of the experiments were given in Chapter 5.

This final chapter is divided into four sections. The first section discusses the results of the experiments used to determine the methodology. It also discusses modifications to SHAPSO that can be made in the light of the experimental results. These modifications are demonstrated by applying SHAPSO to the system modeled in Chapter 4. The second section discusses potential improvements that could be made to this methodology in the future. The third section summarizes the contributions of this thesis to the state of the art, and the final section examines future work on the problem of Hybrid Electric Power Scheduling.

Summary of Experimental Results and Changes to SHAPSO

The methodology detailed at the end of Chapter 5 was created based on the answers to research questions first posed in Chapter 3 pertaining to the impact of optimal operational schedules on the performance of the hybrid architecture. Each of those questions had a corresponding hypothesis which was confirmed or disproved by the experiments detailed in Chapter 5. These experiments showed that for the representative hybrid architecture used in this analysis the performance of a Constant Power baseline schedule was significantly better than that of the other baseline schedules tested, which were Start Power, End Power, and Climb Power. This fuel burn savings for the Constant Power schedule was largely due to the influence of the battery resistance on the hybrid system's efficiency. The experiments also showed that the performance of a Constant Power baseline power schedule was slightly worse than the performance of the power

schedules determined using Dynamic Programming and the variants of Optimal Control across multiple ranges and battery sizes. However the small margin between the performances of Constant Power and the optimization methods merits changes to SHAPSO in order to take advantage of near optimal baseline schedules

Modifications to SHAPSO from Experimental Results
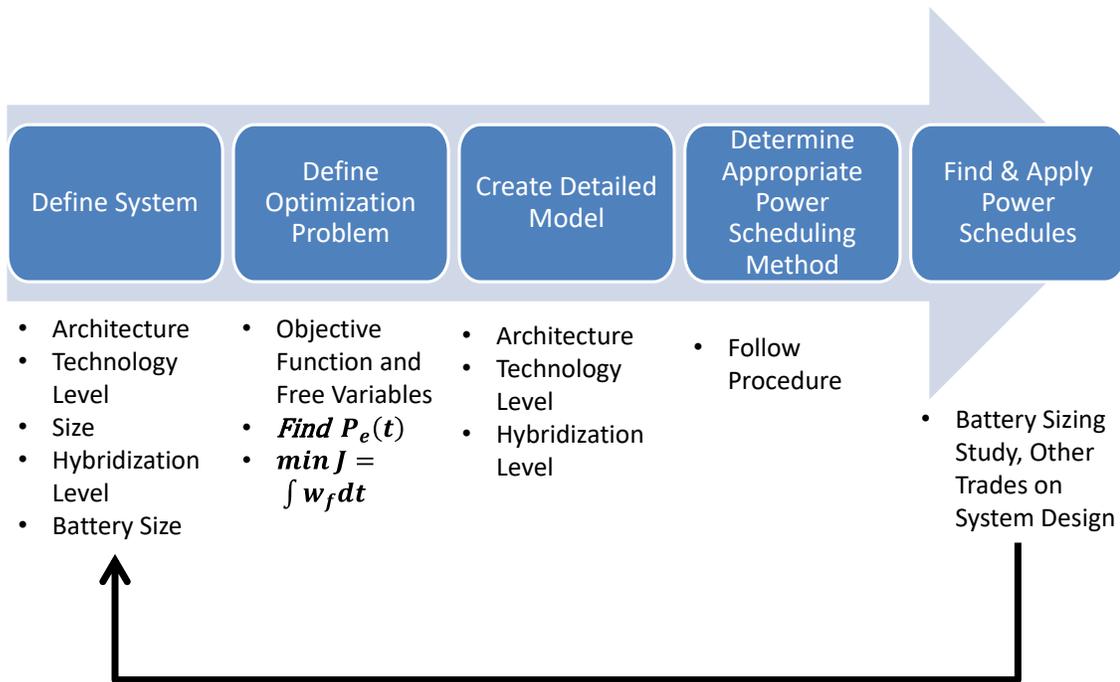
Figure 69: Systematic Hybrid Aircraft Power Schedule Optimizer (SHAPSO)

SHAPSO is the methodology proposed at the end of Chapter 3 and shown in Figure 69 above to determine operational schedules for any hybrid electric architecture. The experimental results revealed some shortcomings in the fourth step of SHAPSO, in which the power scheduling method is selected. The sub procedure originally laid out in Figure 24 only decided between using Dynamic Programming and Optimal Control. It

neglected the potential utility of simple baseline schedules. The final power scheduling selection procedure is seen in Figure 70 below, with changes or additions to the original depicted in green.
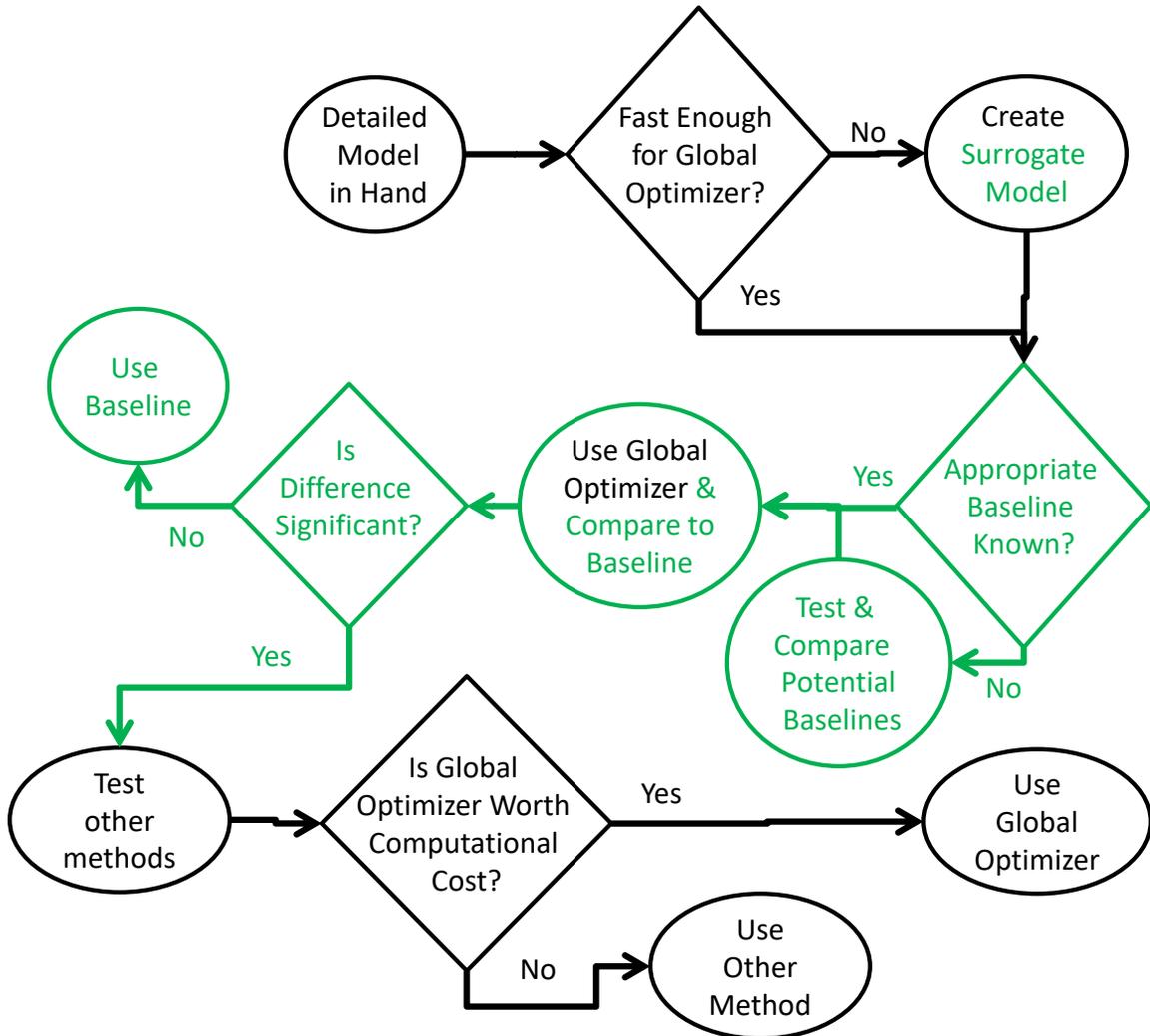
Figure 70: Updated Methodology for Determining Optimal Operational Schedules for Hybrid Electric Architectures

The first change in the methodology is the inclusion of a surrogate model instead of an engine deck. The engine deck introduces a strong bias towards choosing the points sampled from the detailed model, as revealed during the development of Optimal

175

Control. A surrogate model can be smoother than an engine deck, enabling intermediate points to be chosen. It is important however that the surrogate model be a very good fit to the source data, as any ripples in the fit can produce anomalies in the power schedule, as was discovered during the development of Experiment #2.

The next step in the procedure is to identify the appropriate baseline method for power scheduling the architecture. For some systems there is an established baseline in the literature, but for others there are multiple candidate baseline power schedules from which to choose. In the latter case each should be implemented and tested in order to identify the best known power schedule. If the best baseline schedule is not listed or tested, it may become apparent in a later step from looking at the global optimal schedules, similar to the discovery of the Linear schedule in Experiment #1.

The following step is to run a small sample of points through a global optimizer method such as Dynamic Programming, and compare the results to the baseline. The number of points examined depends on the available computational resources, but should sample different ranges and battery sizes to find the optimum performance across the possible missions.

The next decision point depends on the stage of design, the confidence in the model, and the confidence in the underlying technology and mission assumptions made in the modeling effort. There is a threshold value of the smallest fuel savings that is held to be significant. A 1% fuel burn savings when multiplied by the amount of fuel an aircraft burns in its lifetime is a large amount, significant in cost and in CO_2 emissions. A .01% fuel burn savings on the other hand is likely smaller than the modeling error, or the impacts of other unknown variables such as the weather, air traffic congestion, or even

the exact weight of the passengers. The threshold at which significant fuel savings occurs must be decided by the designer based on their knowledge of their model and the estimated error due to known and unknown sources. This threshold of significant fuel savings becomes the margin of significance used in comparing schedules.

If the amount of fuel savings predicted by the global optimum is a smaller improvement over the amount predicted by the baseline schedule than this margin of significance, the methodology concludes that the baseline is sufficient and should be used until the uncertainty in the model is reduced to less than the difference. If the difference in fuel burn is greater than the margin of significance, the global optimizer may still not be the best option due to the computational burden. For this reason the next step in the methodology is to evaluate alternative methods such as Optimal Control, Two Level Optimal Control, and Weighted Optimal Control, in order of increasing computational burden.

The methodology's selection of operational scheduler therefore chooses the least computationally expensive method which predicts fuel savings within the margin of significance of the global optimum. If none of the other methods produce savings within this margin, a final decision is made after evaluating both the difference between the savings of the best of these methods and the global optimizer and the difference in computational cost. If the computational cost is prohibitive, the less computationally expensive method is used. Otherwise the global optimizer is the final choice.

Example Application of the Methodology
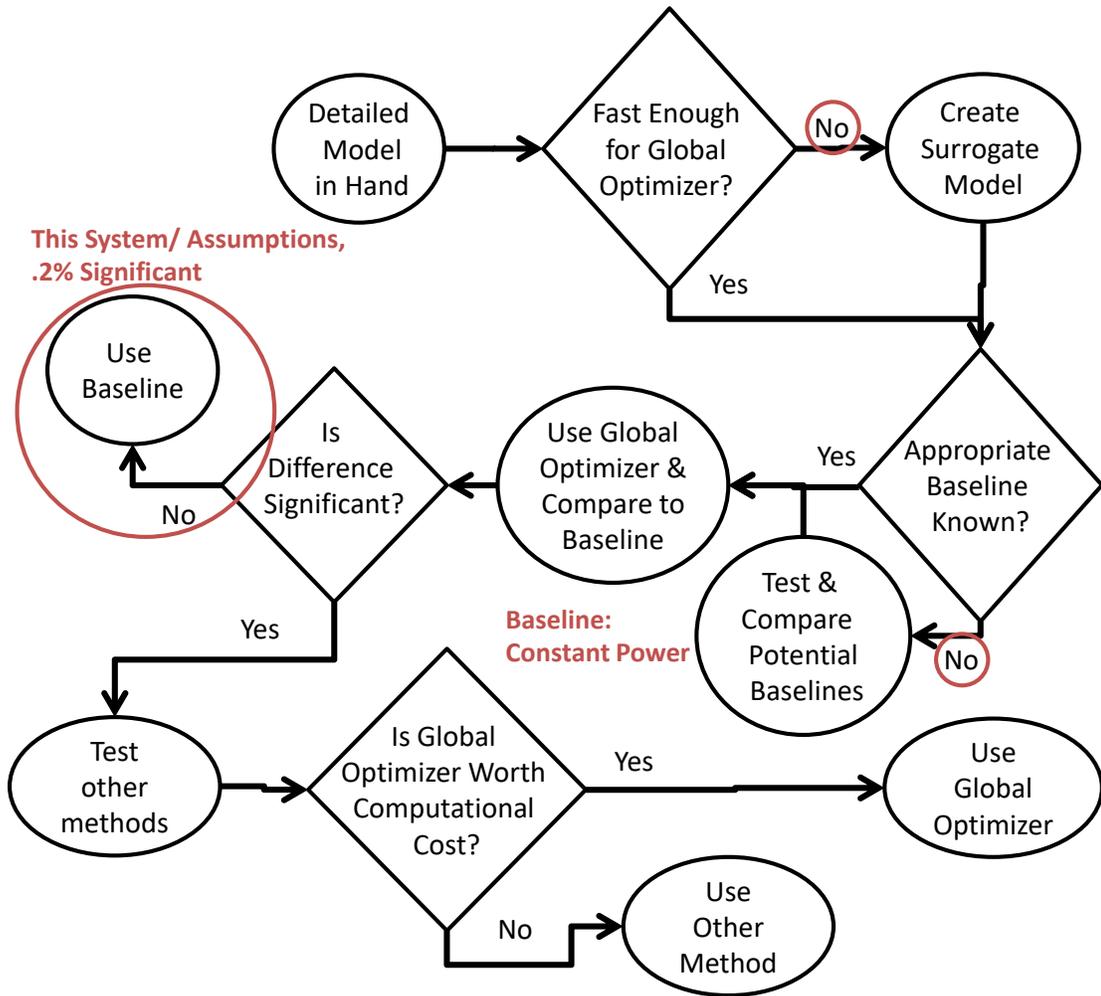
Figure 71: Procedure Example, Experiment #2 System/Assumptions, .2% Fuel Burn Significant

Using the results of Experiment #2 the application of the SHAPSO power scheduler selection method can be demonstrated as illustrated in Figure 71, with branch choices taken shown in red. The detailed model was examined and found to be too slow to use with Dynamic Programming. Therefore a surrogate model was created. With the surrogate model in hand, the appropriate baseline schedule was unknown so the different

baseline schedules were compared. Constant Power was found to save the most fuel. Using Dynamic Programming as the global optimizer, the maximum observed difference in fuel burn between the Constant Power schedule and the Dynamic Programming schedule was .021% using the original assumption about battery resistance. If the confidence interval for the model is .2%, this would complete the methodology with Constant Power selected as the final schedule, as shown in the flowchart in Figure 71 above.
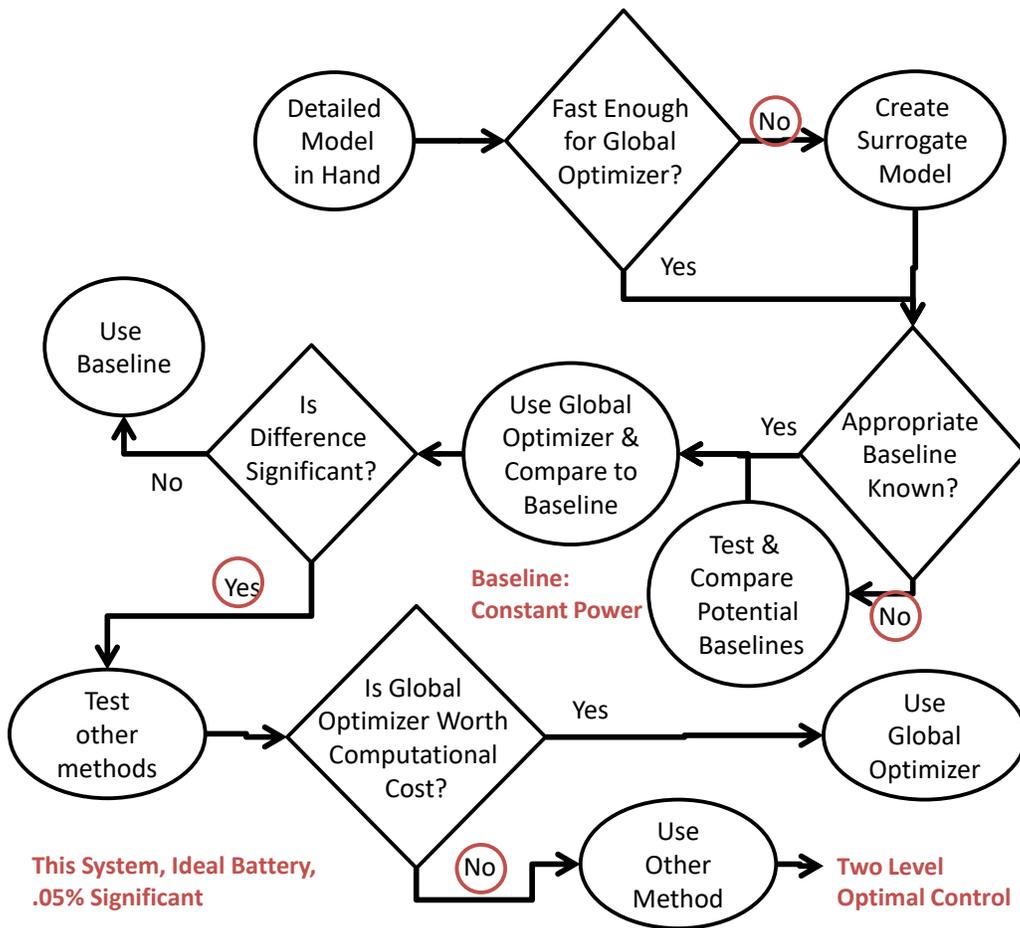
Figure 72: Procedure Example, Experiment #2 System, Ideal Battery, .05% Fuel Burn Significant

However, if the battery assumption was changed to the ideal battery and the confidence interval of the model was .05%, the .09% increase in fuel burn of the baseline methods over Dynamic Programming would cause the methodology to turn to the Optimal Control variants as illustrated in Figure 72. In this case the methodology would settle on Two Level Optimal Control because it is the fastest method which stays within the .05% bounds of Dynamic Programming.

This logical progression from the least expensive scheduler to the most expensive in search of the first one with sufficient performance should work for all hybrid architectures. Depending on the architecture, different baseline schedules may be required, and different optimization methods may be added to the "Test Other Methods" step. However this procedure should still identify the optimal operational schedules for hybrid electric architectures.

Technology, Operational, and Architectural Causes of Near Constant Optimal Schedules

As detailed in Chapter 5, we can have sufficient confidence in the results to adopt a modified version of SHAPSO. However questions remain on why a baseline schedule performed so well compared to a globally optimized schedule. This may be caused by the technology assumptions, the design of the hybrid gas turbine and the operational assumptions inherited from previous studies.

The technology assumptions impacting the efficiency of the electrical system in offsetting fuel at different power levels influence the ideal battery power schedule. These assumptions were included in the efficiency maps baked into the engine surrogate

models. According to these efficiency maps the motor and power electronics are inefficient at low power settings. This made low nonzero power choices uncommon among the optimal schedules. Another assumption is the efficiency loss within the gas turbine engine caused by the engine's acceptance of additional shaft power. This could be addressed in the future by an engine optimized for the acceptance of additional power, possibly even at the expense of fuel consumption during conventional operation.

The most conspicuous technology assumption is the battery resistance, which drives the motor power down with losses that are proportionate to the square of the power. This was shown in Experiments #2 and #3 to be the single largest factor determining the poor performance of the non-constant baseline schedules. Battery resistance severely penalized any use of full hybrid power during a mission. The resistance level of the baseline batteries was set by comparison with modern batteries such as those shown in Figure 73. Batteries of the future may be expected to be available with a lower internal resistance and a higher power density than those modeled in this thesis. However, as seen in Figure 73 this would reduce the available energy density of a fixed technology level battery. It is expected that an aircraft application will use the battery with the highest energy density it can afford, especially considering the battery's reserve capacity, not considered in this thesis, which reduces the effective energy density. Because of the battery's reserve capacity, this may require the actual energy density to be 1,000 Wh/kg to achieve these results.
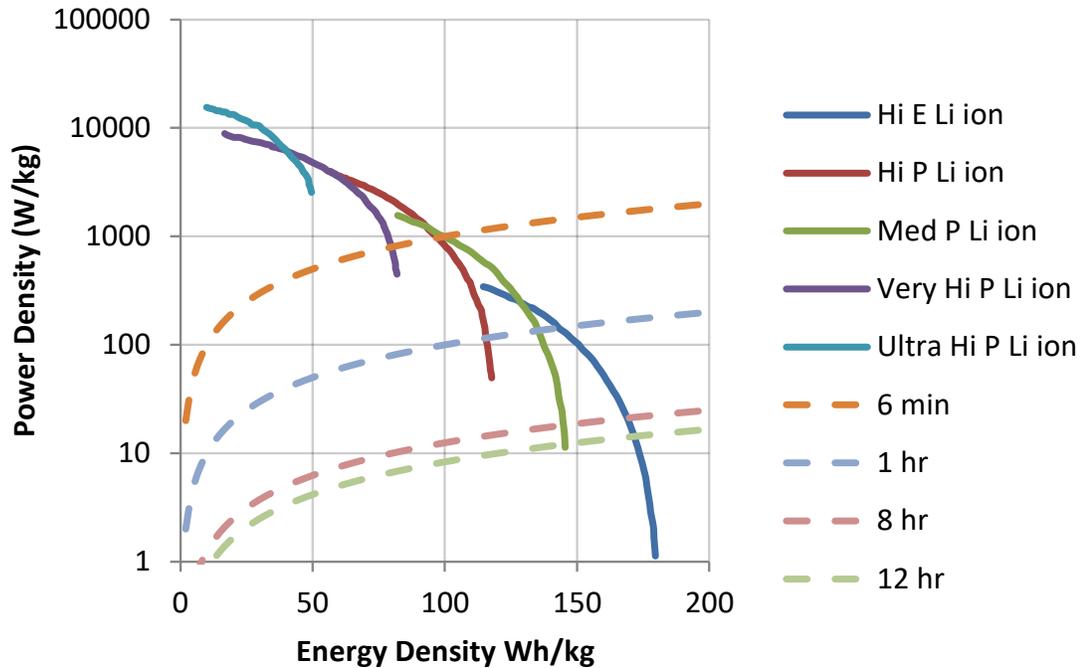
Figure 73: Ragone Chart for 2010 State of the Art Batteries[85]

The design of the hybrid gas turbine may also influence the optimal power schedule. Whenever hybrid power is added to the hybrid turbofan the turbine components downstream of the fan have to handle additional airflow mismatched with the amount of fuel being burned. This can produce engine stability issues as seen in Trawick et al. [90]. In that paper, the stability issues were handled with an operability bleed which reduced the engines efficiency. A different hybrid architecture with separate flow paths for the electric fans and the gas turbines would eliminate this problem and may allow more efficient low power operation of the gas turbines.

In addition to these technology assumptions these experiments inherited operational assumptions from Armstrong et al. [45]. The engine model contains the assumption that the engine thrust can never exceed the maximum value achievable

without electric assist, prohibiting boosting the engine thrust with the motor to achieve a higher climb rate. In addition, the engine was designed under the assumption that the core would never shutdown, dictating a minimum fuel burn even during descent. This differed from the core shutdown configuration seen in the Boeing SUGAR Phase II report[18].

Surprisingly another factor affecting the power schedule is the drag polar of the aircraft. The architecture used in these studies ultimately inherits the truss braced wing from Armstrong et al.[45] and has an extremely high L/D ratio of 22.75. This high ratio means that as the 8,000 lbs. of fuel burns in some of these cases, the required thrust of the vehicle only increases by 300 lbs., a relatively small change in the operation of a 150,000 lb. vehicle. If the induced drag were higher a larger change in thrust could change the operating point of the engine, encouraging a less constant use of hybrid power. On the other hand the higher penalty on weight makes it less likely that a hybrid propulsion system would ever be used on such an aircraft.

A final factor worth mentioning is the limited power of the hybrid system. The Chevrolet Volt, whose optimization in Tribioli et al. [17] drove the formulation of Hypothesis #4, is capable not only of shutting down and restarting its engine, but of maintaining all but the highest required output power on electrical power alone. The batteries carried in the 120 mile case (which they optimized by an additional 20% in fuel burn) were large enough to carry the Volt 1/3 of the distance (40 miles) without any gasoline usage. The only comparable hybrid architecture for aircraft is the SUGAR Volt Core Shutdown case. Unlike the Chevrolet Volt, it cannot relight its engines and pays a penalty for carrying so much weight[18]. However the larger motors and batteries

involved in the Core Shutdown model would give the optimizers more freedom to find the most optimal schedule.

Further work developing SHAPSO may benefit from a test case with a more varied ideal schedule. The first assumption to change for such an architecture is the requirement that the core remains lit during the entire mission. A system enabling core shutdown and relight would likely require a larger hybrid power level which would also enable more operational schedules. It may even be possible to shut down one core and leave the other burning, maintaining symmetric flight by utilizing electric power on one engine and jet fuel on the other. Architectures such as the eConcept with separate flow paths may be a good choice as well.

An additional consideration which would drive more interesting schedules is recharging. Although the electricity generated by burning jet fuel at altitude is unlikely to be cheaper than electricity generated at the ground, in systems where the net battery use in a mission is constrained to be zero a non-constant power schedule is guaranteed, and optimization of the recharging schedule may be an interesting test case.

Potential Improvements to the Methodology

The methodology as stated in Chapter 5 is capable of determining the optimal operational schedules for hybrid electric architectures, but it has room for improvement. A test case with more varied optimal operational schedules may assist in developing its improvements.

Resolution

The time step used during Experiment #1 was identified as being too large for use in the climb and descent segments of Experiment #2. This was due to the integration errors on the rate of climb. More problematic in the experimental results is the propensity of the other methods to edge out the global optimizer, Dynamic Programming, due to the resolution of Dynamic Programming's choice of power. The minimum power step during climb which is required to drain 1/100,000 of the battery in .001 hr., works out to ~26 HP. or about .75% of the maximum available hybrid power. Increasing the number of battery states that Dynamic Programming is allowed to have by a factor of 10 or 100 would bring this down to 2.6 or .26 HP. respectively. This calculation would most likely be sufficient to find the global optimum schedule. However this would increase the computational burden 100 or 10,000 fold and require the implementation of parallel processing and possibly a move off of desktop systems into a parallel computing cluster.

Additional Methods

The methodology as expressed in Chapter 5 does not specify exact methods to be used such as Dynamic Programming and Optimal Control. It is compatible with any method which meets the criteria of being a guaranteed global optimizer or a power schedule optimization method. Replacing the global optimizer with a faster one and/or finding other suitable methods could improve the execution time or final answer of the methodology.

<u>Global Optimizers</u>

Dynamic Programming was chosen as the global optimizer due to the prevalence of its use in the literature for hybrid electric cars, in which it is the benchmark for other, faster, methods[17]. However, once the discretization scheme used for Dynamic Programming has reduced the problem to one of the shortest path between nodes, many other algorithms are available that could find the solution.

One well known method for solving shortest path problems is Dijkstra's algorithm, first published by E. W. Dijkstra in 1959[96]. This method is closely related to Dynamic Programming, as Dijkstra also worked from the principle that any subset of the ideal path is itself the ideal path from the intermediate point to the end[97]. Dijkstra's original algorithm is designed for more general sets of nodes than the time step defined ones used in the hybrid car problem, where each state transition must go from one time step to the next. However modifications of Dijkstra's algorithm for such graphs have been made which make it much faster and suitable for such problems[98].

Even faster convergence might be possible using A* algorithms, which attempt to reduce the number of state transitions that have to be modeled by using a heuristic to estimate the minimum possible fuel burn from each state to the end[99]. This can eliminate areas of the space where too much fuel has already been burned to possibly be optimal. However, if this heuristic is too conservative, it only slows down the algorithm, and if it is too aggressive, it may not find the global optimum. It may be difficult to split the difference and achieve a net time savings compared to Dynamic Programming.

The methodology of this thesis can be adapted to test any algorithm that can be applied to the power scheduling problem. Depending on the factors included in the system model, different methods may be needed. In later stages of design it may be of interest to add stochastic effects to the system model, such as wind or reserve mission requirements, and to test algorithms that can handle such effects, such as Model Predictive Control or Stochastic Dynamic Programming which are used in hybrid cars. These algorithms could show the sensitivity of the ideal fuel burn to stochastic effects by comparing their performance to that of the global optimizer [100, 101].

Additional Variables

Experiments #1-#3 only considered an aircraft which flies a specific climb and descent schedule to a fixed cruise condition of Mach = .7 at 37,700 ft., however there may be gains to be had from flying a hybrid system at different flight conditions. If the cruise conditions were added to the algorithm, the algorithm might find that certain power schedules enable or favor flying at a higher or lower cruise altitude. Aircraft typically fly a step cruise, slowly increasing their altitude throughout a mission as they get lighter. Hybrid power considerations may favor a schedule in which fuel is burned early in the mission to step to a higher altitude where there is less drag. At this higher altitude the hybrid components could outperform the gas turbine further due to the decrease in thrust lapse. This would increase the efficiency of the system.

The climb and descent schedules were also fixed for this thesis using conventional fuels, attempting to get the best range per pound of fuel over the total climb segment.

This optimum climb schedule may change with the addition of electric power, especially if the hybrid system is sized to allow a higher thrust with power added than it can achieve in conventional operation. If core shutdown or other hybrid operation is allowed during descent the descent schedule may change as well.

Including additional variables such as climb rate or altitude in the optimization schemes would increase the computational burden on the optimizer, adding an entire extra dimension to the space optimized by Dynamic Programming and hence a drastic increase in the computation time. This could be offset by use of more advanced computational hardware.

Optimization Objective

In the fixed battery case considered by this thesis, the only objectives of the optimization methodology were to reduce the fuel burn during the mission and find the best method for doing so. The energy carried in the battery was completely used. This was under the justification that most of the cost of using the energy would still be expended if it was not used. That cost would be that incurred by carrying the battery's weight. Completely using all of the energy in the battery remains the strategy even if the objective becomes decreasing carbon emissions. In fact, carbon emissions could potentially be worse for electricity than for jet fuel. Therefore a smaller battery or no battery should be carried if the entire battery is not to be used.

In the 2017 update to NASA on the Rolls-Royce Electrically Variable Engine, Armstrong et al. pointed out that hybrid operation of parallel hybrid turbofans reduces the temperature at the exhaust of the burner and hence increases engine life if used to offset

the hottest part of the mission [46]. This raises the prospect of scheduling power not only to minimize fuel burn over the course of the mission but to maximize engine life, weighing a turbine temperature decrease in one part of the mission against a fuel burn increase from not having hybrid power available at a different part of the mission. This is particularly interesting because maximum life increase would require maximum hybrid power application. This would directly counter the penalty on maximum hybrid power imposed by the battery resistance.

Contributions

Hybrid Engine Modeling

In order to capture the performance of the electric components of a hybrid electric propulsion system, and their interplay with the gas turbine components, a set of electric component models was created in the gas turbine modeling tool NPSS. Models created for the motor, bus, power electronics, cable, and battery components, along with a scheme for interconnecting these electrical components, allowed for the modeling of many different hybrid electric architectures. With the addition of a generator element these models can be used to model most turboelectric architectures as well. These components are not specific to propulsion system modeling and have the potential to be used to model the electric part of gas turbine based power generation systems for terrestrial or airborne applications.

Hybrid Aircraft Mission Modeling

The mission simulation equations that govern the change in fuel weight, battery state of charge and aircraft altitude and distance were implemented in a MATLAB tool to enable analysis of hybrid aircraft mission performance from an engine surrogate model, aircraft weight and drag polar. This tool is not specific to the drag polar and engine model seen in this thesis, as can be seen from the iterations on the surrogate model performed in the setup of Experiments #1 and #2. Any hybrid electric aircraft could be modeled in the system by entering its weight, drag polar and surrogate and having its performance over the mission determined with any power schedule or scheduling method desired. With only slight modifications this could include propulsion systems incorporating recharging or asymmetric propulsion system operations.

Hybrid Aircraft Operational Schedules

The hybrid system chosen as the example system is based on a popular hybrid architecture seen in studies by NASA and Rolls-Royce. This system has been operated under different power schedules by different authors[18, 46, 93]. The superior performance of the Constant Power schedule is therefore of interest, even though it is only known to apply to this particular engine model operating under this set of technology assumptions and operational requirements. For systems with different architectures, sizes, or even higher fidelity models, the operational scheduling tool developed in this thesis has direct application for determining its power schedule and performance. This is particularly true of the Dynamic Programming method, which can be used to identify the global minimum fuel burn and the shapes of the optimal schedules

themselves. After the shapes of the schedules are found, they may admit capture by a simpler parametric scheme.

Future Work

This thesis has concentrated on the optimization of the power schedules for hybrid electric aircraft under a certain set of assumptions in isolation from other aspects of aircraft design and operation. Although hybrid electric aircraft such as the one modeled in this thesis are years away from commercial adoption and many of their technologies remain uncertain, the power scheduling problem is significant due to the effect it can have on other problems within hybrid electric aircraft design. In addition to potentially improving the methodology mentioned above, future work is needed on these larger problems impacted by the operational schedules' performance.

Battery Selection

As seen in Experiment #3, the energy savings curves for a given hybrid architecture are a strong function of the battery size at each range the hybrid aircraft flies and are improved through the application of optimal operational schedules. The battery size can therefore be chosen based on an expected distribution of missions for a proposed aircraft. One aspect of this problem which has not been considered is the application of multiple sizes of battery. This would involve allowing a single airframe to have different detachable batteries to use depending on payload and range. The number of batteries and ultimate feasibility of interchanging batteries at each airport is an economic consideration but the proper sizes to choose and the fuel burn savings they would achieve can be computed using the framework developed in this thesis.

Hybrid Propulsion System Selection and Sizing

Although no air carrier will be optimizing a fleet of hybrid electric airliners in the next couple of years, designers of the next generation of aircraft are already starting to make choices about the level of hybridization future aircraft will have. In this thesis the test scenario given at the end of Experiment #3 demonstrated the change in performance that occurs if the previously fixed electric motor size of 3,500 Hp. on each fan was reduced to 2,500 or 2,000 Hp. There is a tradeoff to be made in this sizing, trading extra weight on long missions against additional savings on short missions. A higher fidelity engine model may also examine the tradeoff between the difficulty in designing an engine with a larger embedded motor and potential energy losses from bending the flow path around the electric machine against the energy savings the larger machines provide when they are turned on. The analysis of each option requires solving the nested battery sizing and power scheduling problems and will determine if the core shutdown scheduling option is viable. This problem also will determine the final capability of a hybrid architecture and will enable the selection or rejection of each hybrid electric architecture altogether.

APPENDIX A: ADDITIONAL OPTIMAL SCHEDULES

In Chapter 5 only some of power schedules found using the different methods were plotted as needed to demonstrate the utility of the methods. The full set of optimal power schedules found may be of interest, as well as the full table of the raw fuel burn values. These are included below.

Table 16: Experiment #2 Absolute Fuel Burn, lbs.

| Batt R	Range (nmi)	Battery Weight (lbs.)	Global Optimizer Dynamic Prog	Baseline Schedules End Power	Climb Power	Const.	Optimal Control Original	Weight.	Two Level
100%	1500	20000	8251.30	8393.43	8301.24	8251.74	8252.71	8250.88	8251.44
100%	1479	10000	8837.76	9019.02	9004.34	8840.29	8840.09	8839.66	8839.33
100%	1000	20000	5012.32	5089.52	5026.98	5013.39	5012.93	5012.35	5012.54
100%	1000	10000	5803.62	5964.37	5920.51	5803.66	5803.80	5803.51	5803.62
50%	1500	20000	8216.24	8304.12	8250.05	8216.66	8217.29	8215.44	8216.21
50%	1500	10000	8951.34	9045.43	9047.86	8955.94	8955.61	8954.90	8950.19
50%	1000	20000	4906.79	4951.51	4916.33	4908.81	4907.07	4906.76	4906.95
50%	1000	10000	5771.59	5855.04	5830.68	5771.59	5771.71	5771.28	5771.43
0%	1500	20000	8177.49	8220.56	8201.58	8180.55	8180.01	8178.26	8179.18
0%	1500	10000	8929.16	8958.88	8984.58	8938.12	8937.30	8933.03	8929.62
0%	1000	20000	4896.58	4918.29	4904.26	4900.03	4897.14	4895.54	4896.97
0%	1000	10000	5739.59	5768.92	5768.28	5742.31	5741.92	5741.43	5741.64
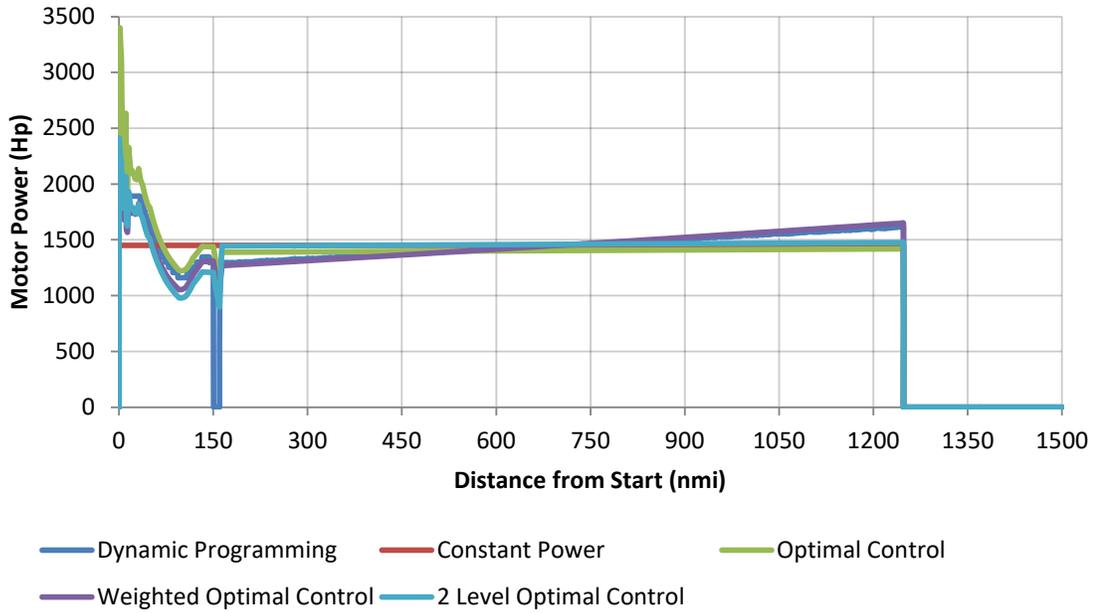
**Figure 74: Original Resistance, 20,000 lb. Battery, 1,500 nmi.**
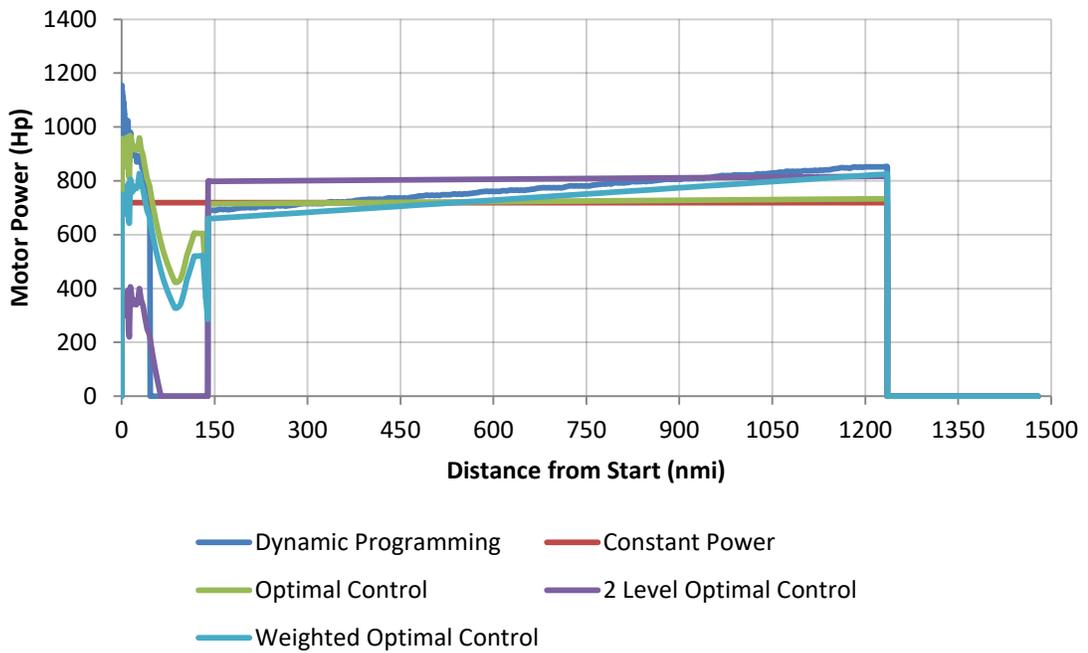
**Figure 75: Original Resistance, 10,000 lb. Battery, 1,500 nmi.**
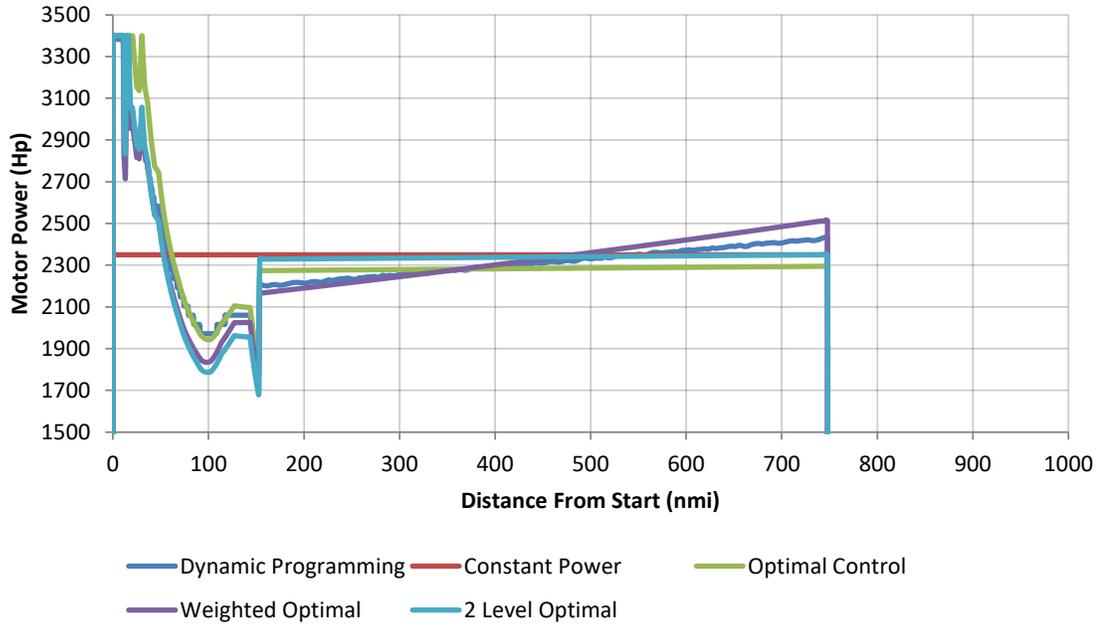
Figure 76: Original Resistance, 20,000 lb. Battery, 1,000 nmi.
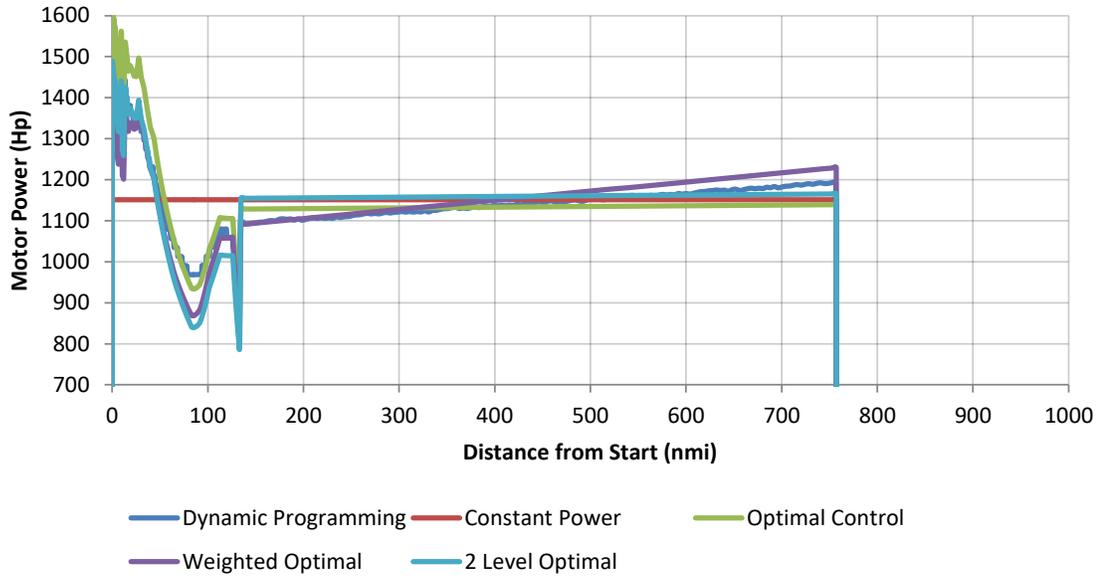

Figure 77: Original Resistance, 10,000 lb. Battery, 1,000 nmi.
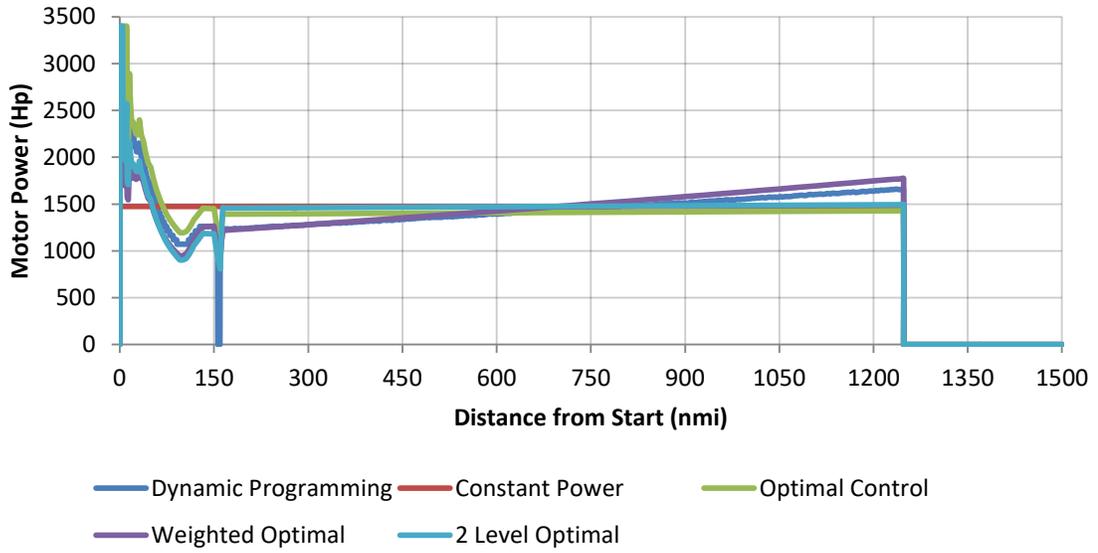
Figure 78: 50% Resistance, 20,000 lb. Battery, 1,500 nmi.
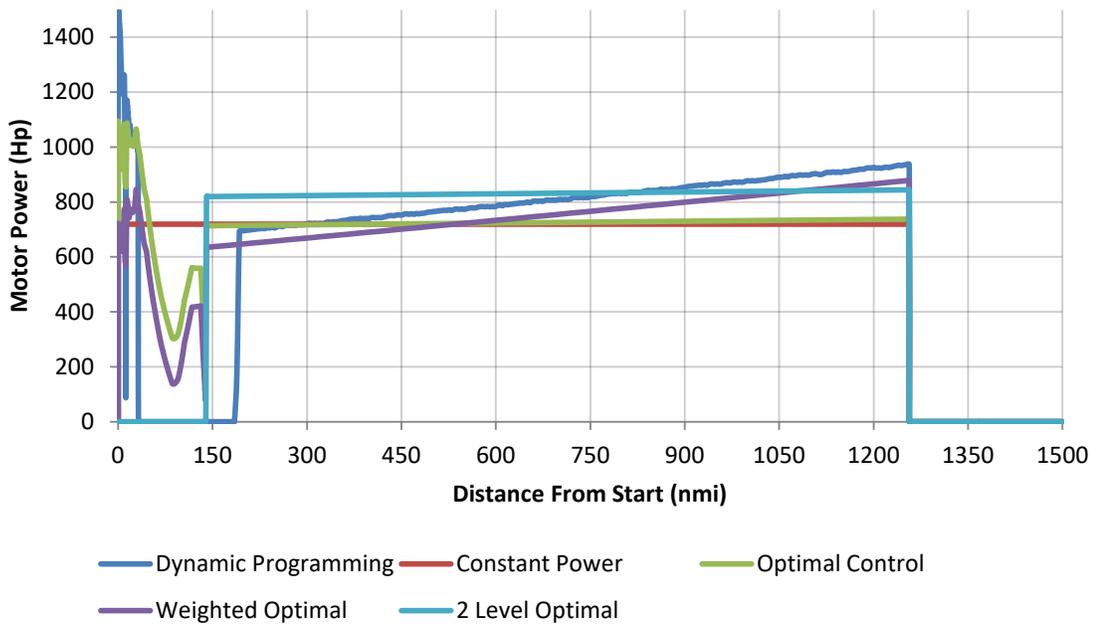
Figure 79: 50% Resistance, 10,000 lb. Battery, 1,500 nmi.
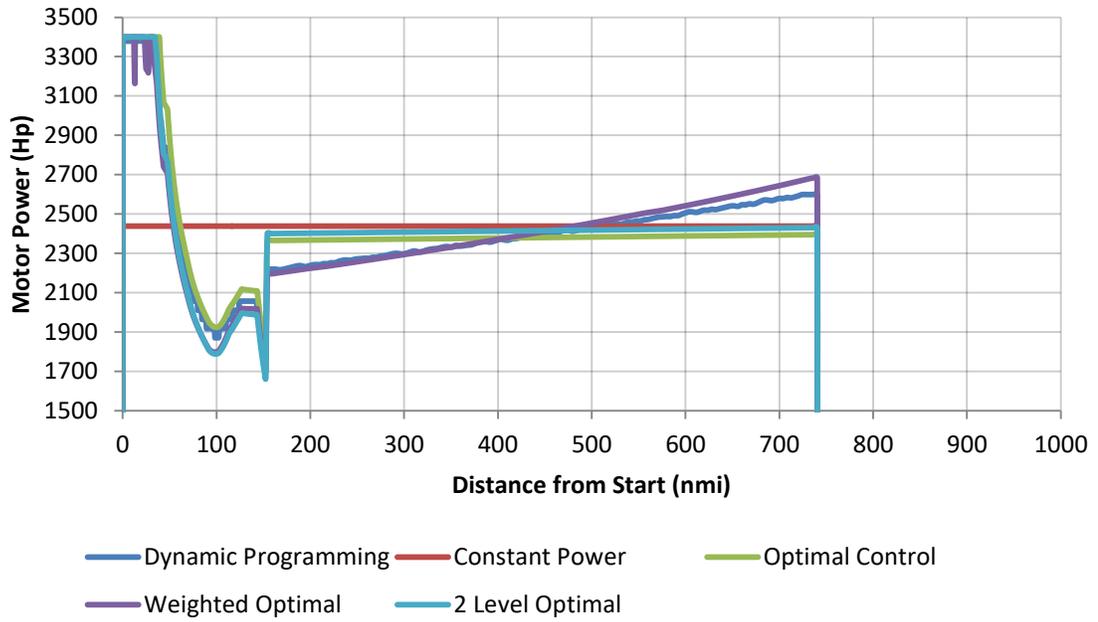
Figure 80: 50% Resistance, 20,000 lb. Battery, 1,000 nmi.
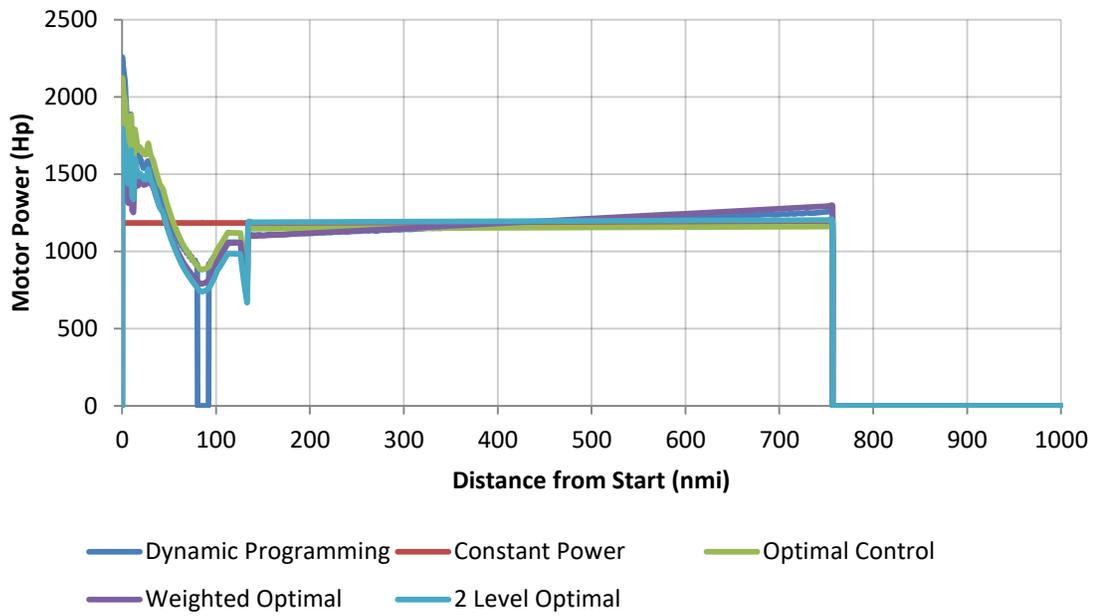
**Figure 81: 50% Resistance, 10,000 lb. Battery, 1,000 nmi.**

197
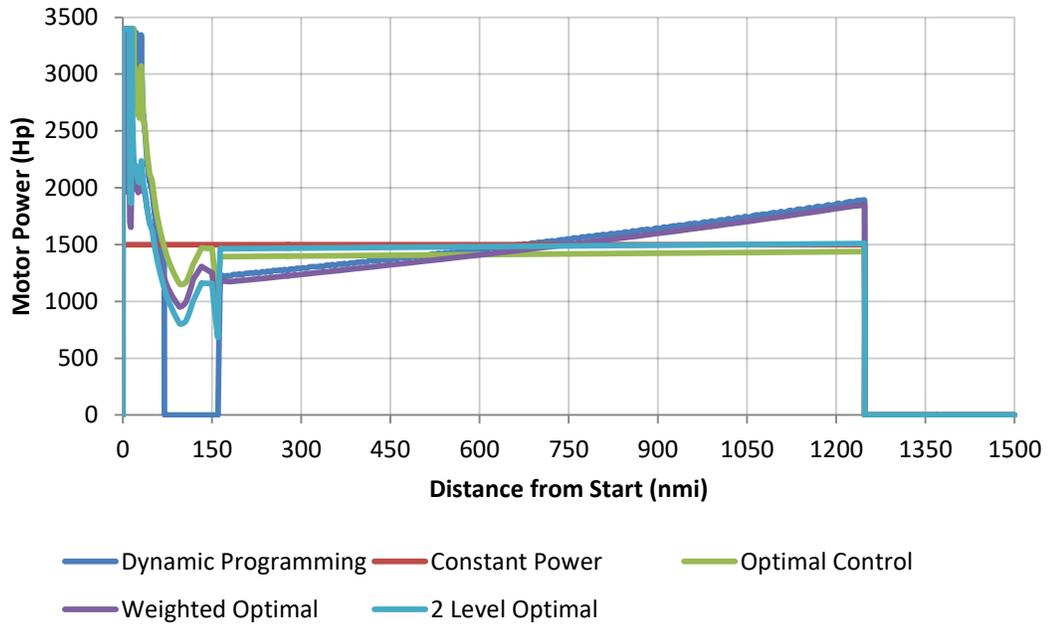
**Figure 82: 0% Resistance, 20,000 lb. Battery, 1,500 nmi.**
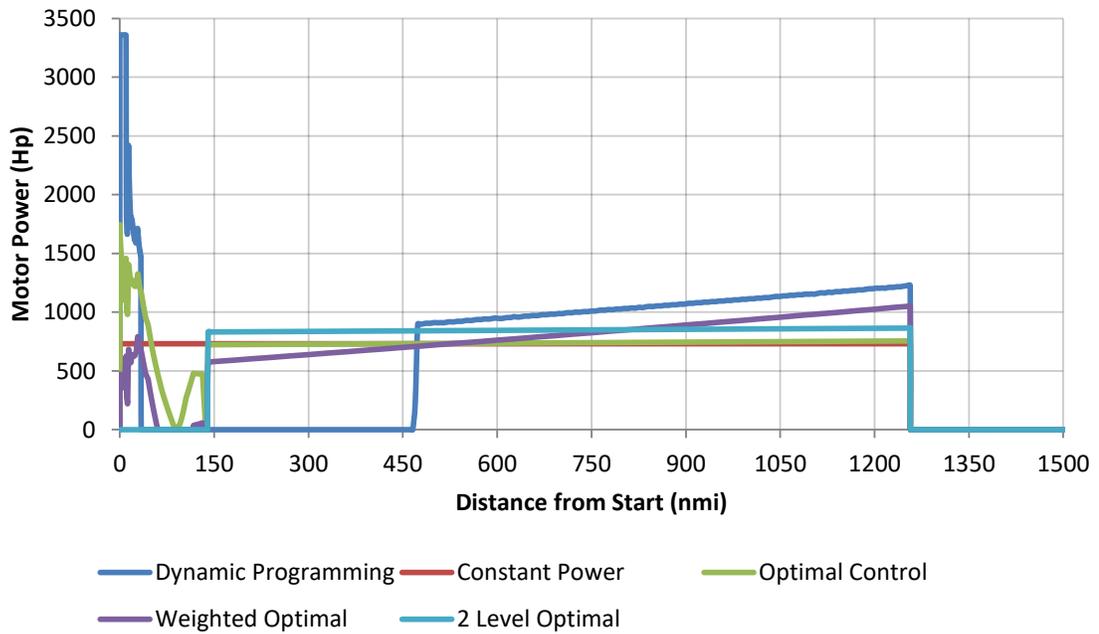
Figure 83: 0% Resistance, 10,000 lb. Battery, 1,500 nmi.
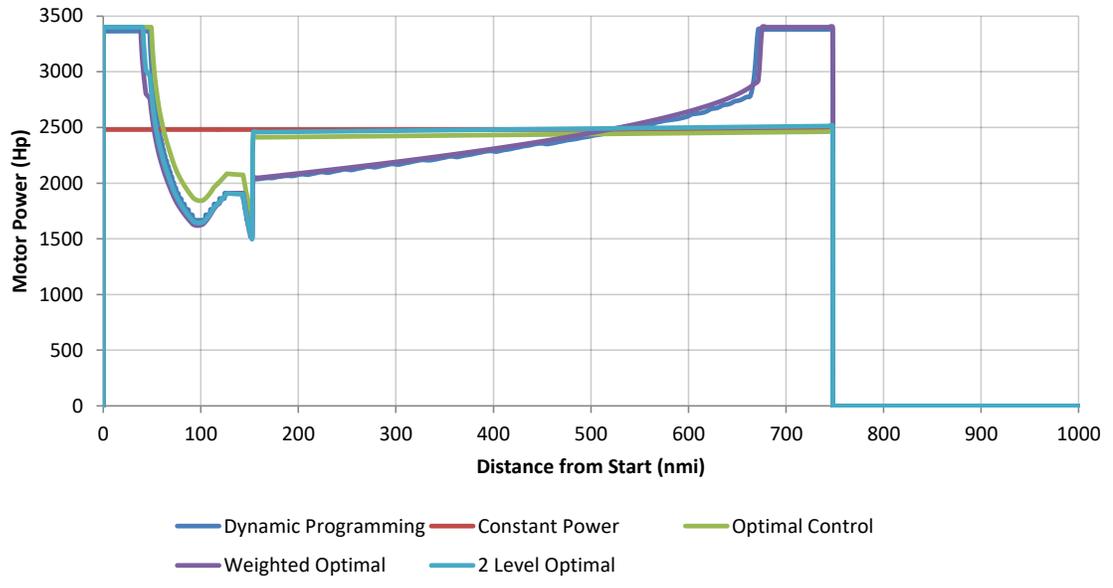
Figure 84: 0% Resistance, 20,000 lb. Battery, 1,000 nmi.
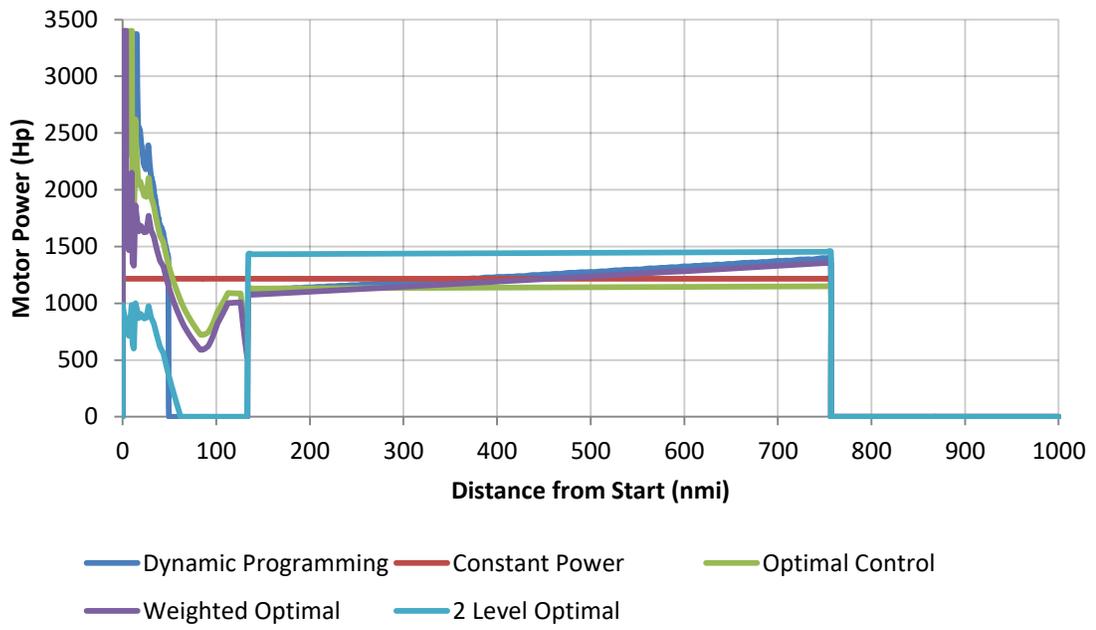

Figure 85: 0% Resistance, 10,000 lb. Battery, 1,000 nmi.

REFERENCES

1.   NASA, *Advanced Concept Studies for Subsonic and Supersonic Commercial Transports Entering Service in the 2030-2035 Period*, in *NASA Research Announcement, Pre-Proposal Conference*. 2007, National Aeronautics and Space Adminstration.

2.   Pornet, C. and A.T. Isikveren, *Conceptual design of hybrid-electric transport aircraft.* Progress in Aerospace Sciences, 2015. **79**: p. 114-135.

3.   Jankovsky, A.L. *Overview of Advanced Air Transport Technololgy (AATT) and Hybrid Gas-Electric Propulsion (HGEP)*. in *HGEP NRA Review Meeting*. 2017. Cleveland, Ohio.

4.   Jankovsky, A.L., C. Bowman, and R. Jansen, *Building Blocks for Transport-Class Hybrid and Turboelectric Vehicles*. 2016, NASA Glenn Research Center: Cleveland, OH. p. 15.

5.   National Academies of Sciences, E.M., et al., *Commercial Aircraft Propulsion and Energy Systems Research: Reducing Global Carbon Emissions*. 2016: National Academies Press.

6.   Bowman, R., *Electrical Materials Research for NASAs Hybrid Electric Commercial Aircraft Program*. 2017, NASA Glenn Research Center: Cleveland, OH United States. p. 34.

7.   Gao, Y., M. Ehsani, and J.M. Miller. *Hybrid electric vehicle: Overview and state of the art*. in *Industrial Electronics, 2005. ISIE 2005. Proceedings of the IEEE International Symposium on*. 2005. IEEE.

8.   Felder, J., H. Kim, and G. Brown, *Turboelectric Distributed Propulsion Engine Cycle Analysis for Hybrid-Wing-Body Aircraft.* 2009.

9.   Madavan, N.K., R. Del Rosario, and A.L. Jankovsky, *Hybrid-Electric and Distributed Propulsion Technologies for Large Commercial Transports: A NASA Perspective.* 2015.

10.   Warwick, G. *eConcept - EADS's Hybrid-Electric Airliner*. Things With Wings 2013 [cited 2016 April 4th]; Available from: http://aviationweek.com/blog/econcept-eadss-hybrid-electric-airliner.

11.   Matthé, R. and U. Eberle, *The voltec system: Energy storage and electric propulsion.* Lithium-Ion Batteries: Advances and Applications; Pistoia, G., Ed, 2014: p. 151-176.

12.   Brown, G.V. *Weights and efficiencies of electric components of a turboelectric aircraft propulsion system*. in *49th AIAA aerospace sciences meeting including the new horizons forum and aerospace exposition*. 2011.

13.   Schutte, J., J. Tai, and D. Mavris. *Multi-Design Point Cycle Design Incorporation into the Environmental Design Space*. in *48th AIAA/ASME/SAE/ASEE Joint Propulsion Conference & Exhibit*. 2012.

14.   Gladin, J.C., et al., *A Parametric Study of Gas Turbine Propulsion as a Function of Aircraft Size Class and Technology Level*, in *55th AIAA Aerospace Sciences Forum*. 2017, AIAA: Grapevine, Texas. p. 37.

15. Salmasi, F.R., *Control Strategies for Hybrid Electric Vehicles: Evolution, Classification, Comparison, and Future Trends.* IEEE Transactions on Vehicular Technology, 2007. **56**(5): p. 2393-2404.

16. Chevrolet, *Plugging into your 2011 Volt: It's more car than electric.*, G. Motors, Editor. 2011, General Motors. p. 16.

17. Tribioli, L.a.O., Simona, *Analysis of Energy Management Strategies in Plug-in Hybrid Electric Vehicles: application to the GM Chevrolet Volt*, in *2013 American Control Conference*. 2013: Washington DC. p. 5966-5971.

18. Bradley, M.K. and C.K. Droney, *Subsonic Ultra Green Aircraft Research: Phase 2. Volume 2; Hybrid Electric Design Exploration.* 2015.

19. Bradley, M.K. and C.K. Droney, *Subsonic Ultra Green Aircraft Research: Phase I Final Report.* 2011: p. 207.

20. Hathaway, M.D., R. Del Rosario, and N. Madavan, *NASA Fixed Wing Project Propulsion Research and Technology Development Activities to Reduce Specific Energy Consumption*, in *49th AIAA/ASME/SAE/ASEE Joint Propulsion Conference*. 2013, American Institute of Aeronautics and Astronautics.

21. Cantemir, C.-G., et al., *10 MW Ring Motor*, in *Hybrid Electric Concept & Motor Development NRA Awards Annual Review*. 2016, Ohio State University: Cleveland, Ohio. p. 39.

22. Okai, K., et al., *Preliminary Design Investigation of Electromagnetic Motors for Turbofan-Drive Assist*, in *53rd AIAA Aerospace Sciences Meeting*. 2015, American Institute of Aeronautics and Astronautics.

23. Wahls, R., *N+3 Technologies and Concepts*. 2010, NASA Ames Research Center: Moffett Field, California. p. 11.

24. Jagannath, R., et al. *A Simplified Method To Calculate The Fuel Burn Of A Hybrid-Electric Airplane*. in *50th AIAA/ASME/SAE/ASEE Joint Propulsion Conference*. 2014.

25. Singh, R., et al., *Cost-based flight technique optimization for hybrid energy aircraft.* Aircraft Engineering and Aerospace Technology: An International Journal, 2014. **86**(6): p. 591-598.

26. Lents, C.E., et al., *Parallel Hybrid Gas-Electric Geared Turbofan Engine Conceptual Design and Benefits Analysis*, in *52nd AIAA/SAE/ASEE Joint Propulsion Conference*. 2016, American Institute of Aeronautics and Astronautics.

27. Perullo, C., et al., *Cycle Selection and Sizing of a Single-Aisle Transport with the Electrically Variable Engine(TM) (EVE) for Fleet Level Fuel Optimization*, in *55th AIAA Aerospace Sciences Meeting*. 2017, American Institute of Aeronautics and Astronautics.

28. Warwick, G. *NASA's Slower X-Plane Pace Could Have An Impact On Industry*. Aviation Week & Space Technology, 2017.

29. Jansen, R., K.P. Duffy, and G. Brown, *Partially Turboelectric Aircraft Drive Key Performance Parameters*, in *53rd AIAA/SAE/ASEE Joint Propulsion Conference*. 2017, American Institute of Aeronautics and Astronautics.

30. Welstead, J. and J.L. Felder, *Conceptual Design of a Single-Aisle Turboelectric Commercial Transport with Fuselage Boundary Layer Ingestion.* 2016.

31. Kim, H., *Distributed Propulsion Vehicles*, in *27th International Congress of the Aeronautical Sciences*. 2010: Nice, France. p. 11.

32. Armstrong, M., et al., *Stability, transient response, control, and safety of a high-power electric grid for turboelectric propulsion of aircraft*. 2013.

33. Liou, M.-F., et al., *Aerodynamic Design of the Hybrid Wing Body with Nacelle: N3-X Propulsion-Airframe Configuration*, in *34th AIAA Applied Aerodynamics Conference*. 2016, American Institute of Aeronautics and Astronautics.

34. Kim, H. and M.-S. Liou, *Optimal Shape Design of Mail-Slot Nacelle on N3-X Hybrid Wing Body Configuration*, in *31st AIAA Applied Aerodynamics Conference*. 2013, American Institute of Aeronautics and Astronautics.

35. Berton, J.J. and W.J. Haller, *A Noise and Emissions Assessment of the N3-X Transport*, in *52nd Aerospace Sciences Meeting*. 2014, American Institute of Aeronautics and Astronautics.

36. Goldberg, C., et al., *Economic Viability Assessment of NASA?s Blended Wing Body N3-X Aircraft*, in *53rd AIAA/SAE/ASEE Joint Propulsion Conference*. 2017, American Institute of Aeronautics and Astronautics.

37. Williamson, M., *Air power the rise of electric aircraft.* Engineering & Technology, 2014. **9**(10): p. 77-79.

38. Van Bogaert, J., *Assessment of Potential Fuel Saving Benefits of Hybrid-Electric Regional Aircraft*. 2015, TU Delft, Delft University of Technology.

39. Gibson, A., et al., *Superconducting Electric Distributed Propulsion Structural Integration and Design in a Split-Wing Regional Airliner*, in *49th AIAA Aerospace Sciences Meeting including the New Horizons Forum and Aerospace Exposition*. 2011, American Institute of Aeronautics and Astronautics.

40. Green, M., B. Schiltgen, and A. Gibson, *Analysis of a Distributed Hybrid Propulsion System with Conventional Electric Machines.* 2012.

41. Friedrich, C. and P.A. Robertson, *Design of Hybrid-Electric Propulsion Systems for Light Aircraft.* 2014.

42. Fredericks, W.J., M.D. Moore, and R.C. Busan, *Benefits of Hybrid-Electric Propulsion to Achieve 4x Increase in Cruise Efficiency for a VTOL Aircraft*. 2012, AIAA.

43. Ausserer, J. and F. Harmon, *Integration, Validation, and Testing of a Hybrid-Electric Propulsion System for a Small Remotely Piloted Aircraft.* 2012.

44. Trawick, D., C. Perullo, and D. Mavris. *Examining Non-Uniform Generator and Propulsor Control Schemes for a Hybrid Electric Propulsion Concept*. in *48th AIAA/ASME/SAE/ASEE Joint Propulsion Conference & Exhibit*. 2012.

45. Armstrong, M. and C. Perullo, *NASA Hybrid Gas-Electric Propulsion System*. 2015, Rolls-Royce.

46. Armstrong, M., M. Starr, and D. Stamm, *Electrically Variable Engine (EVE) NASA Annual Review*. 2017, Rolls-Royce LibertyWorks: Cleveland, OH. p. 24.

47. Zhang, X., et al., *Prius and Volt: Configuration Analysis of Power-Split Hybrid Vehicles With a Single Planetary Gear.* Vehicular Technology, IEEE Transactions on, 2012. **61**(8): p. 3544-3552.

48. Energy, U.D.o.E.O.o.E.E.a.R. *Plug-in Hybrids*. 2017 [cited 2017 November 6th 2017]; Available from: https://www.fueleconomy.gov/feg/phevtech.shtml.

49. Hofman, T., et al., *Rule-based energy management strategies for hybrid vehicles.* International Journal of Electric and Hybrid Vehicles, 2007. **1**(1): p. 71-94.

50. Koot, M., et al., *Energy management strategies for vehicular electric power systems.* Vehicular Technology, IEEE Transactions on, 2005. **54**(3): p. 771-782.

51. Lin, C.-C., et al., *Power management strategy for a parallel hybrid electric truck.* Control Systems Technology, IEEE Transactions on, 2003. **11**(6): p. 839-849.

52. Borhan, H., et al., *MPC-based energy management of a power-split hybrid electric vehicle.* Control Systems Technology, IEEE Transactions on, 2012. **20**(3): p. 593-603.

53. Ripaccioli, G., et al. *A stochastic model predictive control approach for series hybrid electric vehicle power management.* in *American Control Conference (ACC).* 2010.

54. Heinrich, M.T.E., et al., *Regenerative Braking Capability Analysis of an Electric Taxiing System for a Single Aisle Midsize Aircraft.* IEEE Transactions on Transportation Electrification, 2015. **1**(3): p. 298-307.

55. Hellmund, R.E., *Regenerative braking of electric vehicles.* Proceedings of the American Institute of Electrical Engineers, 1917. **36**(1): p. 1-56.

56. *Chevrolet Volt Features and Specs.* 2017 [cited 2017 November 8, 2017]; Available from: https://www.caranddriver.com/chevrolet/volt/specs.

57. Enthaler, A. and F. Gauterin. *Significance of internal battery resistance on the remaining range estimation of electric vehicles.* in *2013 International Conference on Connected Vehicles and Expo (ICCVE).* 2013.

58. Armstrong, M.J., M. Blackwelder, and C. Ross, *Sensitivity of TeDP Microgrid System Weight and Efficiency to Operating Voltage.* 2014.

59. *DC-DC Converter Efficiency Map.* [cited 2014 August 24, 2014]; Available from: http://connectedplanetonline.com/images/archive/Rectifier%20Efficiency%20Curve%20TCO2.jpg.

60. Pilawa, R., et al., *Modular and Scalable High Efficiency Power Inverters for Extreme Power Density Applications.* 2017, University of Illinois at Urbana-Champaign: NASA AATT NRA Annual Meeting, Cleveland, OH. p. 83.

61. Sarma, M.S., *Electric Machines: Steady-state Theory and Dynamic Performance.* 1994: PWS Publ.

62. Perullo, C., D. Trawick, and D. Mavris, *Assessment of Engine and Vehicle Performance Using Integrated Hybrid-Electric Propulsion Models.* Journal of Propulsion and Power, 2016. **32**(6): p. 1305-1314.

63. Bradley, T., et al., *Energy Management for Fuel Cell Powered Hybrid-Electric Aircraft.* 2009.

64. Bellman, R., *On the Theory of Dynamic Programming.* Proceedings of the National Academy of Sciences of the United States of America, 1952. **38**(8): p. 716-719.

65. Sniedovich, M., *A new look at Bellman's principle of optimality.* Journal of Optimization Theory and Applications, 1986. **49**(1): p. 161-176.

66. Musardo, C., et al., *A-ECMS: An adaptive algorithm for hybrid electric vehicle energy management.* European Journal of Control, 2005. **11**(4): p. 509-524.

67.   Kolmanovsky, I., I. Siverguina, and B. Lygoe. *Optimization of powertrain operating policy for feasibility assessment and calibration: Stochastic dynamic programming approach*. in *American Control Conference, 2002. Proceedings of the 2002*. 2002. IEEE.

68.   Perullo, C. and D. Mavris, *A review of hybrid-electric energy management and its inclusion in vehicle sizing*. Aircraft Engineering and Aerospace Technology, 2014. **86**(6): p. 550-557.

69.   Miyazawa, Y., et al., *Dynamic Programming Application to Airliner Four Dimensional Optimal Flight Trajectory*. 2013.

70.   Serrao, L. and G. Rizzoni. *Optimal control of power split for a hybrid electric refuse vehicle*. in *Proceedings of the 2008 American Control Conference*. 2008.

71.   Kim, N., S. Cha, and H. Peng, *Optimal control of hybrid electric vehicles based on Pontryagin's minimum principle*. Control Systems Technology, IEEE Transactions on, 2011. **19**(5): p. 1279-1287.

72.   Paganelli, G., et al. *Equivalent consumption minimization strategy for parallel hybrid powertrains*. in *Vehicular Technology Conference, 2002. VTC Spring 2002. IEEE 55th*. 2002. IEEE.

73.   Sciarretta, A., M. Back, and L. Guzzella, *Optimal control of parallel hybrid electric vehicles*. Control Systems Technology, IEEE Transactions on, 2004. **12**(3): p. 352-363.

74.   Franco, A., D. Rivas, and A. Valenzuela, *Minimum-fuel cruise at constant altitude with fixed arrival time*. Journal of guidance, control, and dynamics, 2010. **33**(1): p. 280-285.

75.   Norris, G., *Truss-Braced Wings May Find Place on Transonic Aircraft*, in *Aviation Week & Space Technology*. 2016, Penton

76.   Fassbender, M., *Boeing's Sweet Vision For SUGAR Concepts*. 2015, Advantage Buisness Media: Manufacturing.net.

77.   Perullo, C. and D.N. Mavris. *Assessment of Vehicle Performance Using Integrated NPSS Hybrid Electric Propulsion Models*. in *50th AIAA/ASME/SAE/ASEE Joint Propulsion Conference*. 2014.

78.   Miyairi, Y., C. Perullo, and D.N. Mavris, *A Parametric Environment for Weight and Sizing Prediction of Motor/Generator for Hybrid Electric Propulsion*, in *51st AIAA/SAE/ASEE Joint Propulsion Conference*. 2015, American Institute of Aeronautics and Astronautics.

79.   Brown, G.V., et al., *NASA Glenn Research Center program in high power density motors for aeropropulsion*. 2005.

80.   Haran, K., et al., *High Speed, High Frequency Air-Core Machine and Drive*. 2017, NASA Hybrid Electric NRA Annual Review: Cleveland, OH.

81.   Perullo, C.a.M., Dimitri N., *Assesement of Vehicle Performance Using NPSS Hybrid Electric Propulsion Models*, in *50th AIAA/ASME/SAE/ASEE Joint Propulsion Conference*. 2014: Cleveland, OH.

82.   Vrancik, J., *Prediction of windage power loss in alternators*, NASA, Editor. 1968.

83.   Huynh, C., L. Zheng, and D. Acharya, *Losses in high speed permanent magnet machines used in microturbine applications*. Journal of engineering for gas turbines and power, 2009. **131**(2): p. 022301.

84.   *Inverter Efficiency Map.*   [cited 2015 May 12, 2015]; Available from: http://www.powersystemsdesign.com/library/resources/images/articles/special_re ports/april2011/cree/figure6.jpg.

85.   Zanardelli, S., *US Army's Ground Vehicle Energy Storage R&D Programs and Goals.* 2010, DTIC Document.

86.   OXIS, *Ultra Light Lithium Pouch Cell.* 2014, OXIS Energy Ltd.: http://oxisenergy.com/.

87.   Stückl, S., J. Van Toor, and H. Lobentanzer. *VoltAir–The All Electric Propulsion Concept Platform–A Vision for Atmospheric Friendly Flight.* in *28th International Congress of the Aeronautical Sciences (ICAS).* 2012.

88.   Lytle, J.K., *The numerical propulsion system simulation: A multidisciplinary design system for aerospace vehicles.* 1999.

89.   *NPSS User Guide.* 2013, NPSS Consortium.

90.   Trawick, D., et al., *Development and Application of GT-HEAt to the design of the Electrically Variable Engine (EVE),* in *55th AIAA Aerospace Sciences Meeting.* 2017: Grapevine, Texas.

91.   Kestner, B., et al., *Integrated Engine and Aircraft Mission Performance Analysis Using NPSS,* in *50th AIAA Aerospace Sciences Meeting including the New Horizons Forum and Aerospace Exposition.* 2012, American Institute of Aeronautics and Astronautics.

92.   Coogan, S.B., *Object-Oriented Aircraft Mission Analysis Using NPSS,* in *54th AIAA Aerospace Sciences Meeting.* 2016, American Institute of Aeronautics and Astronautics.

93.   Armstrong, M. and C. Perullo, *NASA Hybrid Gas-Electric Propulsion System Phase II Review.* 2015, Rolls-Royce LibertyWorks: Cleveland OH.

94.   *MATLAB Documentation.* 2017   [cited 2017 November 26, 2017]; Available from: https://www.mathworks.com/help/matlab/index.html.

95.   McCullers, L.A., *Flight Optimization System* in *User's Guide.* 2004, NASA Langley Research Center: Hampton, Va.

96.   Dijkstra, E.W., *A note on two problems in connexion with graphs.* Numerische mathematik, 1959. **1**(1): p. 269-271.

97.   Sniedovich, M., *Dijkstra's algorithm revisited: the dynamic programming connexion.* Control and cybernetics, 2006. **35**(3): p. 599-620.

98.   Cormen, T.H., *Introduction to algorithms.* 2nd ed. ; Eastern Economy ed.. ed. Algorithms. 2005, New Delhi-110001: New Delhi-110001 : Prentice-Hall of India Private Limited.

99.   Hart, P.E., N.J. Nilsson, and B. Raphael, *A formal basis for the heuristic determination of minimum cost paths.* IEEE transactions on Systems Science and Cybernetics, 1968. **4**(2): p. 100-107.

100.   Vagg, C., et al., *Stochastic Dynamic Programming in the Real-World Control of Hybrid Electric Vehicles.* IEEE Transactions on Control Systems Technology, 2016. **24**(3): p. 853-866.

101.   Tang, J., et al. *Energy management of a parallel hybrid electric vehicle with CVT using model predictive control.* in *2016 35th Chinese Control Conference (CCC).* 2016.